



## THESIS APPROVAL

### GRADUATE SCHOOL, KASETSART UNIVERSITY

Master of Science (Chemistry)

DEGREE

Chemistry

FIELD

Chemistry

DEPARTMENT

**TITLE:** Experimental and Theoretical Studies on Resveratrol Oligomer Compounds from the Bark of Dipterocarpaceae Family against HIV-1 Reverse Transcriptase

**NAME:** Miss Chompoonuch Tancharoen

**THIS THE SIS HAS BEEN ACCEPTED BY**

THESIS ADVISOR

( Mr. Songwut Suramitr, Ph.D. )

THESIS CO-ADVISOR

( Associate Professor Supa Hannongbua, Dr.rer.nat. )

DEPARTMENT HEAD

( Associate Professor Supa Hannongbua, Dr.rer.nat. )

APPROVED BY THE GRADUATE SCHOOL ON

DEAN

( Associate Professor Gunjana Theeragool, D.Agr. )

THESIS

EXPERIMENTAL AND THEORETICAL STUDIES ON  
RESVERATROL OLIGOMER COMPOUNDS FROM  
THE BARK OF DIPTEROCARPACEAE FAMILY AGAINST  
HIV-1 REVERSE TRANSCRIPTASE

CHOMPOONUCH TANCHAROEN

A Thesis Submitted in Partial Fulfillment of  
the Requirements for the Degree of  
Master of Science (Chemistry)  
Graduate School, Kasetsart University  
2012

Chompoonuch Tancharoen 2012: Experimental and Theoretical Studies on Resveratrol Oligomer Compounds from the Bark of Dipterocarpaceae Family against HIV-1 Reverse Transcriptase. Master of Science (Chemistry), Major Field: Chemistry, Department of Chemistry. Thesis Advisor: Mr. Songwut Suramitr, Ph.D. 82 pages.

In this work, a new resveratrol trimer together with three known compounds were isolated including Gnetin C, Anigopreissin A and Hopeafuran from the stem-bark of *Shorea siamensis* Miq. All isolated compounds were evaluated for their anti-HIV-1 reverse transcriptase by using Nevirapine as reference drug. From the IC<sub>50</sub> values, it showed that Anigopreissin A can inhibit wild-type HIV-1 RT activity as same as Nevirapine. In addition, orientations of all isolated compounds were investigated by molecular docking simulations. The results of GoldScore were found in the order of a new resveratrol trimer (83.40) > Anigopreissin A (65.39) > Gnetin C (60.63) > Nevirapine (62.82) > Hopeafuran (19.81). IC<sub>50</sub> results of a new resveratrol trimer corresponded to partial interaction. Whereas, the results of partial interaction and docking calculations of the other ligands contravened to the experimental IC<sub>50</sub> values. Thus, a new resveratrol trimer and Anigopreissin A are found to be potent compounds to further study as novelistic drugs.

\_\_\_\_\_  
Student's signature

\_\_\_\_\_  
Thesis Advisor's signature

/ /

## ACKNOWLEDGEMENTS

I sincerely thank my advisor, Dr. Songwut Suramitr for his support and attention throughout the duration of my graduate study and research. I also wish to express my deep and sincere gratitude to my advisory committee Associate Professor Supa Hannongbua, who gave me a great opportunity to work at Nanjing University, China under collaborative research with Prof. Ren Xiang Tan and Dr. Hui-Ming Ge. I have not only a great experience about the experimental but also have a beautiful memory in that time. I wish to thank Dr. Srunya Vajrodaya for helping about identification of plants. I also wish thank Dr. Supanna Techasakul who provided facilities on experimental laboratory and valuable suggestion. I deeply appreciate to Dr. Patchreenart Saparpakorn, Dr. Phornphimon Maitarad and Dr. Darinee Phromyothin who took the time to help and suggest in technical computational calculations. Furthermore, I am also grateful to Ms. Ratsupa Thammaporn who performed anti-HIV 1 RT activity testing and spent time discussing about the results with me.

I would like to express my deep gratitude to the National Center of Excellence in Petroleum, Petrochemical and Advanced Materials (NCE-PPAM), Kasetsart University Research and Development Institute (KURDI), Laboratory of Computational and Applied Chemistry (LCAC) for research facilities. The Thailand Research Fund (DBG5280018), (RTA 5380010) is sincere thanked for scholarship. The High Performance Computing Center of the National Electric and Computer Technology (NECTEC), was provide SYBYL program. I wish to thank the Chulabhorn Research Institute (CRI) of Thailand for HRMS measurements. And I would also like to thank all of LCAC members and staffs at the Department of Chemistry, Faculty of Science, Kasetsart University for research supporting.

Finally, I owe my loving thanks to my lovely parents, my younger brother, cousin and neighbor for constant supports and encouragement throughout the duration of my educations.

Chompoonuch Tancharoen

April, 2012

**TABLE OF CONTENTS**

	<b>Page</b>
TABLE OF CONTENTS	i
LIST OF TABLES	ii
LIST OF FIGURES	iii
LIST OF ABBREVIATIONS	vi
INTRODUCTION	1
OBJECTIVES	10
LITERATURE REVIEW	11
MATERIALS AND METHODS	17
RESULTS AND DISCUSSIONS	26
CONCLUSION	43
LITERATURE CITED	44
APPENDICES	51
Appendix A $IC_{50}$ for HIV-1RT assay	52
Appendix B NMR and Mass Spectrum	54
Appendix C Theoretical Background	70
Appendix D Oral and Poster Presentation	77
CURRICULUM VITAE	81

## LIST OF TABLES

<b>Table</b>		<b>Page</b>
1	List of Thai Dipterocarpaceous family plants from Khonkaen.	3
2	Structures of resveratrol derivatives and experimental biological activities against the aromatase enzyme.	25
3	Extracted compounds and weight are extracted from the stem bark of <i>Shorea siamensis</i> Miq.	27
4	Determination of IC <sub>50</sub> values of Anigopreissin A, Gnetin C, Hopeafuran, New resveratrol and Nevirapine against HIV-1 RT	30
5	GOLD Scores of Nevirapine, Gnetin C, Anigopressin A, Hopeafuran and New resveratrol trimers in wild type HIV-1 RT.	32
6	Partial interaction energies (kcal/mol) of Nevirapine, Gnetin C, Anigopressin A and New resveratrol trimmer with individual residues, calculated by the M062x/6-31G(d,p) level compared with reference.	38
7	Partial interaction energies (kcal/mol) of Nevirapine, Gnetin C, Anigopressin A and New resveratrol trimmer with individual residues, calculated by the M062x/6-31G(d,p) level with BSSE-CP and compared with reference.	39
<b>Appendix Table</b>		
B1	Spectroscopic data of New resveratrol trimer.	61

## LIST OF FIGURES

<b>Figure</b>		<b>Page</b>
1	Structure of resveratrol.	1
2	Percent inhibition of HIV-1 RT of 14 samples from Thai Dipterocarpaceae plants.	4
3	Bounded structure of NNRTI in HIV-1 RT.	6
4	Chemical structure of NNRTIs.	7
5	Ribbon representation of the active site. The p66 and p51 subunits of HIV-1 RT are colored red and blue.	8
6	Chart diagram for isolation and extraction the stem bark.	19
7	Adopted model system of Nevirapine bound to the HIV-1 RT binding site.	22
8	Structure of the HIV-1 RT heterodimer in complex with Nevirapine (atom-type color) (PDB code 1VRT).	31
9	Orientation of Nevirapine in HIV-1 RT binding pocket (PDB code 1VRT). Geometries obtained from X-ray (yellow color) and docking (atomtype color) using GoldScore fitness function.	32
10	Docked orientations of Nevirapine (yellow) compared with orientations of New resveratrol trimers (blue), Anigopressin A (orange), Gnetin C (green) and Hopeafuran (pink) in wild type HIV-1RT binding pocket by using GoldScore fitness function.	33
11	Docked orientations of Gnetin C in wild type HIV-1RT binding pocket.	35
12	Docked orientations of Anigopreissin A in wild type HIV-1RT binding pocket.	35

## LIST OF FIGURES (Continued)

<b>Figure</b>		<b>Page</b>
13	Docked orientations of Hopeafuran in wild type HIV-1RT binding pocket.	36
14	Docked orientations of New resveratrol trimer in wild type HIV-1RT binding pocket.	36
15	Docked orientations of Nevirapine in wild type HIV-1RT binding pocket.	37
16	Interaction energy with CP correction of Nevirapine, Gnetin C, Anigopressin A and New resveratrol trimmer with individual amino acid surrounding the binding pocket of wild type by the M062x/6-31G(d,p) level.	40
17	Graphical plot between experimental and predicted PIC50 values obtaining from the CoMSIA model.	41
18	Contour maps of CoMSIA model.	42
 <b>Appendix Figure</b>		
B1	<sup>1</sup> H NMR spectrum (Acetone- <i>d</i> 6) of Gnetin C.	55
B2	<sup>1</sup> H NMR spectrum (Acetone- <i>d</i> 6) of Gnetin C (Continued).	56
B3	<sup>1</sup> H NMR spectrum (Acetone- <i>d</i> 6) of Anigopressin A.	57
B4	<sup>1</sup> H NMR spectrum (Acetone- <i>d</i> 6) of Anigopressin A (Continued).	58
B5	<sup>1</sup> H NMR spectrum (Acetone- <i>d</i> 6) of Hopeafuran.	59
B6	<sup>1</sup> H NMR spectrum (Acetone- <i>d</i> 6) of Hopeafuran (Continued).	60
B7	<sup>1</sup> H NMR spectrum (Acetone- <i>d</i> 6) of New resveratrol trimer.	62

**LIST OF FIGURES (Continued)**

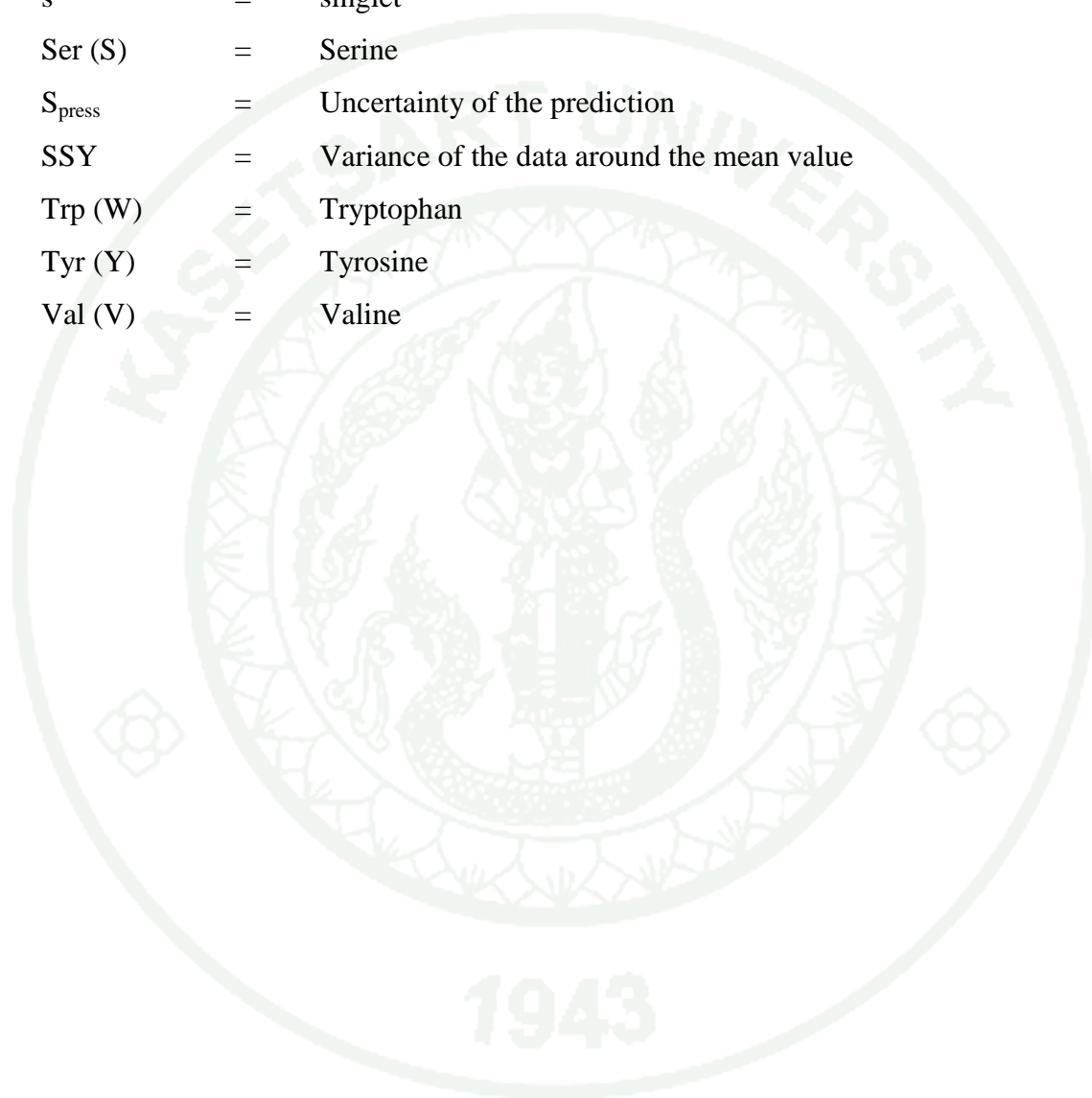
<b>Appendix Figure</b>		<b>Page</b>
B8	<sup>1</sup> H NMR spectrum (Acetone- <i>d</i> <sub>6</sub> ) of New resveratrol trimer (Continued).	63
B9	<sup>13</sup> C-NMR spectrum (Acetone- <i>d</i> <sub>6</sub> ) of New resveratrol trimer (Continued).	64
B10	DEPT 90 and 135 spectrum (Acetone- <i>d</i> <sub>6</sub> ) of New resveratrol trimer.	65
B11	HMBC spectrum (Acetone- <i>d</i> <sub>6</sub> ) of New resveratrol trimer.	66
B12	HSQC spectrum (Acetone- <i>d</i> <sub>6</sub> ) of New resveratrol trimer.	67
B13	ROESY spectrum (Acetone- <i>d</i> <sub>6</sub> ) of New resveratrol trimer	68
B14	Mass Spectrum of New resveratrol trimer.	69
C1	Key flowchart for all docking protocols.	72
C2	Gaussian-type functional form of CoMSIA field defines a significantly smoother distance dependence compared to the Lennard-Jones and Coulomb potential of CoMFA field.	74
C3	Cross-validated procedure.	76

## LIST OF ABBREVIATIONS

AIDS	=	Acquired immunodeficiency syndrome
B3LYP	=	Becke's three parameter hybrid functional using the LYP correlation functional
br	=	broad
CoMFA	=	Comparative molecular field analysis
CoMSIA	=	Comparative Molecular Similarity Indices Analysis
d	=	doublet
dd	=	doublet of doublets
DFT	=	Density Functional Theory
3D-QSAR	=	Three-dimensional quantitative structure-activity relationship
Glu (Q)	=	Glutamine
Gly (G)	=	Glycine
His (H)	=	Histidine
HIV	=	Human immunodeficiency virus
Ile (I)	=	Isoleucine
Leu (L)	=	Leucine
Lys (K)	=	Lysine
M06-2X	=	Meta exchange correlation function with 54% of Hartree–Fock exchange
MP2	=	The second-order Møller-Plesset perturbation theory
NNRTIs	=	Non-nucleoside reverse transcriptase inhibitors
NRTIs	=	Nucleoside reverse transcriptase inhibitors
PDB	=	Protein Data Bank
Phe (F)	=	Phenylalanine
PRESS	=	Prediction error sum of squares
Pro (P)	=	Proline
$r_{cv}^2$	=	Predictive ability of cross-validation
$r_{nv}^2$	=	Predictive ability of non-cross validation

**LIST OF ABBREVIATION (Continued)**

rmsd	=	Root mean square deviation
Rnase H	=	ribonuclease H
s	=	singlet
Ser (S)	=	Serine
S <sub>press</sub>	=	Uncertainty of the prediction
SSY	=	Variance of the data around the mean value
Trp (W)	=	Tryptophan
Tyr (Y)	=	Tyrosine
Val (V)	=	Valine



# EXPERIMENTAL AND THEORETICAL STUDIES ON RESVERATROL OLIGOMER COMPOUNDS FROM THE BARK OF DIPTEROCARPACEAE FAMILY AGAINST HIV-1 REVERSE TRANSCRIPTASE

## INTRODUCTION

The family of Dipterocarpaceae is mainly tropical lowland rainforest tree in Southeast Asia (Abe *et al.*, 2010), consisting of 17 genera which are *Anisoptera*, *Cotylelobium*, *Dipterocarpus*, *Dryobalanops*, *Hopea*, *Marquesia*, *Monotes*, *Neobalanocarpus*, *Pakaraimaea*, *Parashorea*, *Pseudomonotes*, *Shorea*, *Stemonoporus*, *Upuna*, *Vateria*, *Vateriopsis* and *Vatica*, and it also has approximately 600 species. Recently, the structural variations in these genera have been examined and about 120 new resveratrol oligomers have been reported (Ito, 2011). In Thailand, Dipterocarpaceae family is known as Yang-na, Ka-bag, Rang and Teng plants. This family produces a wide variety of natural products such as terpenoids, flavonoids, arylpropanoids and oligomer resveratrol (Wan Zuraida *et al.*, 2010). These oligomers derive from the resveratrol monomer (Saroyobudiono *et al.*, 2008). So, plants of this family have variety bioactive compounds which functionalized as antialzheimer, antibacterial, antiviral, and cytotoxicity (Ito *et al.*, 2004; Vingtdoux *et al.*, 2008).

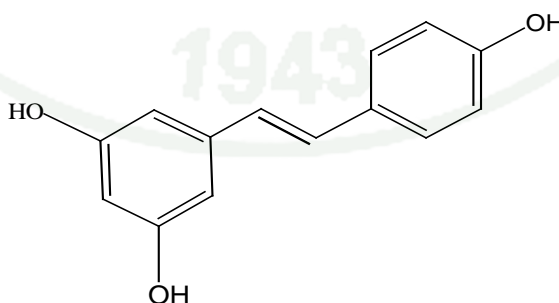


**Figure 1** Structure of resveratrol.

The resveratrol is the first member of the Shikimic path way via polymerization of stilbene. Resveratrol (3,5,4'-trihydroxystilbene) (Figure 1) consists of two phenolic rings linked by a styrene double bond to generate 3,4',5, - trihydroxystilbene (Aggarwal *et al.*, 2004). It was first isolated from the roots of the white *hellebore lily Veratrum* O.Loos since 1940. Then, in 1963, there was reported that resveratrol can be also extracted from the roots of *Polygonum cuspidatum*, a plant used in traditional Chinese and Japanese medicine (Baur and Sinclair, 2006, Sun *et al.*, 2010).

Nowadays, people pay more attention about healthy and cure a sickness with natural route because natural drugs have safer than chemical drugs. So, this work aimed to extract the resveratrol compounds from Thai Dipterocarpaceous family plants consisting 14 samples of crude extraction from Khonkaen province, Thailand as shown in Table 1 and then to screen their biological activities against HIV-1 reverse transcriptase bioassay as shown preliminary test of HIV-1 RT percent inhibition in Figure 2. The experiments provide that a crude extraction from *Shorea siamensis* Miq. (sample 12) locally known as “Rang” in Thailand, shows high anti HIV-1 RT activity. This plant is a deciduous and medium to large-sized tree widely distributed in many parts of Thailand.

Moreover, the theoretical parts using molecular docking and quantum chemical calculations will also be performed to find the orientation and particular interaction of the inhibitor and binding site of HIV-1 RT.

**Table 1** List of Thai Dipterocarpaceous family plants from Khonkaen.

Sample	Name	Year
1	<i>Dipterocarpus alatus</i> Roxb. (yang-na)	80
2	<i>Dipterocarpus alatus</i> Roxb. (yang-na)	200
3	<i>Dipterocarpus alatus</i> Roxb. (yang-na)	70
4	<i>Dipterocarpus alatus</i> Roxb. (yang-na)	100
5	<i>Dipterocarpus alatus</i> Roxb. (yang-na)	30
6	<i>Dipterocarpus turbinatus</i> Gaertn. f. (yang-dang)	60
7	<i>Dipterocarpus tuberculatus</i> Roxb. (yang-plung)	30
8	<i>Dipterocarpus obtusifolius</i> Teijsm. ex Miq. (yang-hiang)	35
9	<i>Shorea roxburghii</i> G. Don. (pa-yom)	30
10	<i>Dipterocarpus baudii</i> Korth. (yang-khon)	30
11	<i>Anisoptera costata</i> Korth. (yang-khao)	20
12	<i>Shorea siamensis</i> Miq. (rang)	30
13	<i>Shorea obtusa</i> Wall. (teng)	30
14	<i>Dipterocarpus turbinatus</i> Gaertn. f. (yang-dang)	70

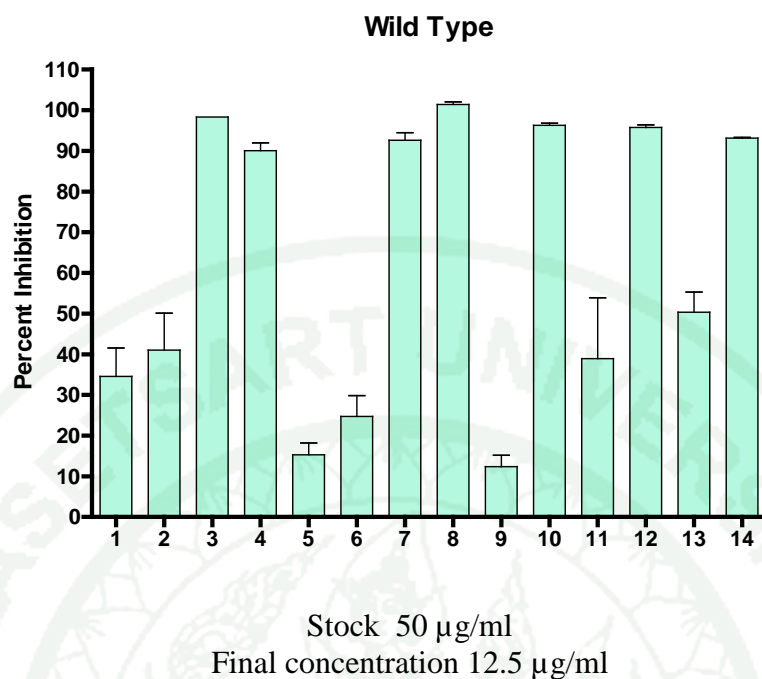


**Figure 2** Percent inhibition of HIV-1 RT of crude extraction from 14 Thai Dipterocarpaceae plants.

### Acquired Immunodeficiency Syndrome (AIDS)

Acquired Immunodeficiency Syndrome (AIDS) is an infectious and fatal disease that has spread throughout many parts of the world, especially in Africa and Southeast Asia (Silprasit et al., 2011a). AIDS caused by Human Immunodeficiency Virus (HIV) which is divided two types including HIV-1 and HIV-2. HIV-1 is more widespread than HIV-2 which is prevalent in individuals at West Africa (Rambaut et al., 2004). Herein, this study was focused on the HIV-1 which has been present therapies based on the inhibition of two key viral enzymes: HIV reverse transcriptase (RT) and HIV protease (PI) as well as the inhibition of viral fusion (Sahlberg and Zhou, 2008).

## HIV-1 Reverse Transcriptase

HIV-1 RT consists of two subunits including p66 and p51, both having the same N terminus. Subunit p66 is larger (p66 has 560 amino acid residues and p51 has 440 residues) and resembles the human right hand. Its domains have been termed fingers (residues 1–85, 118–155), palm (86–117, 156–237), thumb (238–318), connection (319–426) and RNase H (427–554) (Jaeger *et al.*, 1998). In the palm of the p66 subdomain is the polymerase active site, whereas near the finger domain is the RNase H sub domain (Figure3). The two main activities of RT are polymerization and ribonuclease H activity.

In general, the inhibitors of HIV-1 RT are classified into two main categories: nucleoside/nucleotide inhibitors (NRTIs) and non-nucleoside inhibitors (NNRTIs), depending upon their mechanism of action. NRTIs are substrate analogs of normal nucleotides that act competitively at the catalytic site of HIV-1 RT and terminating DNA synthesis, whereas NNRTIs are chemically diverse groups of compounds that noncompetitively bind to the unique allosteric hydrophobic binding pocket located about 10 Å away from the catalytic site (Sahlberg and Zhou, 2008); Shen *et al.*, 2003). Moreover, NNRTIs are a group of small (<600 Da) hydrophobic compounds with diverse structures that specifically inhibit HIV-1 RT, but not HIV-2 RT (De Clercq, 1998).

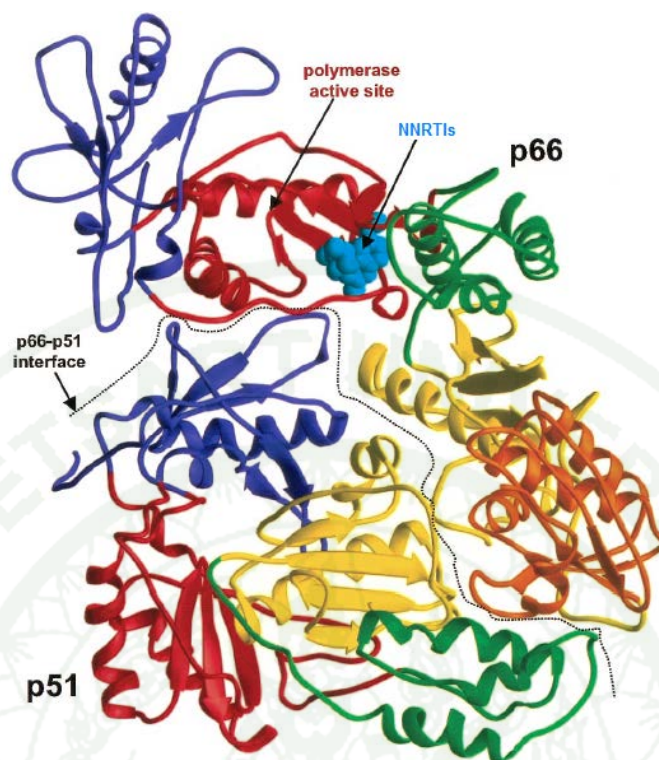


**Figure 3** Bounded structure of NNRTI in HIV-1 RT.

The structure of HIV-1 RT is bounded with NNRTI. The p66 subunit is on the upper right; the p51 subunit is on the lower left. The interface between the subunits is shown by a dotted line. The individual subdomains of the two subunits are color coded: blue, fingers; red, palms; green, and thumbs; yellow, connection domains. The RNase H domain is gold and the NNRTI (HBY) is cyan color. The approximate position of the polymerase active site is indicated by an arrow. The figure was prepared from the coordinates of Hsiou et al. (ref. 4; Protein Data Bank ID code 1BQM) (Hughes, 2001) as shown in Figure 3.

Treatments of HIV-1 RT infection, patients are normally advised to continue taking medication for longer durations to subside the viral load and to improve the blood count of CD4+ T-lymphocyte cells. However, the researchers have also studied intensively to find new drugs for safer anti-HIV-1 molecules that are cost effective and with few or no toxic effects in patients.

Nowadays, FDA has been approved 12 drugs therapy that used in clinic to inhibit HIV-1 RT. The non-nucleoside reverse transcriptase has been interested for the clinical, because it is over advantage than NRTIs. According to the several report, NNRTIs perform as noncompetitive inhibitor by binding to one specific pocket of the enzyme as well-known as hydrophobic pocket. It is a chemically diverse class of compound that composes of over 50 classes of compound. Now, there are four NNRTIs such as nevirapine, delavirdine, efavirenz and etravirine that have been improved and used in clinical as shown in Figure 4 (Marie-Pierre, 2010).

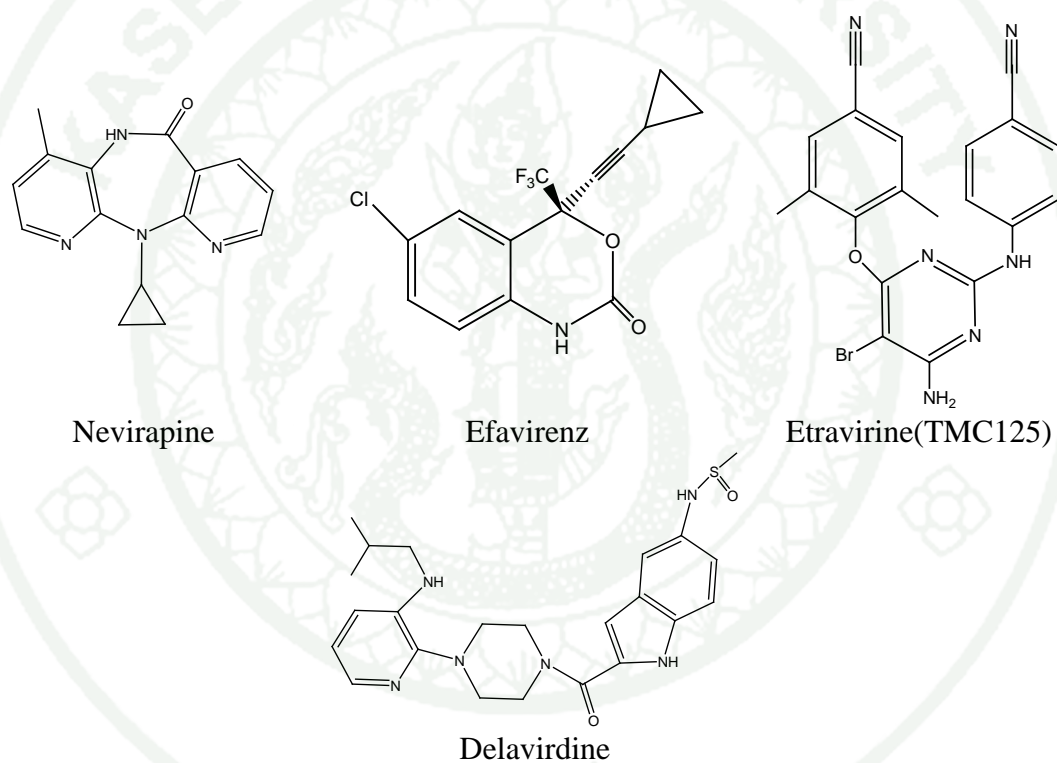


**Figure 4** Chemical structure of NNRTIs (Marie-Pierre, 2010).

### HIV-1 RT active site and Binding Pocket

It is believed that p51 plays a role in maintaining the overall structure of the RT. The p66 finger and thumb domains are rather flexible and the nucleic acid template and primer are bound in this cleft passing between the fingers and in front of the thumb domain. When dNTP is bound to the complex, the fingers bend towards the

palm forming a catalytic pocket. Actually, HIV-1 RT has 3 areas that are considerable for the active site including DNA polymerase active site, non-nucleoside inhibitor binding pocket (NNIBP) and RNase H active site. In this work, NNIBP was focused which is hydrophobic region and it can be interacted with non-nucleoside inhibitor. This pocket is located on the palm subdomain and surrounded by several stranded  $\beta$ -sheets (Sahlberg and Zhou, 2008). It lies near the DNA polymerase active site, polymerase primer grip and the base of thumb subdomain, which serve as the hinge for the movement of the thumb. The suitable location of this pocket is 10 Å away from the DNA polymerase active site and 60 Å away from the RNase H active site as shown in Figure 5 (Sluis-Cremer and Tachedjian, 2008).

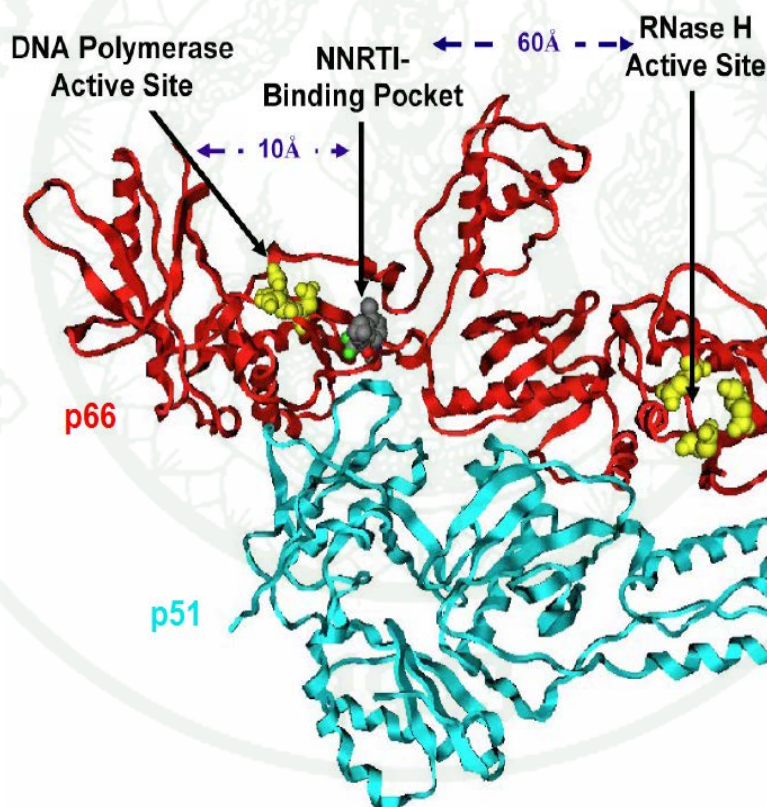
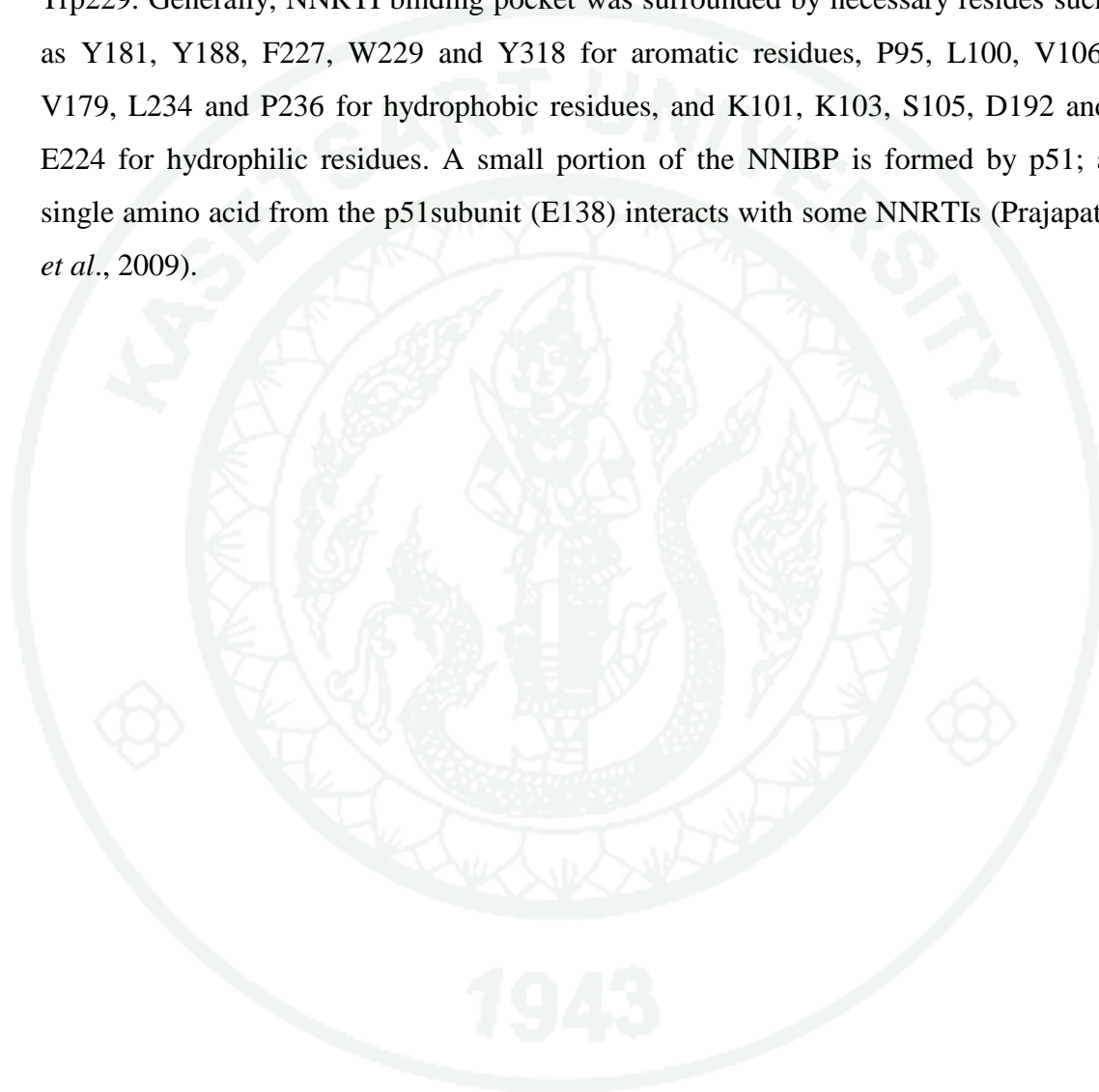


**Figure 5** Ribbon representation of the active site. The p66 and p51 subunits of HIV-1 RT are colored red and blue, respectively (Sluis-Cremer and Tachedjian, 2008).

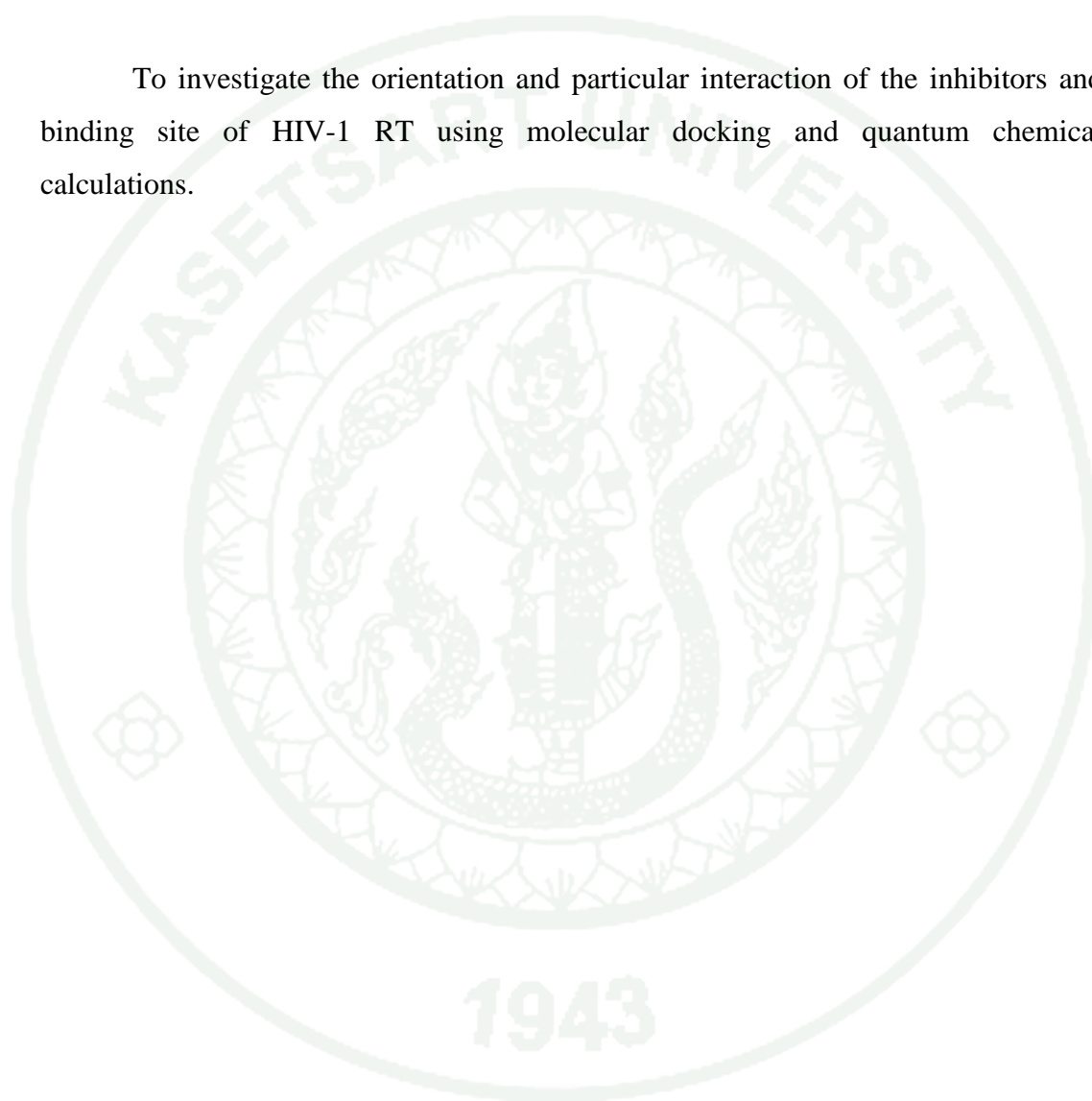
The residues in the NNIBP contribute at a varied degree to the affinity between the inhibitor and the enzyme. Some aromatic residues are crucial and play an important role in a majority of the NNRTIs that have hydrophobic  $\pi$ -interactions with  $\pi$ -electron containing components of the inhibitors such as Tyr181, Tyr188 and Trp229. Generally, NNRTI binding pocket was surrounded by necessary residues such as Y181, Y188, F227, W229 and Y318 for aromatic residues, P95, L100, V106, V179, L234 and P236 for hydrophobic residues, and K101, K103, S105, D192 and E224 for hydrophilic residues. A small portion of the NNIBP is formed by p51; a single amino acid from the p51 subunit (E138) interacts with some NNRTIs (Prajapati *et al.*, 2009).



## OBJECTIVES

To extract the natural bioactive compounds from the bark of Dipterocarpaceae family and screen for HIV-1 RT biological activity inhibitor.

To investigate the orientation and particular interaction of the inhibitors and binding site of HIV-1 RT using molecular docking and quantum chemical calculations.



## LITERATURE REVIEWS

Dipterocarpaceous family plants are widely distributed in Southeast Asia. In Thailand, this family of plant has received much attention as several potential bioactive compounds have been identified.

In 1999, Department of Chemistry, Mahidol University and Program for Collaborative Research in the Pharmaceutical Sciences collaborate with Department of Medicinal Chemistry and Pharmacognosy, College of Pharmacy, University of Illinois at Chicago reported on investigation of resveratrol tetramers, Vattediospyroidol and Vaticaphenol A from stems of *Vatica diospyroides* (plant in the family Dipterocarpaceae). Resveratrol tetramers, Vattediospyroidol and Vaticaphenol A exhibited more potent cytotoxicity against the oral epidermoid carcinoma (KB, EC<sub>50</sub> 1.0 µg/ML), colon cancer (Col2 EC<sub>50</sub> 1.9 µg/ML), and breast cancer (BC1, EC<sub>50</sub> 3.8 µg/ML) cell lines in the in vitro tumor cell panel whereas Vaticaphenol A was displayed as non-cytotoxic constituents (Seo *et al.*, 1999).

In 2004-2006, Sittisombut and coworkers, Faculty of Pharmacy, Silpakorn University, studied Dipterocarpaceae in Thailand, survey of potential products as anti-cancer agents and found that *Dipterocarpus costatus* Gaertn.f. (Yang-pai) and *Hopea odorata* Roxb. (Takian-tong) exhibited potent anti-cancer activity (Sittisombut *et al.*, 2005; Sittisombut *et al.*, 2006).

In 2006, Kaewamatawong and coworkers, Ubon Rajathanee University, extracted phenolic compounds such as stilbene from *Dipterocarpus intricatus* Dyer using ethyl acetate and ethanol. These obtained compounds showed DPPH free radical scavenging activity (Kaewamatawong *et al.*, 2006).

In 2011, Patcharamun and coworkers reported isolation a new resveratrol dimer, Roxburghiol A together with eleven known compounds from the roots of *Shorea roxburghii* (Pha-yom). These compounds were tested cytotoxicity against the human cervical carcinoma (HeLa) and human epidermoid carcinoma (KB). Two known

compounds (compound 8 and 9) exhibited more potent cytotoxicity (KB, IC<sub>50</sub> 6.5, 8.5 µg/ML and HeLa, IC<sub>50</sub> 8.7, 10.1 µg/ML). Whereas other compounds were inactive to both cell (Patcharamun *et al.*, 2011).

Furthermore, resveratrol oligomers in Dipterocarpaceae family have attracted recent much attention as potential bioactivities from different countries. In China 2006, the stem bark of *Hopea exalata* has received considerable attention by Ge and coworkers. Six known compounds were isolated and tested for antifungal activity and inhibitory effects against jack bean urease. Hopeanolin demonstrated antifungal activity in the MIC value range 0.1- 22.5 µg/mL (Ge *et al.*, 2006). In 2008, the ethanol extracts of the stem bark of *Hopea hainanensis* were investigated. The structure of three new polyphenols and one known compound which isolated was elucidated by analysis of the spectroscopic data including single-crystal X-ray spectroscopy and computational methods. Hopeahainol A, the most important compound, showed acetylcholinesterase inhibition with IC<sub>50</sub> value of 4.33 µM (Ge *et al.*, 2008). The next year later, four new oligo stilbenoids, Hopeahainols C-F, and eight known compounds were obtained. All of polyphenols were tested for their radical scavenging and total reducing capacities by measuring their capacity to scavenge the 2, 2-diphenyl-1-picrylhydrazyl (DPPH) radical, anion superoxide radical, and also to induce the reduction of Mo (VI) to Mo (V). Actually, Malibatol A was a known compound, which could be candidate for pharmaceutical use or food additives (Ge *et al.*, 2009).

In Indonesia 2006, Muhtadi and coworkers extracted the tree bark of *Dipterocarpus hasseltii* as Yang-tai in thai plant using acetone. They got a new resveratrol tetramer (Diptoindonesin E), and five known resveratrol oligomers. All of these compounds were tasted cytotoxicity testing. The result showed that Hopeaphenol strongly inhibited murine leukemia P-388 cells (Muhtadi *et al.*, 2006). In the same year, Ito and coworkers isolated three new resveratrol oligomers Cotylelophenol C and Cotylelosides A and B, together with four known glucosides of resveratrol oligomers from the stem of *Cotylelobium lanceolatum* as Kiam in thai plant with acetone (Ito *et al.*, 2006).

In 2008, Sri and colleague investigated *Hopea* which is one of the main genera of Dipterocarpaceae. They isolated seven known compounds which consist of dimer, trimer and tetramer resveratrol from the stem bark of *Hopea odorata* (as Takian-Tong in Thai plant), *H. mengarawan* and *H. nigra*. They got four compounds from *Hopea odorata* (Balanocarpol, Hopeaphenol, Ampelopsin H and Hemlesyanol C). Hopeaphenol showed the highest activity as antioxidant (IC<sub>50</sub> 61.8 µg/mL), whereas Ampelopsin H and Vaticanol B gave the highest cytotoxic effect against HeLa-S3 (LC<sub>50</sub>, 129.72 µg/mL, 92.81 µg/mL) and Raji cell (LC<sub>50</sub>, 34.69 µg/mL, 34.45 µg/mL) (Sri *et al.*, 2008).

In 2009, two new resveratrol trimers, Grandiphenols C and D were isolated from the stem bark of *Dipterocarpus grandiflorus* as Yang-Young in Thai plant. These structure were elucidated by spectral analysis including 1D- and 2D- NMR experiments and by computer-aided molecular modeling (Ito *et al.*, 2009)

In Malaysia 2011, Wibowo and coworkers isolated a new resveratrol trimer, Malaysianol A and five known resveratrol oligomers from the acetone extract of the stem bark of *Dryobalanops aromatic* (as Pim-sean in Thai plant) by combination of vacuum and radial chromatography techniques. These compounds were tested cytotoxicity against HL-60 (human leukemia), MCF-7 (human breast cancer), HepG2 (human hepatocellular liver carcinoma), A-549 (human lung adenocarcinoma epithelial) and WRL-68 (normal liver) cell lines. Compound 4 was found to inhibit very strong the growth of HL-60 cell lines (IC<sub>50</sub> 2.7 µg/mL). Moreover, compounds 3 and compound 4 were also found to display moderate activity against MCF-7 cell line (IC<sub>50</sub> 14.3 and 15.7 µg/mL), while weak activity was shown by against MCF-7 and HepG2 (IC<sub>50</sub> 25.1 and 29.8 µg/mL) (Wibowo *et al.*, 2011a). The later year, three compounds were isolated from the same plant. So, the total compounds were ten which made this plant chemotaxonomic important (Wibowo *et al.*, 2011b).

In India and Sri Lanka, local people have been used the resin of the woody plant *Vateria indica* LINN. (Dipterocarpaceae family) as traditional medicine for sore throat, chronic bronchitis, rheumatism and diarrhea. In 2010, Ito and colleague

investigated the isolation a novel resveratrol dimeric dimer having a C<sub>2</sub>-symmetric structure, Vatriaphenol F, two new O-glucosides of resveratrol oligomers which Vatriosides A (resveratrol dimer) and B (resveratrol tetramer), along with a new natural compound and 33 known compounds including 26 resveratrol derivatives (Ito *et al.*, 2010).

Nowadays, the computational chemistry calculations were used for studying in order to understand detail of interaction or mechanism in the binding pocket of enzymes. In 2007, Billes and colleague investigated the vibrational spectra were recorded; density functional calculations were carried out resulting in the optimized geometry and several properties of trans-resveratrol (3, 5, 4-trihydroxy-transstilbene) of diverse beneficial biological activity. The results showed that the enzymatic methylation and demethylation of these compounds play an important role in the regulation of the formaldehyde concentration in cells (Billes *et al.*, 2007).

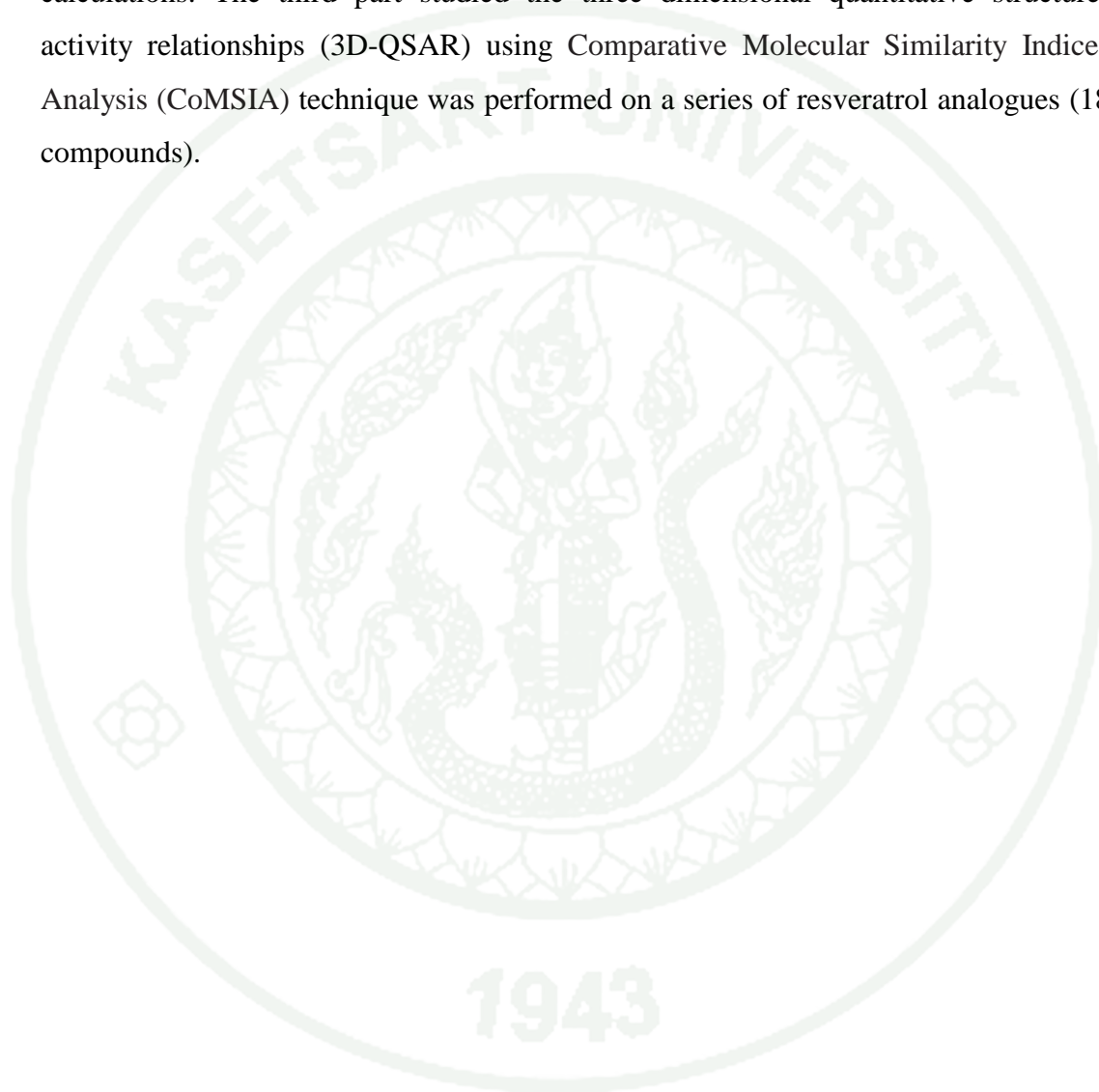
In 2008, Molnár and colleague used quantum chemical calculations which supported the possibility of interaction between resveratrol and HCHO in biological systems in which methoxy and formyl derivatives can be formed. These derivatives can participate in the different beneficial effects of resveratrol. With this, it can be helpful to biochemists to screen compounds which are worth for synthesis (Molnár *et al.*, 2008).

In 2009, the structure–activity relationship has been used to study the determination of antioxidant pharmacophore for resveratrol using quantum chemistry calculations by the Functional of Density Theory. According to the geometry obtained by using a B3LYP/6-31G\*, the HOMO, ionization potential, bond dissociation energies, stabilization energies, and spin density distribution, the electron or hydrogen abstraction in *para* position is more favored than in meta positions for resveratrol and related derivatives because of the resonance effects. Comparison with structurally related compounds revealed that the antioxidant pharmacophore of resveratrol is 4-hydroxystilbene. The results explain the activity difference between resveratrol and its hydroxylated derivatives (Queiroz *et al.*, 2009).

In 2010, quantum calculations based on the density functional theory (DFT) had been employed the relation between the structure and antioxidant activity of resveratrol and derivatives in the gas phase and water environment. The results show that the antioxidant activity of trans-stereo isomers of the compounds considered related to their phenoxy radicals that represent a planar and semiquinone conformation that allows delocalization of the unpaired electron through the whole trans-stilbene skeleton. The obtained results demonstrate that the H-transfer mechanism for scavenging of the free radicals is more preferable than the single-electron transfer in both types of environment (Mikulski et al., 2010).

Moreover, a series of new resveratrol analogues were designed and synthesized and their inhibitory activities against aromatase were evaluated. Since breast cancer is the most commonly diagnosed type of cancer in women and is the second leading cause of death from cancer in women. Estrogens are known to play pivotal role in the cancer cell proliferation. High levels of estrogens promote the progression of breast cancer. Aromatase enzyme catalyzes the rate limiting step in estrogen biosynthesis. This enzyme is an important enzyme responsible for converting androgens to estrogens as a target of other biological interest for the development of new agents for the treatment of breast cancer (Roy and Roy, 2010). Thus, inhibition of the enzyme aromatase is an attractive target for Endocrine treatment of breast cancer depending on hormones. The crystal structure of human aromatase (PDB code 3EQM) was used to rationalize the mechanism of action of the aromatase inhibitor 32 (IC<sub>50</sub> 0.59 μM) through docking, molecular mechanics energy minimization, computer graphics molecular modeling, and the information that was utilized to design several potent inhibitors, including compounds 82 (IC<sub>50</sub> 70 nM) and 84 (IC<sub>50</sub> 36 nM). The aromatase and quinone reductase inhibitors resulting from these studies have potential value in the treatment and prevention of cancer (Sun *et al.*, 2010). From their work, investigation on the three-dimensional quantitative structure activity relationship (3D-QSAR) with synthesized resveratrol analogues were performed for aromatase inhibitory activity using the Comparative Molecular Similarity Indices Analysis (CoMSIA) technique.

So, in this work were divided into three parts. The first part included about isolation of bioactive compounds from the stem bark of *Shorea siamensis* Miq. The second part investigated the orientation and particular interaction of the inhibitors in binding site of HIV-1 RT using molecular docking and quantum chemical calculations. The third part studied the three dimensional quantitative structure-activity relationships (3D-QSAR) using Comparative Molecular Similarity Indices Analysis (CoMSIA) technique was performed on a series of resveratrol analogues (18 compounds).



## MATERIALS AND METHODS

### Extraction and Isolation

#### Dipterocarpaceous Barks

The stem-bark of *Shorea siamensis* Miq. was collected during February-March 2011 from the Sam Sung District, Khon Kaen Province, Thailand. The stem-bark was separated and then left air-dried for 2 weeks and cut into small pieces before being ground into powder.

#### Preparation of Crude Ethanolic Extract

Ground samples were macerated in ethanol for 7 days. The slurry was filtered and the obtained ethanolic extracts were dried by a rotary evaporator under reduced pressure at 40 °C. The dried extracts were tested for biological activities in order to select bioactive extracts for further isolation. The chart diagram for isolation and extraction in this work are shown in Figure 6.

#### Instrumentation

The ethanolic crude extract of the stem-bark of *Shorea siamensis* Miq. was isolated by a medium-pressure liquid chromatography MPLC was perform using a 400 x 40mm (The Lisui, China).

Proton nuclear magnetic resonance ( $^1\text{H}$  NMR) spectra at 500 MHz and carbon nuclear magnetic resonance ( $^{13}\text{C}$  NMR) spectra at 125 MHz were recorded with tetramethylsilane (TMS) or solvent signals as internal references, at 303 K on a Bruker DRX-500 NMR spectrometer at Laboratory of Pharmaceutical Biotechnology School of Medicine, Nanjing University, Nanjing, China. Chemical shifts were recorded as  $\delta$  values in ppm. Coupling constants ( $J$ ) are given in Hz, and

multiplicity is defined as follows: br = broad, s = singlet, d = doublet, dd = doublet of doublets.

The semipreparative HPLC was performed using a 250 x 10mm, 5  $\mu$ m, Hypersil ODS column (Thermo Fisher Scientific, USA) on a Hitachi HPLC system consisting of a L-7110 pump (Hitachi) with a L-7400 UV/Vis Detector (Hitachi) and an Apollo C18 column (5  $\mu$ m, 250 x 4.6 mm; Alltech Associates, Inc. Chicago, IL, USA). Mass spectra were measured on LC-Q instrument at Laboratory of Pharmaceutical Biotechnology School of Medicine, Nanjing University, Nanjing, China.

Mass spectra (MS): EI-MS (direct insertion probe, 70eV) were measured using a Finnigan POLARIS Ion Trap Mass Spectrometer, HR-APCI-MS (direct infusion) were recorded on a Bruker MicroTOF Mass Spectrometer at Chulabhorn Research Institute, Bangkok, Thailand.

## **Chemicals**

Analytical grade ethanol, methanol, acetone, ethyl acetate, chloroform, were purchased from Nanjing Chemical Reagent Co., Ltd., Nanjing. Acetone and chloroform deuteriated solvents for NMR measurement were purchased from Merck, Inc. Analytical TLC was performed on GF254 (10-20 mm) plates with 0.2 mm layer thickness. Column chromatography, Sephadex LH-20 was purchased by Pharmacia Biotech, Uppsala, Sweden and Silica gel (200-300 mesh) was produced by Qingdao Marine Chemical Factory, Qingdao, People's Republic of China.

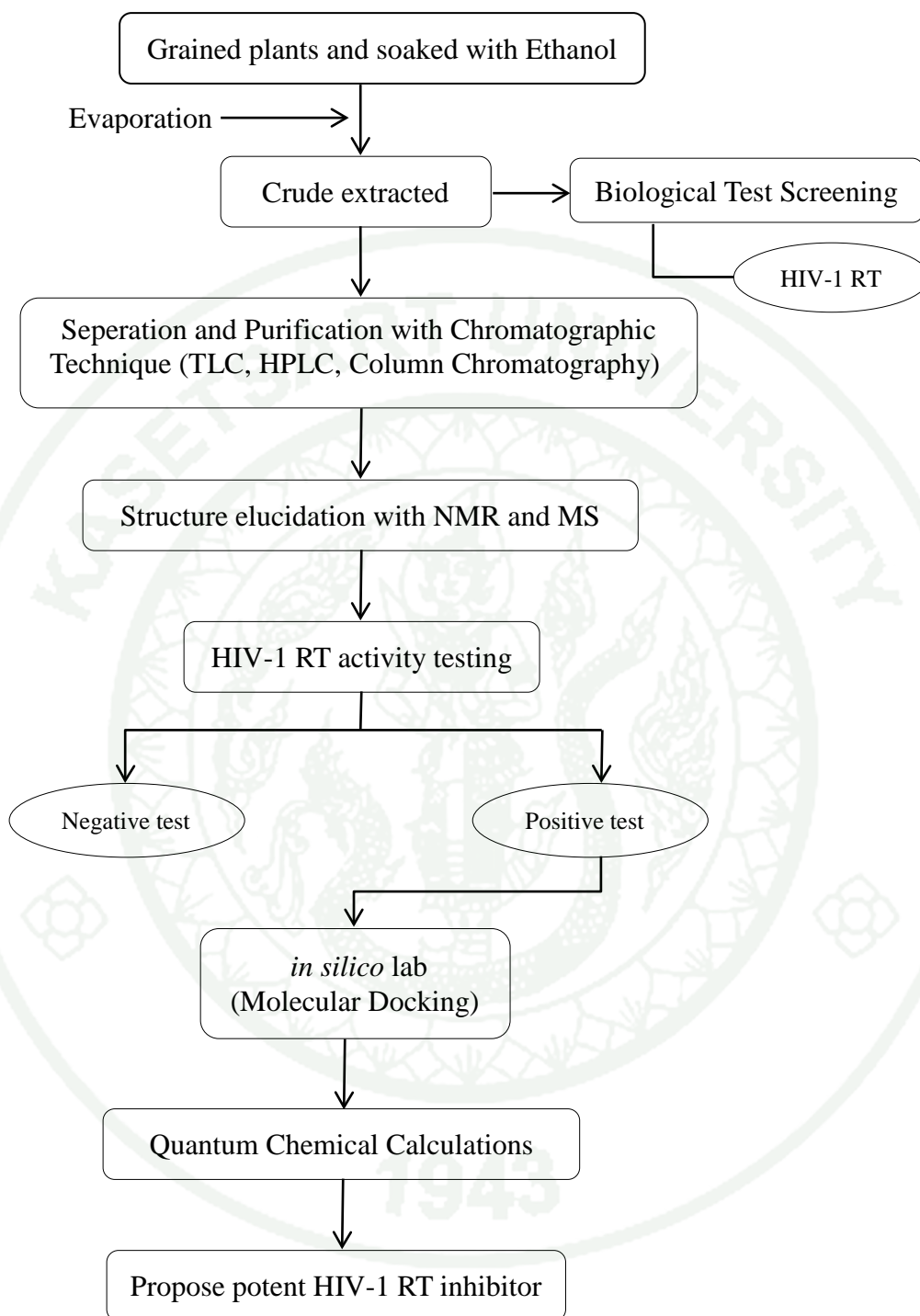


**Figure 6** Chart diagram for isolation and extraction the stem bark.

## Molecular Modeling and Quantum Chemical Calculations

### Molecular Modeling

#### Receptor X-ray structure

The X-ray crystal structure of HIV-1 reverse transcriptase, PDB code 1VRT (resolution = 2.20 Å), in complex with inhibitor Nevirapine (Ren et al., 1995) was recovered from the Protein Data Bank. Although residues of the enzyme were missing from 1 to 3, 444 to 454, 540 to 600 of chain A and 1 to 4, 89 to 91, 216 to 230, 357 to 361 and 429 to 440 of chain B in the enzyme structure, these are not included in the binding site and hence repairing was not done.

#### Ligands Structure

All of the resveratrol derivatives, isolated from the plants and including Nevirapine were docked into the active site of HIV-1 RT using GOLD, version 5.0. The active site was defined based on the bound inhibitor as Nevirapine in a crystal structure. Water molecules were discarded from the pdb file, added hydrogens were reconstructed. For protein, the ligand and water molecules were removed from each structure. All hydrogen atoms were added into the protein structure in order to set the complex to be the neutral molecule.

#### Docking of Nevirapine and Resveratrol Derivatives from Plant

In this work used the molecular docking program GOLD (Genetic Optimisation for Ligand Docking) for virtual ligand screening based on docking, consensus scoring and ranking was employed to generate classes using GOLD score. The GOLD docking was done according to the following step. Initially, theprotein.pdb and ligand.mol2 were downloaded into GOLD program. Then, the binding site was defined as a spherical region which encompasses referent ligand as Nevirapine and the active site within 7.0 Å of each crystallographic ligand atom. For

each ligand, the number of GA run was set to 15 runs. For each independent GA run, the slow speed (most accurate) were selected. This value equates to 100,000 operations. Automatic GA settings (Population size = 100, Selection pressure = 1.1, Number of islands = 5, Niche size = 2, Crossover, Mutation and Migration frequency = 95, 95 and 10, respectively.) were defined and search efficiency was set to 100%. To further speed up the calculations, the GA docking was terminated when the top three solutions were within 1.5 Å RMSD of each other. GOLD scores recorded on each binding mode using a fitness function that accounts for the steric and electrostatic complementarity between the ligand and receptor. The GOLD scoring function includes the terms for hydrogen bonding, van der Waals interaction (vdW) and intramolecular energies. The first ranked solutions of the ligands were taken for further observation of binding orientation and H-bond interactions. In order to validate the method, the Nevirapine was docked back to its binding pocket. Then, resveratrol derivatives (New resveratrol trimmers, Gnetin C, Anigopreissin A and Hopeafuran) were docked into PDB code 1VRT of HIV-1 RT. The docked ligands were saved in mol2 format.

### Particular Interaction

The studied binding pocket included 22 residues are Pro95, Leu100, Lys101, Lys102, Lys103, Lys104, Ser105, Val106, Val179, Ile180, Tyr181, Tyr188, Val189, Gly190, Phe227, Leu228, Trp229, Leu234, His235, Pro236 and Tyr318 of the p66 domain of RT, Glu138 of the p51 domain (Figure 7). Calculations of Nevirapine with concerned 22 residues by Kuno et al. which the backbone atoms of the residue were fixed (Kuno *et al.*, 2006). Then, a partial interaction energies (kcal/mol) of Nevirapine, Gnetin C, Anigopressin A and New resveratrol trimer with individual residues were calculated by the M062x/6-31G (d, p) level. In order to evaluate the intermolecular interaction, using the basis set superposition error (BSSE) based on the counterpoise scheme of Boys-Bernardi as following equation (1).

$$E_{\text{int}}^{\text{CP}}(\text{AB}) = E(\text{AB}^{\text{AB}}) - E(\text{A}^{\text{AB}}) - E(\text{B}^{\text{AB}}) \quad (1)$$

where  $E(AB)$  is the energy of the complex  $AB$  with the basis set of the  $AB$ , while  $E(A^{AB})$  and  $E(B^{AB})$  are the energies of monomer  $A$  and monomer  $B$ , respectively, with the basis set of  $AB$  at their respective geometries adopted from the complex of  $AB$ .

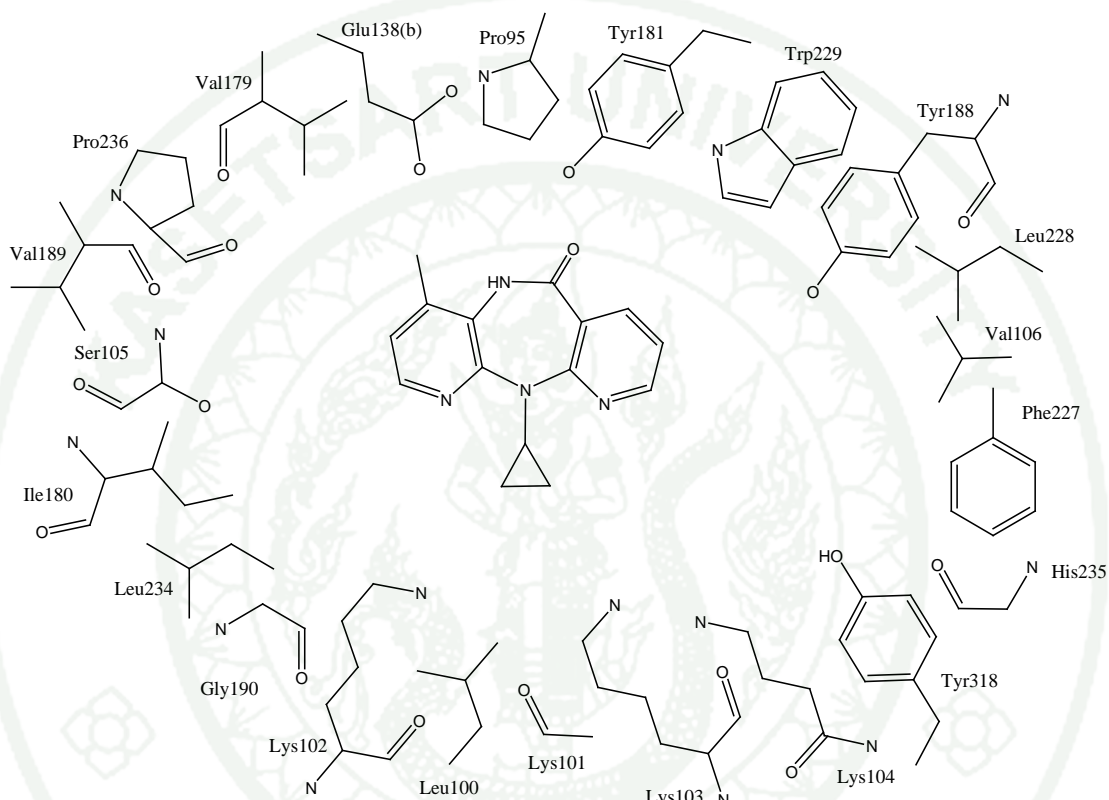


**Figure 7** Adopted model system of Nevirapine bound to the HIV-1 RT binding site.

### Comparative Molecular Similarity Indices Analysis (CoMSIA)

All synthesized resveratrol analogues were tested for aromatase inhibitory activity by Sun and coworkers (Sun *et al.*, 2010); the structures and activities listed in Table 3. The dependent potency values were defined as  $pIC_{50}$ , where  $IC_{50}$  is the concentrations corresponding to 50% inhibition of the human aromatase (CYP19) enzyme. All derivatives were built according to the skeleton template of X-ray structure of resveratrol (PDB code 3EQM) (Ghosh *et al.*, 2009). The processes of structural modifications, optimizations and Gasteiger-Hückel charge calculations were performed on the Sybyl 8.0 program package on a Silicon Graphics Octane2 workstation.

An atom-base superposition alignment of 18 compounds was performed using a common template with 14 aligned positions as marked by asterisks in the structure of the insert figure of Table 2. Then, to calculate CoMSIA descriptors fields, grid spacing with 2 Å was set to generate a cubic lattice around these molecules based on the molecular volume of the structures. It was ensured that the grid extended the molecular dimensions by 4.0 Å in all directions. Molecular interactions between probe atoms and aligned molecules were then calculated. CoMSIA descriptors were computed using a default  $sp^3$  carbon atom with +1 charge served as the probe atom. This model considered the steric, electrostatic, hydrogen-bond donor and acceptor terms.

To obtain 3D-QSAR models, the CoMSIA descriptors, steric, electrostatics, hydrogen bond donor and hydrogen bond acceptor, were used as independent variables and  $pIC_{50}$  values were employed as dependent variables in Partial least square (PLS) regression analysis. The predictive ability of the models was evaluated by leave-one-out (LOO) cross-validation. The analyses were carried out with a maximum of six components, and subsequently, using the number of components (noc) at which the difference in the  $r^2_{cv}$  value to the next one was less than 0.05. Consequently, a non-cross validated analysis was performed using the optimal number of components previously identified and was then employed to analyze the

results (Hannongbua *et al.*, 1999; Maitarad *et al.*, 2009b; Pungpo *et al.*, 2006; Suphavanich *et al.*, 2009).

The predictive ability of the model derived from the training set is expressed as the cross-validation predictive ( $r^2_{cv}$ ) value. The  $r^2_{cv}$  value is defined as

$$r^2_{cv} = 1.0 - \frac{PRESS}{SSY} \quad (2)$$

where SSY represents the variance of the biological activities of molecule around the mean value and PRESS is the prediction error sum of squares derived from the leave-one-out (LOO) method.

$$PRESS = \sum y (y_{pred} - y_{actual})^2 \quad (3)$$

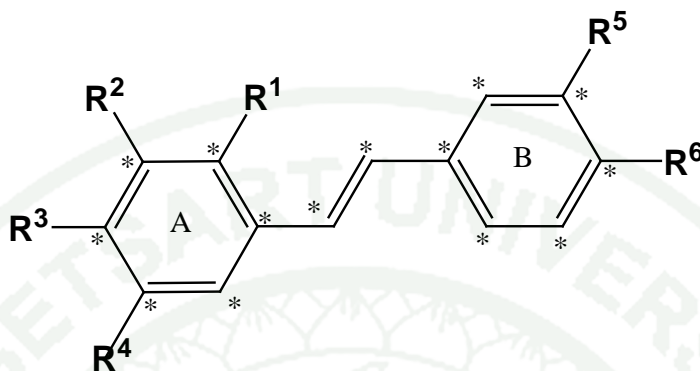
$$SSY = \sum y (y_{actual} - y_{mean})^2 \quad (4)$$

The uncertainty of the prediction is defined as

$$S_{PRESS} = \sqrt{\frac{PRESS}{n - k - 1}} \quad (5)$$

where  $k$  is the number of variables in the model and  $n$  is the number of compounds used in the study (Maitarad *et al.*, 2009a; Thengyai *et al.*, 2010).

**Table 2** Structures of resveratrol derivatives and experimental biological activities against the aromatase enzyme.



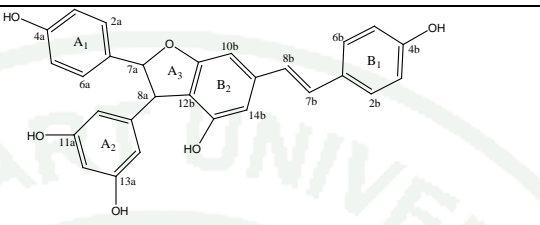
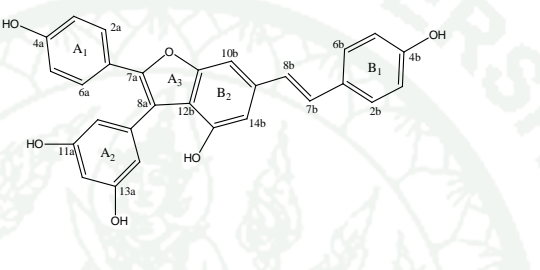
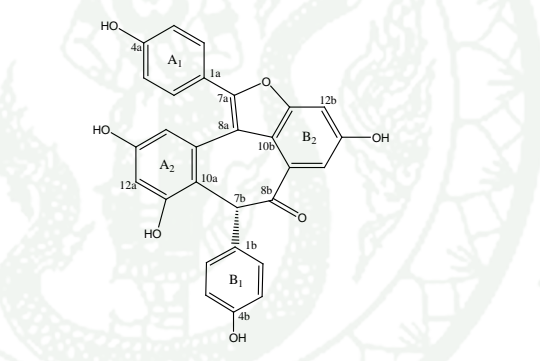
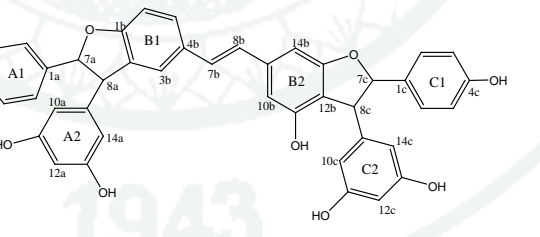
No.	R <sup>1</sup>	R <sup>2</sup>	R <sup>3</sup>	R <sup>4</sup>	R <sup>5</sup>	R <sup>6</sup>	IC <sub>50</sub> ( $\mu$ M)	pIC <sub>50</sub>
1	H	OCH <sub>3</sub>	H	OCH <sub>3</sub>	H	NH <sub>2</sub>	0.59	6.2291
2	OCH <sub>3</sub>	H	OCH <sub>3</sub>	H	H	NH <sub>2</sub>	0.76	6.1192
3	OCH <sub>3</sub>	H	OCH <sub>3</sub>	H	NH <sub>2</sub>	H	11.14	4.9531
4	OCH <sub>3</sub>	H	H	OCH <sub>3</sub>	H	NH <sub>2</sub>	80.94	5.7399
5	OCH <sub>3</sub>	OCH <sub>3</sub>	H	H	H	NH <sub>2</sub>	91.22	6.0088
6	H	OCH <sub>3</sub>	OCH <sub>3</sub>	H	H	NH <sub>2</sub>	78.93	4.8383
7	H	OCH <sub>3</sub>	OCH <sub>3</sub>	OCH <sub>3</sub>	NH <sub>2</sub>	H	83.5	4.7846
8	H	OCH <sub>3</sub>	OCH <sub>3</sub>	OCH <sub>3</sub>	H	NH <sub>2</sub>	0.90	6.0458
9	OCH <sub>3</sub>	OCH <sub>3</sub>	OCH <sub>3</sub>	H	H	NH <sub>2</sub>	3.57	5.4473
10	OCH <sub>3</sub>	OCH <sub>3</sub>	H	OCH <sub>3</sub>	H	NH <sub>2</sub>	2.28	5.6421
11	H	-OCH <sub>2</sub> O-	H	H	NH <sub>2</sub>	H	21.86	4.6604
12	H	-OCH <sub>2</sub> O-	H	H	H	NH <sub>2</sub>	8.49	5.0711
13	H	H	NO <sub>2</sub>	H	NO <sub>2</sub>	H	8.33	5.0794
14	H	OCH <sub>3</sub>	H	H	H	NH <sub>2</sub>	3.08	5.5114
15	H	NH <sub>2</sub>	H	H	H	NH <sub>2</sub>	7.47	5.1267
16	H	NH <sub>2</sub>	H	NH <sub>2</sub>	H	NH <sub>2</sub>	8.51	5.0701
17	H	OAc	H	OAc	H	NH <sub>2</sub>	2.94	5.5316
18	H	OH	H	OH	H	NH <sub>2</sub>	5.00	5.3010

## RESULTS AND DISCUSSIONS

### Extraction and Isolation of Bioactive Compounds against HIV-1 Reverse Transcriptase

One kilogram of dried powdered bark was macerated with ethanol at room temperature for a period of 7 days. After filtration, the process was repeated three times using 2.5 L methanol each time. The slurry was filtered and the obtained ethanolic extract was dried with a rotary evaporator under reduced pressure at 40 °C. The dried extract (200 g) was prepared by grinding and dissolved in methanol, mixed with silica gel (400 g), then dried in hot air oven at 60 °C for 1 day. The sample was separated using C18 medium-pressure liquid chromatography (MPLC). Then, ethanolic extract with silica gel was subject onto a glass column packed with silica gel (200-300 mesh) on the top of columns (2 columns of (500 mm x 50 mm i.d.) and 500 mm x 50 mm i.d.). The extract was eluted with different proportions of mixture of dichloromethane–methanol (100:0, 100:5, 100:10, 100:20, 100:30, 100:50, 0:100) with a gradient pump at a flow rate of 45ml/min and eluent was detected at 254 nm with a UV detector. Eluent was collected in bottles of 500 ml with an automatic fraction collector and analyzed by TLC to give a total of 128 fractions. Fraction number 4-7 was purified using SephadexLH-20 eluted with MeOH to afford compound Gnetin C ( $C_{28}H_{22}O_6$ , Mw: 454) and Anigopreissin A ( $C_{28}H_{20}O_6$ , Mw: 452). Using the same methodology for fraction number 10-11 to get 2 compounds, Hopeafuran,  $C_{28}H_{18}O_7$ , Mw: 466 was obtained from RP-18 HPLC-UV with MeOH/H<sub>2</sub>O solution (55:45) and the other compound ( $C_{42}H_{32}O_9$ , Mw: 680) was purified using SephadexLH-20 eluted with MeOH by two times. The compounds from the stem-bark of *Shorea siamensis* Miq. which was isolated and extracted are shown in Table 3.

**Table 3** Structures and molecular weight of compounds from the stem-bark of *Shorea siamensis* Miq.

Compound	Weight
<p>Gnetin C</p> 	0.0357 g.
<p>Anigopreissin A</p> 	0.0241 g.
<p>Hopeafuran</p> 	0.0050 g.
<p>New resveratrol trimer</p> 	0.1225 g.

Gnetin C ( $C_{28}H_{22}O_6$ , Mw: 454) was obtained as brown solids.  $\delta_H$  (500 MHz;  $CD_3COCD_3$ ) 7.44 (1H, d,  $J=8.5$ , CH), 7.21 (1H, d,  $J=8.5$ , CH), 7.10 (1H, d,  $J=16.1$ , CH), 6.98 (1H, d,  $J=16.1$ , CH), 6.85 (1H, d,  $J=8.5$ , CH), 6.84 (1H, d,  $J=8.5$ , CH), 6.70 (1H, br s, CH), 6.59 (1H, br s, CH), 6.24 (1H, t,  $J=2.2$ , CH), 6.17 (1H, d,  $J=2.2$ , CH), 5.39 (1H, d,  $J=4.9$ , CH), 4.39 (1H, d,  $J=4.9$ , CH).

Anigopreissin A ( $C_{28}H_{20}O_6$ , Mw: 452) was obtained as brown solids.  $\delta_H$  (500 MHz;  $CD_3COCD_3$ ) 8.73 (1H, br s, OH), 8.54 (1H, br s, OH), 8.38 (1H, br s, OH), 7.96 (1H, br s, OH), 7.46 (1H, d,  $J=8.8$ , CH), 7.45 (1H, d,  $J=8.5$ , CH), 7.25 (1H, d,  $J=0.8$ , CH), 7.13 (1H, d,  $J=16.3$ , CH), 7.06 (1H, d,  $J=16.3$ , CH), 6.87 (1H, d,  $J=0.8$ , CH), 6.85 (1H, d,  $J=8.5$ , CH), 6.80 (1H, d,  $J=8.8$ , CH), 6.49 (1H, d,  $J=2.2$ , CH), 6.41 (1H, t,  $J=2.2$ , CH).

Hopeafuran ( $C_{28}H_{18}O_7$ , Mw: 466) was obtained as yellow solids.  $\delta_H$  (500 MHz;  $CD_3COCD_3$ ) 7.70 (2H, d,  $J=8.8$  Hz, H-2/6a), 7.34 (1H, d,  $J=2.1$  Hz, H-14b), 7.04 (1H, d,  $J=2.1$  Hz, H-12b), 6.98 (2H, d,  $J=8.8$  Hz, H-3/5a), 6.85 (2H, dd,  $J=8.3$ , 1,3, H-2/6b), 6.55 (2H, d,  $J=8.4$ , H-3/5b), 6.57 (1H, d,  $J=2.6$ , H-12a), 6.70 (1H, d,  $J=2.6$  Hz, H-14a), 6.12 (1H, br s, H-7b), OH {8.92 (1H, br s, H-4a), 8.80 (1H, br s, H-11a), 8.36 (1H, br s, H-13a), 8.00 (1H, br s, H-4b), and 8.80 (1H, br s, H-13b)}.

The New resveratrol trimer was obtained as brown solids.  $\delta_H$  (500 MHz;  $CD_3COCD_3$ ) 7.46 (1H, d,  $J=8.5$ , CH), 7.28 (1H, br s, CH), 7.25 (1H, d,  $J=8.5$ , CH), 7.20 (1H, d,  $J=8.5$ , CH), 7.15 (1H, d,  $J=16.0$ , CH), 7.00 (1H, d,  $J=16.0$ , CH), 6.89 (1H, d,  $J=8.5$ , CH), 6.84 (1H, d,  $J=8.5$ , CH), 6.86 (1H, d,  $J=8.5$ , CH), 6.71 (1H, br s, CH), 6.59 (1H, br s, CH), 6.30 (1H, br s, CH), 6.21 (1H, d,  $J=2.0$ , CH), 6.26 (1H, br s, CH), 6.16 (1H, d,  $J=2.0$ , CH), 5.47 (1H, d,  $J=8.0$ , CH), 5.38 (1H, d,  $J=5.0$ , CH), 4.48 (1H, d,  $J=8.0$ , CH), 4.39 (1H, d,  $J=5.0$ , CH)

### IC<sub>50</sub> value determination

HIV-1 RT activity was tested by Ms. Ratsupa Thammaporn based on biological activity protocol as reported by Silprasit and coworkers (Silprasit *et al.*, 2011b).

IC<sub>50</sub> (50% inhibitory concentration) is an important evidence to study the interaction of NNRTIs to HIV-1 RT. From the result of screening Thai Dipterocarpaceous family plants consisting 14 samples of EtOH crude extraction, the crude with high percent inhibition (up to 70 percent) have been further investigated for the IC<sub>50</sub> values. So, the stem-bark of *Shorea siamensis* Miq. showed strong HIV-1 RT inhibition. Therefore, this plant was selected to isolate compound and determine IC<sub>50</sub> values. Varying concentration of each inhibitor was assayed to test against the HIV-1 RT activity (detailed biological assay for HIV-1 RT testing is shown in Appendix A). The IC<sub>50</sub> values of Gnetin C, Anigopreissin A, Hopeafuran and New resveratrol trimer are shown in Table 4. The results revealed that HIV-1 RT activity in wild-type was inhibited by Anigopreissin A as Nevirapine more than the other compounds. Gnetin C showed a weak biological activity. For K103N HIV-1 RT, Hopeafuran showed the highest inhibition, while Anigopreissin A showed the highest inhibition for against K103N HIV-1 RT. Significantly, both K103N and Y181C HIV-1 RT were inhibited by New resveratrol trimer. So, both Anigopressin A and New resveratrol trimer were found to be interesting inhibitors for wild-type and mutant HIV-1 RT enzymes.

**Table 4** Determination of IC<sub>50</sub> values of Anigopreissin A, Gnetin C, Hopeafuran, New resveratrol trimer and Nevirapine against HIV-1 RT.

Compounds	IC <sub>50</sub> (μM)			
	wild-type	K103N	Y181C	K103N/Y181C
<b>Anigopreissin A</b>	8.04 ± 0.44 <sup>a</sup>	26.54 ± 7.44	15.77 ± 0.29	22.08 ± 0.68
<b>Gnetin C</b>	76.56 ± 19.2	141.8 ± 38.83	69.94 ± 5.95	86.08 ± 10.49
<b>Hopeafuran</b>	19.67 ± 5.17	14.76 ± 4.08	83.3 ± 17.28	60.13 ± 25.22
<b>New resveratrol trimer</b>	12.25 ± 8.94	23.50 ± 3.88	23.25 ± 15.40	22.28 ± 1.65
<b>Nevirapine</b>	7.82 ± 2.66	>250	>250	>250

<sup>a</sup> Standard deviations obtained from triplicate experiments.

For further studies, investigation on wild-type HIV-1 Reverse Transcriptase was focused. Due to the difficulties and economic cost of the experimental methods for determining the structures of enzyme-inhibitor complex, computational method such as molecular docking is a desired approach for predicting putative binding modes. Therefore, molecular docking has considered to explain behavior of inhibitor in binding pocket of the HIV-1 RT.

## Molecular Modeling and Quantum Chemical Calculations of Resveratrol Oligomers

### Docking with HIV-1 RT

#### Validation of docking method

Structures of the HIV-1 RT heterodimer in complexed with Nevirepine is shown in Figure 8. The GOLD program was used for docking of Nevirapine into its binding pocket of HIV-1 RT. The GoldScore function of docked Nevirapine was 62.82. The root mean square deviation (rmsd) of docking conformation was 0.42 for GoldScore comparing to X-ray structure (PDB code 1VRT). The orientations of x-ray structure and docked Nevirapine with GoldScore are shown in Figure 9. Therefore, GoldScore function was found to reproduce the x-ray conformation of Nevirapine with standard deviation of 2.0 Å.

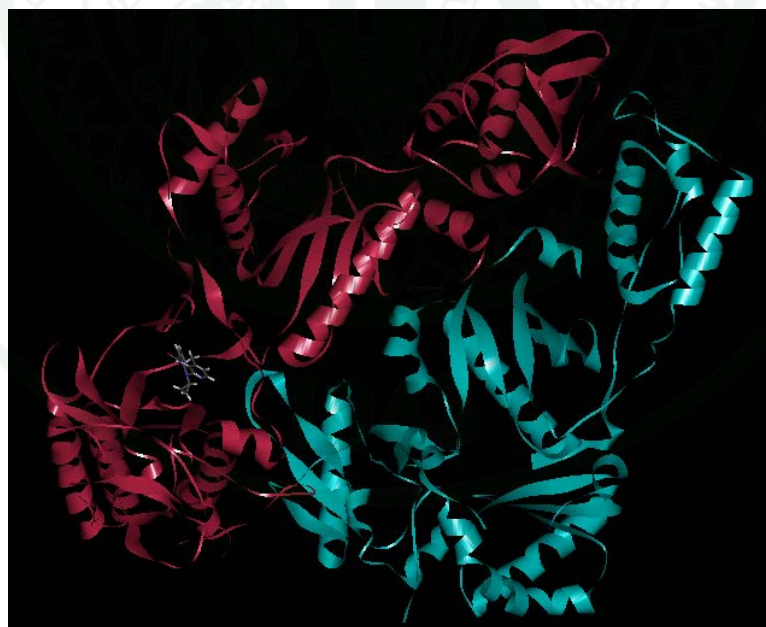


**Figure 8** Structure of the HIV-1 RT heterodimer in complex with Nevirapine (atom-type color) (PDB code 1VRT).

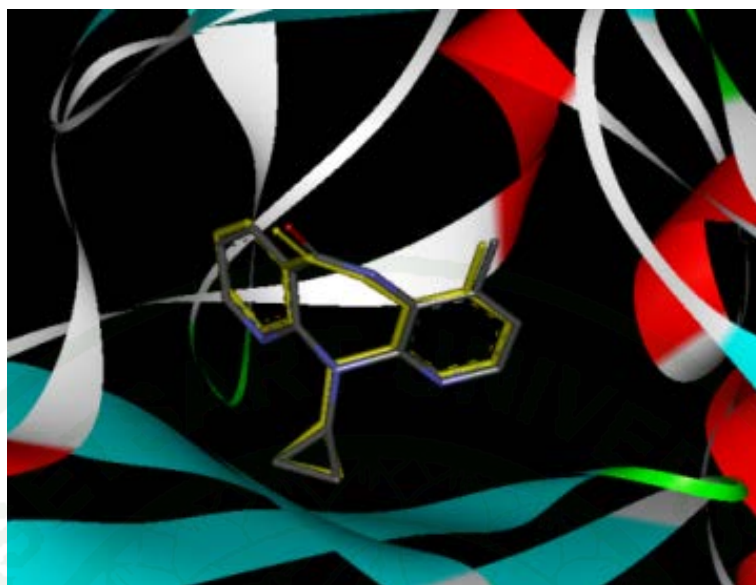


**Figure 9** Orientation of Nevirapine in HIV-1 RT binding pocket (PDB code 1VRT). Geometries obtained from X-ray (yellow color) and docking (atom type color) using GoldScore fitness function.

The overview of the docked conformations of Nevirapine, Gnetin C, Anigopreissin A, Hopeafuran and New resveratrol trimer are shown in Figure 10 and the GOLD Score are shown in Table 5.

**Table 5** GOLD Scores of Nevirapine, Gnetin C, Anigopreissin A, Hopeafuran and New resveratrol trimer in wild-type HIV-1 RT.

Compounds	GoldScore
Nevirapine	62.82
Gnetin C	60.63
Anigopreissin A	65.39
Hopeafuran	19.81
New resveratrol trimer	83.40

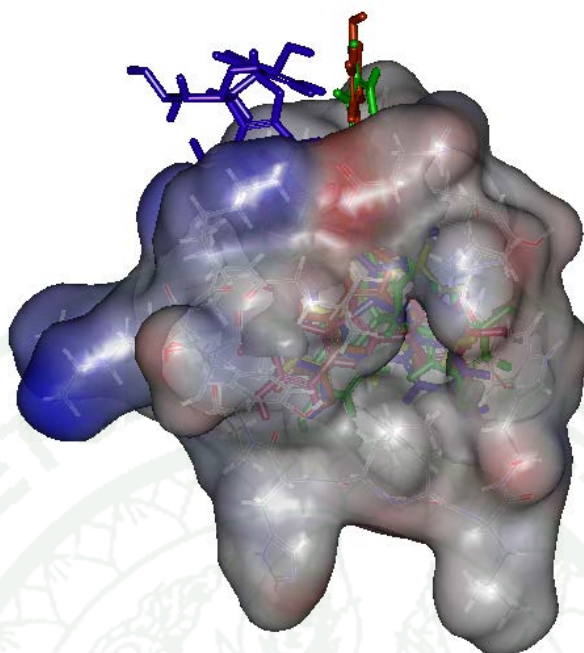


**Figure 10** Docked orientations of Nevirapine (yellow) compared with orientations of New resveratrol trimer (blue), Anigopressin A (orange), Gnetin C (green) and Hopeafuran (pink) in wild-type HIV-1 RT binding pocket by using GoldScore fitness function.

The GoldScore of Anigopressin A and New resveratrol trimer were higher than those of Nevirapine by 2.57 and 20.58 respectively, but Gnetin C and Hopeafuran were lower by 2.19 and 43.01 respectively, in the wild-type binding pocket. From the investigation of H-bond interaction and orientation, all molecules can form in the binding pocket as shown by docking calculations. Moreover, investigation from the particular interaction of docked Nevirapine compared with the result of Nevirapine from reference (Kuno *et al.*, 2006) (Table 6 and Table 7). The partial interaction energy of Nevirapine in this work corresponded to the results of reference, so M06-2x method was accepted.

The result of the partial interaction with BSSE-CP correction of Nevirapine, Gnetin C, Anigopressin A, Hopeafuran and New resveratrol trimer as shown in Table 7 and Figure 16, have attractive interaction less than Nevirapine. Gnetin C formed H-bond (1.983 Å) and  $\pi$ - $\pi$  interaction via phenyl group of Tyr188. Tyr 181 had also

formed  $\pi$ - $\pi$  interaction but steric interaction between phenyl group and aromatic ring A2 of ligand had more effect as shown in Figure 11. Anigopressin A formed H- $\pi$  interaction via Leu100 with side chain as shown in Figure 12. The aromatic ring A2 of Anigopressin A formed strong H-bond interaction with phenyl group of Tyr318 and also formed H-bond interaction with the carbonyl backbone of Pro236. Surprisingly, the structure of Anigopressin A had difference with Gnetin C at only one double bond as displayed in Table 3. IC<sub>50</sub> value showed that Anigopressin A had results close to Nevirapine but Gnetin C had the worse. This is because it might be delocalized electrons of Anigopressin A which could delocalize around molecule but Gnetin C could not. Hopeafuran has more attractive interaction than any other ligands but the IC<sub>50</sub> result was moderate. The important H-bond interaction with side chain of Lys101 by 1.90 Å as shown in Figure 13. Considering structure of Hopeafuran, it was rigid as Nevirapine but was bigger than one. So, the OH functional group of Hopeafuran could bind with amino acid but the steric hindrance in binding pocket would also decrease. New resveratrol trimer formed H-bond interaction with phenyl group of Tyr318 (1.356 and 2.061 Å) and Tyr188 (1.576 Å), backbone oxygen atom of His235 (1.768 Å) and nitrogen atom of side chain (2.663 Å) and backbone (2.820 Å) of Lys103. Moreover, OH group of aromatic ring B2 formed strong H- $\pi$  and cation- $\pi$  interaction via side chain nitrogen atom of Lys101, H- $\pi$  interaction via side chain of Val179 as shown in Figure 14. IC<sub>50</sub> results of New resveratrol trimer corresponded to the result of partial interaction and docking calculations as Nevirapine. Whereas, the results of partial interaction and docking calculations of the other ligands contravened to the experimental IC<sub>50</sub> values.

It is important that the hydrogen bonding between the ligand and Tyr188 play an important role in the binding pocket of the HIV-1 RT by H- $\pi$  interaction via Tyr181 as shown in Figure 15 (He *et al.*, 2005; Kuno *et al.*, 2006; Nunrium *et al.*, 2005). However, in this case, the shape of consequently the steric hindrance for entering the molecule to binding pocket will also decrease. But new resveratrol trimer is interesting compound to develop in Lys103  $\rightarrow$  Asn (K103N) because interaction with Lys103 was better than Nevirapine.

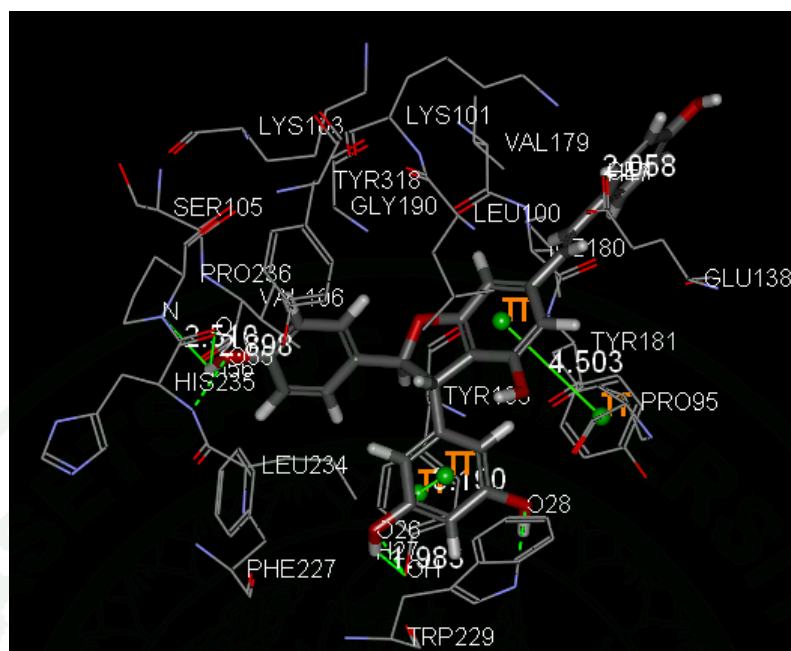


**Figure 11** Docked orientations of Gnetin C in wild-type HIV-1 RT binding pocket.

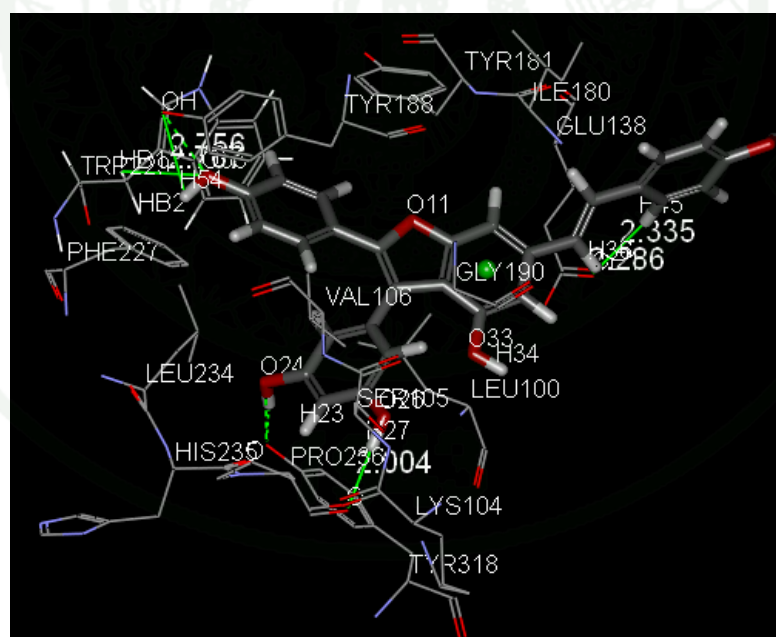


**Figure 12** Docked orientations of Anigopreissina in wild-type HIV-1 RT binding pocket.

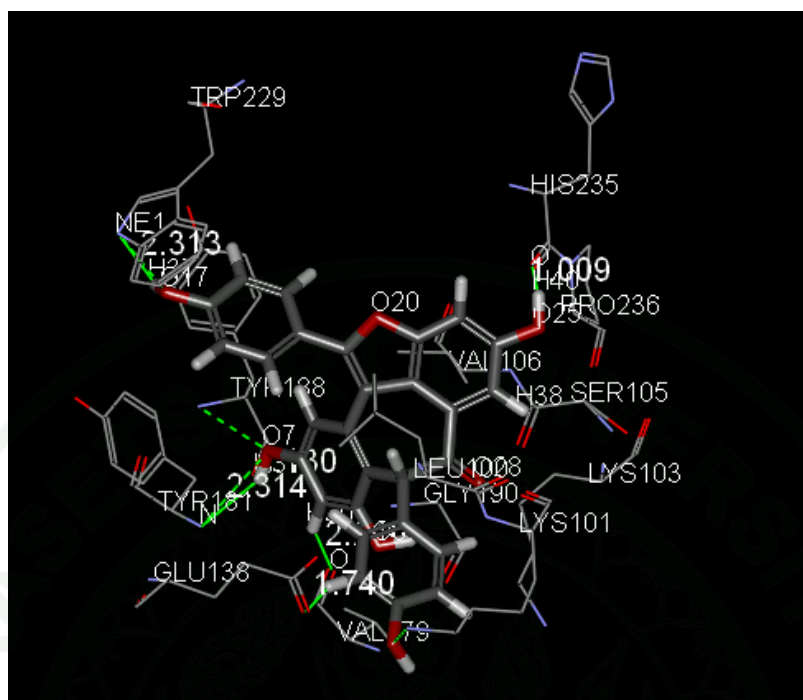


**Figure 13** Docked orientations of Hopeafuran in wild-type HIV-1 RT binding pocket.

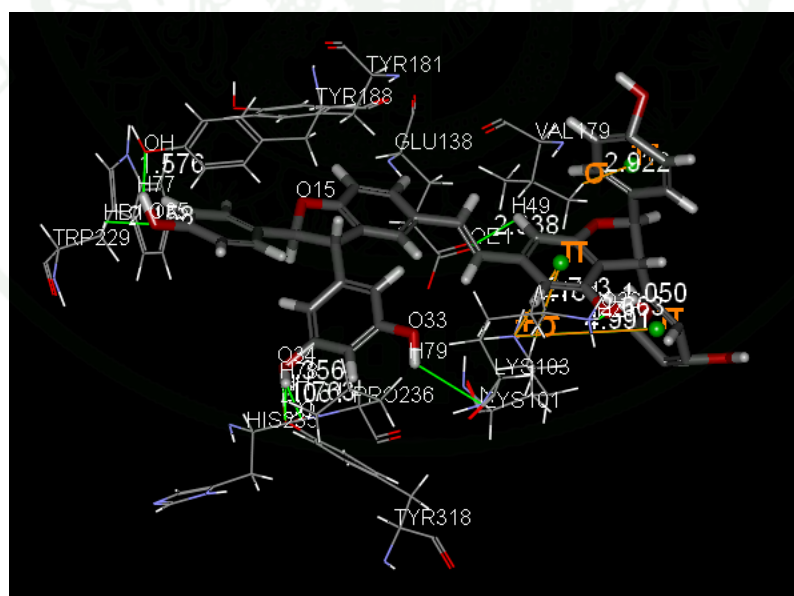


**Figure 14** Docked orientations of New resveratrol trimer in wild-type HIV-1 RT binding pocket.

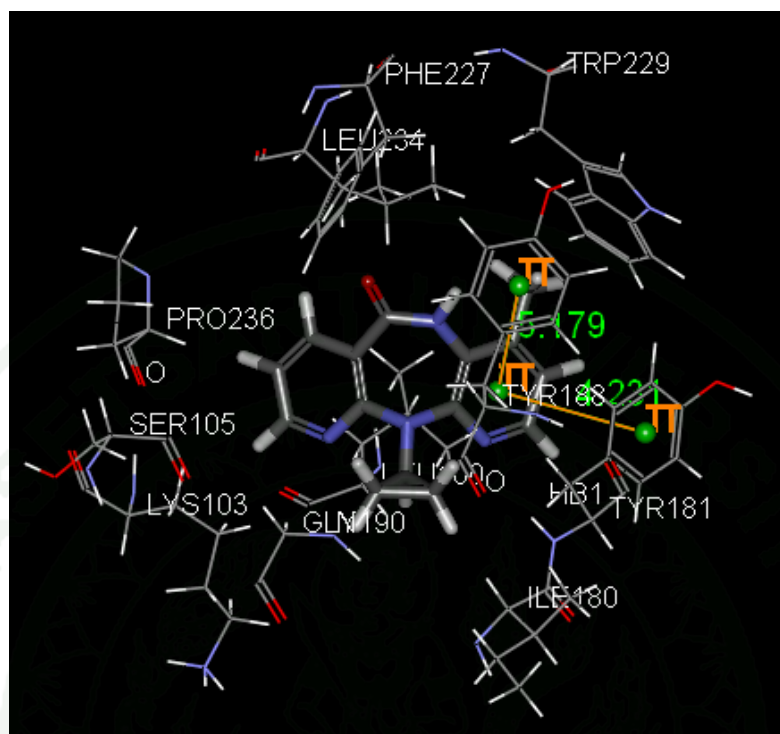


**Figure 15** Docked orientations of Nevirapine in wild-type HIV-1 RT binding pocket.

**Table 6** Partial interaction energies (kcal/mol) of Nevirapine, Gnetin C, Anigopressin A, Hopeafuran and New resveratrol trimmer with individual residues, calculated by the M062x/6-31G(d,p) level of calculations compared with reference.

Residue	Interaction energy (IE, kcal/mol)					
	Gnetin C	Anigopreissin A	Hopeafuran	New resveratrol trimmer	Nevirapine	BBF <sup>a</sup>
PRO095	-1.37	-0.17	-0.14	-0.18	-0.46	-1.39
LEU100	-2.43	7.25	-3.29	0.43	-2.14	-6.58
LYS101	-1.03	0.20	-9.18	-13.20	-1.57	-2.29
LYS102	-0.96	1.17	42.11	2.25	-0.29	-0.58
LYS103	-2.92	0.96	42.11	-5.21	-3.37	-2.04
LYS104	-0.67	-0.51	-1.56	0.92	-0.86	0.02
SER105	0.28	0.24	0.04	0.39	-0.08	-0.16
VAL106	4.18	0.02	-1.41	5.28	-2.53	-2.60
VAL179	-0.43	1.28	27.07	0.89	-0.47	0.41
ILE180	-1.03	-1.09	0.32	-0.38	-0.46	-0.73
TYR181	25.53	-1.79	2.83	3.98	-1.03	-5.14
TYR188	6.36	7.90	106.43	4.78	-5.32	-8.87
VAL189	-0.39	-0.25	-1.75	-0.03	-1.34	-1.14
GLY190	0.08	-0.20	-0.39	-0.24	-0.63	0.07
PHE227	5.72	-0.34	5.72	2.89	-1.51	-2.67
LEU228	-0.71	0.41	0.00	-1.40	-0.12	-0.20
TRP229	13.41	-1.13	17.88	5.04	-2.95	-3.02
LEU234	-1.40	1.17	0.19	2.93	-0.47	-1.21
HIS235	28.87	0.14	71.33	-4.78	-2.18	-4.22
PRO236	7.26	-5.75	24.16	-5.34	-1.39	-2.83
TYR318	-0.67	85.68	88.43	32.64	-1.27	-3.28
GLU138 <sup>b</sup>	-7.25	-9.48	4.25	-6.69	0.07	-0.15
Sum	70.46	85.72	415.14	24.97	-30.36	-48.60

<sup>a</sup> BBF is corrected interaction energy by MP2/6-31G(d,p) level from Kuno *et al.*, 2006

<sup>b</sup> All residues in this study taken from the p66 domain of RT, excepted GLU138 taken from the p51 domain of RT

**Table 7** Partial interaction energies (kcal/mol) of Nevirapine, Gnetin C, Anigopressin A, Hopeafuran and New resveratrol trimmer with individual residues, calculated by the M062x/6-31G(d,p) level with BSSE-CP calculations and compared with reference.

Residue	Interaction energy (IE, kcal/mol)					
	Gnetin C	Anigopressin A	Hopeafuran	New resveratrol trimmer	Nevirapine	BBF <sup>a</sup>
PRO095	-2.72	-0.22	-0.25	-0.38	-0.70	-0.87
LEU100	-4.12	4.90	-5.77	-1.48	-3.41	-3.09
LYS101	-1.03	-1.54	-13.99	-15.35	-2.00	-1.10
LYS102	-0.96	0.76	39.01	2.11	-0.36	-0.37
LYS103	-2.95	-1.43	39.01	-8.45	-3.83	-1.20
LYS104	-0.67	-0.52	-1.56	0.92	-0.86	0.02
SER105	0.28	0.24	0.04	0.39	-0.08	-0.16
VAL106	2.75	-1.15	-2.19	3.60	-4.07	-0.08
VAL179	-1.29	0.15	23.44	-1.86	-1.16	1.47
ILE180	-2.36	-1.52	-0.36	-0.43	-0.69	-0.50
TYR181	21.37	-3.46	-1.67	1.76	-3.70	-2.79
TYR188	1.20	4.17	99.64	0.41	-7.94	-5.05
VAL189	-0.40	-0.25	-3.04	-0.04	-1.83	-0.64
GLY190	0.08	-0.22	-0.86	-0.28	-1.43	1.65
PHE227	4.20	-0.64	4.20	1.29	-2.41	-1.74
LEU228	-0.74	0.41	0.00	-1.59	-0.12	-0.20
TRP229	8.96	-2.97	14.26	2.51	-3.95	-1.19
LEU234	-3.70	-1.43	-1.32	0.35	-1.54	1.22
HIS235	25.60	-2.07	67.39	-7.01	-3.26	-2.39
PRO236	4.71	-8.24	20.64	-7.19	-2.28	-1.63
TYR318	-1.35	81.52	83.10	28.70	-2.47	-1.80
GLU138 <sup>b</sup>	-11.59	-14.64	0.52	-10.56	0.01	-0.09
Sum	35.28	51.86	360.25	-12.57	-48.08	-20.53

<sup>a</sup>BBF is corrected interaction energy by MP2/6-31G(d,p) level from Kuno *et al.*, 2006

<sup>b</sup>All residues in this study taken from the p66 domain of RT, excepted GLU138 taken from the p51 domain of RT

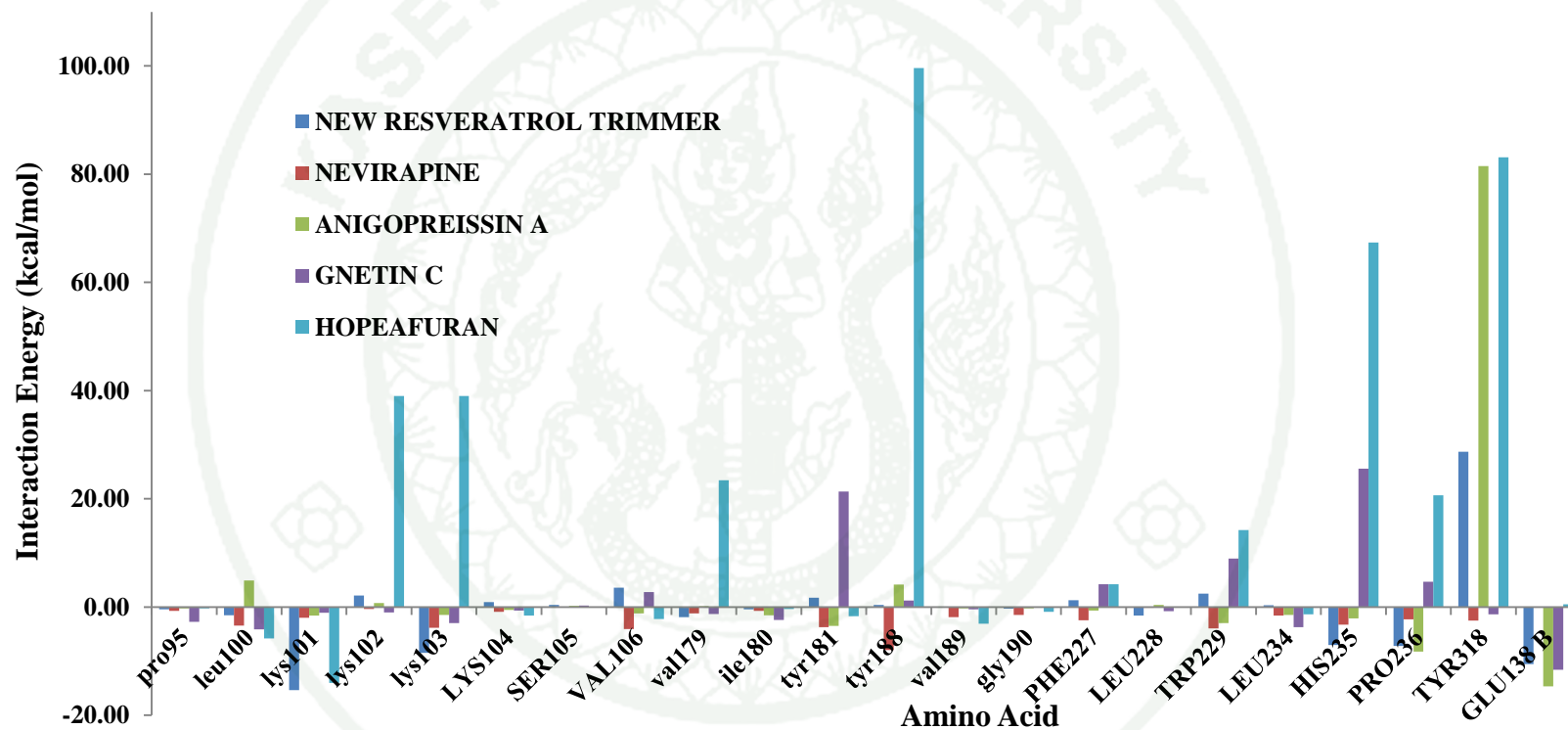


**Figure 16** Interaction energy with CP correction of Nevirapine, Gnetin C, Anigopressin A and New resveratrol trimmer with individual amino acid surrounding the binding pocket of wild-type by the M062x/6-31G(d, p) level.

### 3D-QSAR Study on Resveratrol Analogues as Aromatase Inhibitors

#### CoMSIA Statistical Part

The obtained CoMSIA model gives good statistical results ( $r^2_{cv} = 0.683$ ,  $r^2_{nv} = 0.974$ ,  $S_{press} = 0.355$ ,  $s = 0.101$  and  $F$  value = 56.556). The model can be used to predict the  $pIC_{50}$  of the resveratrol derivatives very well as shown the graphical plot between experimental and predicted  $pIC_{50}$  values in the Figure 17.

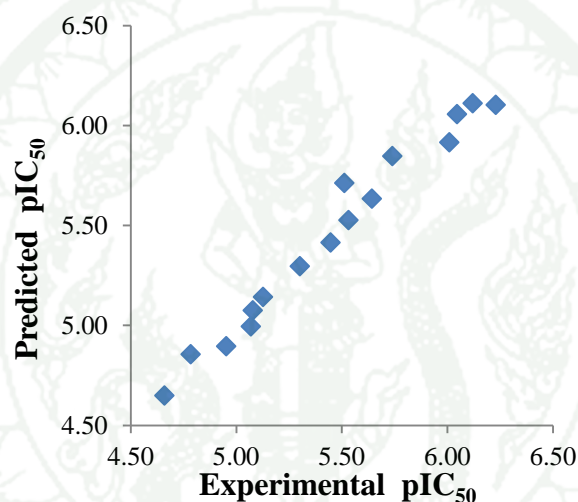


**Figure 17** Graphical plot between experimental and predicted PIC50 values obtaining from the CoMSIA model.

#### CoMSIA Contour Map Part

The CoMSIA contour map (Figure 18) consists of four CoMSIA properties; steric 7.2% contribution, electrostatic 49.1% contribution, hydrogen bond donor 6.8% contribution and hydrogen bond acceptor 36.9% contribution. The displayed map definitions are; the steric property; green areas indicate regions where bulky groups increase activity; yellow areas indicate regions where bulky groups decrease activity, the electrostatic property; blue areas indicate regions where positive groups increase activity; red areas indicate regions where negative charges increase activity, the H-

bond donor property; cyan areas indicate regions where H-bond donor groups increase activity; purple areas indicate regions where H-bond donor groups decrease activity, the H-bond acceptor property; magenta areas indicate regions where H-bond acceptor groups increase activity; orange areas indicate regions where H-bond acceptor groups decrease activity.

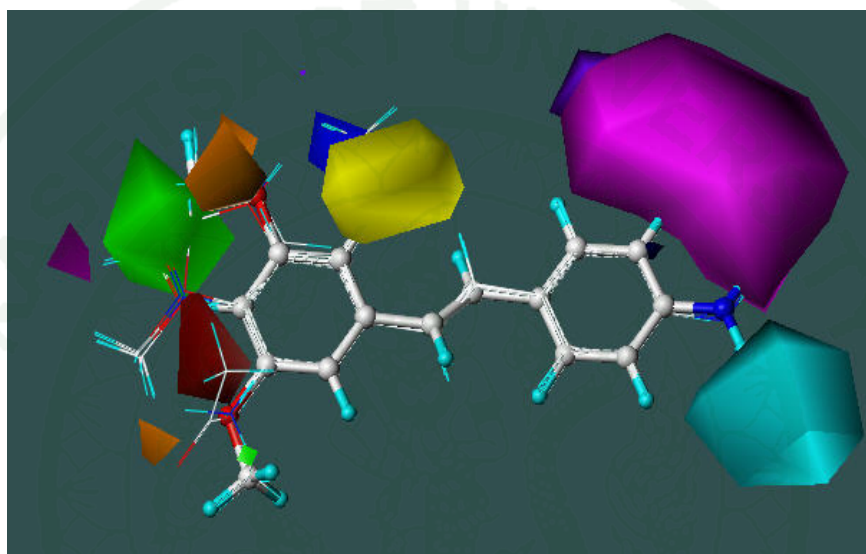


**Figure 18** Contour maps of CoMSIA (stdev\*coeff) model; color code for each contour is as follows; blue positive-electrostatically favored, red positive-electrostatically disfavored, green sterically favored, yellow sterically disfavored, cyan hydrogen bond donor favored, purple hydrogen bond donor disfavored, magenta hydrogen bond acceptor favored and orange hydrogen bond acceptor disfavored.

Considering of CoMSIA contour maps, these can be concluded that (i) the  $R^1$  is favorable the positive charge group or electron donating group, (ii)  $R^2$  is favorable the steric group. (iii)  $R^3$  and  $R^4$  are favorable the negative charge or electron or electron withdrawing group, (iv)  $R^5$  is favored the H-bond acceptor interaction implying that the H-donor group is suitable for this region, whereas the  $R^6$  position has both H-bond donor and H-bond acceptor regions merging together which means that the substituent that can act both H-donor and H-acceptor is fit for this position, such as  $NH_2$  group.

## CONCLUSION

From the investigation of HIV-1 reverse transcriptase from *Shorea siamensis* Miq., four resveratrol analogues were isolated and identified. The orientation of Gnetin C, Anigopreissin A, Hopeafuran and New resveratrol trimer could be a good candidate to be further study for HIV-1 RT inhibitor. Particular interaction calculations with BSSE-CP correction, the obtained results these four molecules showed attractive interaction higher than Nevirapine whereas, New resveratrol trimer was similar to Nevirapine. Surprisingly, New resveratrol trimer demonstrated strong binding with Lys103. This investigation can be exploited in design of new inhibitor for mutant type K103N. Additionally, Anigopreissin A showed good inhibition against wild-type and mutant (K103N and Y181C) HIV-1 RT. Thus, New resveratrol trimer and Anigopreissin A can be considered as high potent for further toxicity study prior to be developed as novelistic drugs.

In additional, from the three-dimensional quantitative structure activity relationship (3D-QSAR) with synthesized resveratrol analogues were tested for aromatase inhibitory activity by Sun and coworkers using the Comparative Molecular Similarity Indices Analysis (CoMSIA) technique. The information of CoMSIA results provides a helpful guideline to design and predict the affinity of resveratrol compounds with enhanced activities prior to synthesis. However, the other analyses, such as partial charge distribution, molecular docking and amino acid interactions, will be involved in the further studies for more molecular details and better understanding on ligand-enzyme interactions

**LITERATURE CITED**

- Abe, N., T. Ito, K. Ohguchi, M. Nasu, Y. Masuda, M. Oyama, Y. Nozawa, M. Ito and M. Inuma. 2010. Resveratrol Oligomers from *Vatica albiramis*. **J. Nat. Prod.** 73(9): 1499–1506.
- Aggarwal, B.B., A. Bhardwaj, R.S. Aggarwal, N.P. Seeram, S. Shishodia and Y. Takada. 2004. Role of resveratrol in prevention and therapy of cancer: preclinical and clinical studies. **Anticancer Res.** 24(5A): 2783-840.
- Baur, J.A. and D.A. Sinclair. 2006. Therapeutic potential of resveratrol: the in vivo evidence. **Nat. Rev. Drug Discov.** 5(6): 493-506.
- Billes, F., I. Mohammed-Ziegler, H. Mikosch and E. Tyihák. 2007. Vibrational spectroscopy of resveratrol. **Spectrochim. Acta A Mol. Biomol. Spectrosc.** 68(3): 669-679.
- De Clercq, E. 1998. The role of non-nucleoside reverse transcriptase inhibitors (NNRTIs) in the therapy of HIV-1 infection. **Antiviral Res.** 38(3): 153-179.
- Ge, H.-M., W.-H. Yang, J. Zhang and R.-X. Tan. 2009. Antioxidant Oligostilbenoids from the Stem Wood of *Hopea hainanensis*. **J. Agric. Food Chem.** 57(13):5756-5761.
- Ge, H.M., B. Huang, S.H. Tan, D.H. Shi, Y.C. Song and R.X. Tan. 2006. Bioactive Oligostilbenoids from the Stem Bark of *Hopea exalata*. **J. Nat. Prod.** 69(12): 1800-1802.
- Ge, H.M., C.H. Zhu, D.H. Shi, L.D. Zhang, D.Q. Xie, J. Yang, S.W. Ng and R.X. Tan. 2008. Hopeahainol A: An Acetylcholinesterase Inhibitor from *Hopea hainanensis*. **ChemInform** 39(20):no-no. **Chem. Eur. J.** 14(1): 376-381.

- Ghosh, D., J. Griswold, M. Erman and W. Pangborn. 2009. Structural basis for androgen specificity and oestrogen synthesis in human aromatase. **Nature** 457(7226): 219-223.
- Hannongbua, S., P. Pungpo, J. Limtrakul and P. Wolschann. 1999. Quantitative structure-activity relationships and comparative molecular field analysis of TIBO derivatised HIV-1 reverse transcriptase inhibitors. **J. Comput.-Aided Mol. Design** 13(6): 563-577.
- He, X., Y. Mei, Y. Xiang, D.W. Zhang and J.Z.H. Zhang. 2005. Quantum computational analysis for drug resistance of HIV-1 reverse transcriptase to nevirapine through point mutations. **Proteins** 61(2): 423-432.
- Hughes, S.H. 2001. Molecular matchmaking: NNRTIs can enhance the dimerization of HIV type 1 reverse transcriptase. **PNAS** 98(13): 6991-6992.
- Ito, T. 2011. Structures of Oligostilbenoids in Dipterocarpaceaeous Plants and Their Biological Activities. **Yakugaku Zasshi** 131(1): 93-100.
- Ito, T., N. Abe, M. Oyama, T. Tanaka, J. Murata, D. Darnaedi and M. Iinuma. 2009. Two Novel Resveratrol Trimers from *Dipterocarpus grandiflorus*. **Helv. Chim. Acta** 92(6): 1203-1216.
- Ito, T., Z. Ali, M. Furusawa, I. Iliya, T. Tanaka, K.-i. Nakaya, J. Murata, D. Darnaedi and M. Iinuma. 2006. Resveratrol Oligomers and Their O-Glucosides from *Cotylelobium lanceolatum*. **Chem. Pharm. Bull.** 54(3): 363-367.
- Ito, T., Y. Masuda, N. Abe, M. Oyama, R. Sawa, Y. Takahashi, V. Chelladurai and M. Iinuma. 2010. Chemical constituents in the leaves of *Vateria indica*. **Chem. Pharm. Bull.** 58(10): 1369-1378.

- Ito, T., T. Tanaka, M. Iinuma, K.-i. Nakaya, Y. Takahashi, R. Sawa, J. Murata and D. Darnaedi. 2004. Three New Resveratrol Oligomers from the Stem Bark of *Vatica pauciflora*. **J. Nat. Prod.** 67(6): 932-937.
- Jaeger, J., T. Restle and T.A. Steitz. 1998. The structure of HIV-1 reverse transcriptase complexed with an RNA pseudoknot inhibitor. **EMBO J.** 17(15): 4535-4542.
- Kaewamatawong, R., Jounmunkong, Z., DPPH free radical scavenging activity and Total phenol compounds content of some Thai medicinal plant extracts, *Journal of Ubon Rajathanee University*, 2, 76 **2006**.
- Kubinyi, H. 1993. QSAR: Hansch Analysis and Related Approaches; *VCH: Weinheim*.
- Kuno, M., R. Hongkengkai and S. Hannongbua. 2006. ONIOM-BSSE scheme for H $\cdot$  $\cdots$  $\pi$  system and applications on HIV-1 reverse transcriptase. **Chem. Phys. Lett.** 424(1-3): 172-177.
- Maitarad, P., S. Kamchonwongpaisan, J. Vanichtanankul, T. Vilaivan, Y. Yuthavong and S. Hannongbua. 2009. Interactions between cycloguanil derivatives and wild type and resistance-associated mutant *Plasmodium falciparum* dihydrofolate reductases. **J. Comput.-Aided Mol. Design** 23(4): 241-252.
- Maitarad, P., P. Saparpakorn, S. Hannongbua, S. Kamchonwongpaisan, B. Tarnchompoo and Y. Yuthavong. 2009. Particular interaction between pyrimethamine derivatives and quadruple mutant type dihydrofolate reductase of *Plasmodium falciparum*: CoMFA and quantum chemical calculations studies. **J. Enzyme Inhib. Med. Chem.** 24(2): 471-479.

- Marie-Pierre, d.B. 2010. Non-nucleoside reverse transcriptase inhibitors (NNRTIs), their discovery, development, and use in the treatment of HIV-1 infection: A review of the last 20 years (1989–2009). **Antiviral Res.** 85(1): 75-90.
- Mikulski, D., R. Górnjak and M. Molski. 2010. A theoretical study of the structure-radical scavenging activity of trans-resveratrol analogues and cis-resveratrol in gas phase and water environment. **Eur. J. Med. Chem.** 45(3): 1015-1027.
- Molnár, V., F. Billes, E. Tyihák and H. Mikosch. 2008. Theoretical study on the vibrational spectra of methoxy- and formyl-dihydroxy-trans-stilbenes and their hydrolytic equilibria. **Spectrochim. Acta A Mol. Biomol. Spectrosc** 69(2): 542-558.
- Muhtadi, E.H. Hakim, L.D. Juliawaty, Y.M. Syah, S.A. Achmad, J. Latip and E.L. Ghisalberti. 2006. Cytotoxic resveratrol oligomers from the tree bark of *Dipterocarpus hasseltii*. **Fitoterapia** 77(7-8): 550-555.
- Nunriam, P., M. Kuno, S. Saen-oon and S. Hannongbua. 2005. Particular interaction between efavirenz and the HIV-1 reverse transcriptase binding site as explained by the ONIOM2 method. **Chem. Phys. Lett.** 405(1–3): 198-202.
- Patcharamun, W., J. Sichaem, P. Siripong, S. Khumkratok, J. Jong-Aramruang and S. Tip-Pyang. 2011. A new dimeric resveratrol from the roots of *Shorea roxburghii*. **Fitoterapia** 82(3): 489-492.
- Prajapati, D.G., R. Ramajayam, M.R. Yadav and R. Giridhar. 2009. The search for potent, small molecule NNRTIs: A review. **Bioorg. Med. Chem.** 17(16): 5744-5762.

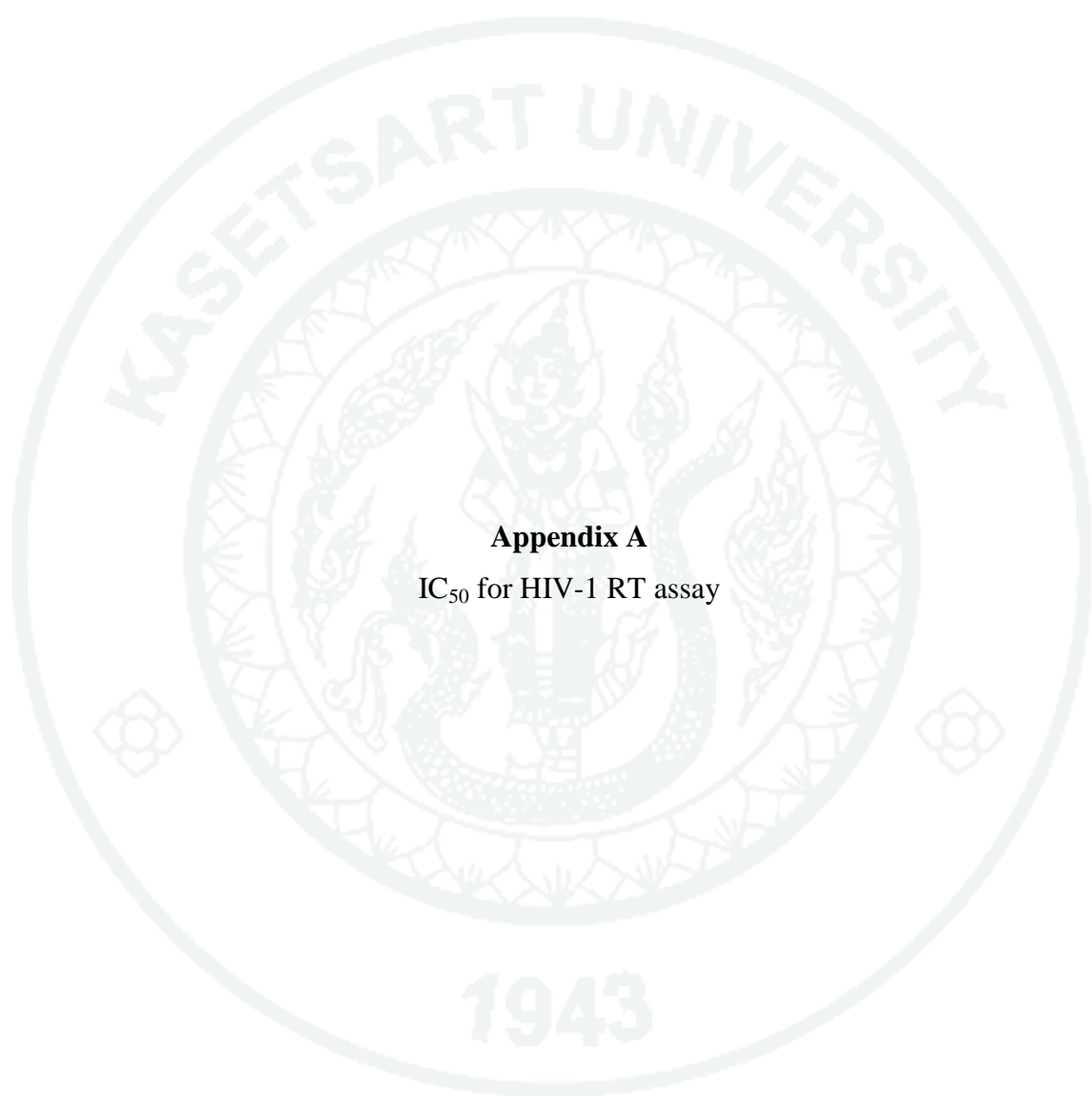
- Pungpo, P., P. Saparpakorn, P. Wolschann and S. Hannongbua. 2006. Computer-aided molecular design of highly potent HIV-1 RT inhibitors: 3D QSAR and molecular docking studies of efavirenz derivatives. **SAR QSAR Environ. Res.** 17(4): 353-370.
- Queiroz, A.N., B.A.Q. Gomes, W.M. Moraes Jr and R.S. Borges. 2009. A theoretical antioxidant pharmacophore for resveratrol. **Eur. J. Med. Chem.** 44(4): 1644-1649.
- Rambaut, A., D. Posada, K.A. Crandall and E.C. Holmes. 2004. The causes and consequences of HIV evolution. **Nat. Rev. Genet.** 5(1): 52-61.
- Ren, J., R. Esnouf, E. Garman, D. Somers, C. Ross, I. Kirby, J. Keeling, G. Darby, Y. Jones, D. Stuart and D. Stammers. 1995. High resolution structures of HIV-1 RT from four RT-inhibitor complexes. **Nat. Struct. Biol.** 2(4): 293-302.
- Roy, P. and K. Roy. 2010. Docking and 3D-QSAR studies of diverse classes of human aromatase (CYP19) inhibitors. **J. Mol. Model.** 16(10): 1597-1616.
- Sahlberg, C. and X.X. Zhou. 2008. Development of non-nucleoside reverse transcriptase inhibitors for anti-HIV therapy. **Anti-Infect. Agents Med. Chem.** 7(2): 101-117.
- Saroyobudiono, H., L. Juliawaty, Y. Syah, S. Achmad, E. Hakim, J. Latip and I. Said. 2008. Oligostilbenoids from *Shorea gibbosa* and their cytotoxic properties against P-388 cells. **J. Nat. Med.** 62(2): 195-198.
- Seo, E.-K., H. Chai, H.L. Constant, T. Santisuk, V. Reutrakul, C.W.W. Beecher, N.R. Farnsworth, G.A. Cordell, J.M. Pezzuto and A.D. Kinghorn. 1999. Resveratrol Tetramers from *Vatica diospyroides*. **J. Org. Chem.** 64(19): 6976-6983.

- Shen, L., J. Shen, X. Luo, F. Cheng, Y. Xu, K. Chen, E. Arnold, J. Ding and H. Jiang. 2003. Steered molecular dynamics simulation on the binding of NNRTI to HIV-1 RT. **Biophys. J.** 84(6): 3547-3563.
- Silprasit, K., S. Seetaha, P. Pongsanaraku, S. Hannongbua and K. Choowongkomon. 2011. Anti-HIV-1 reverse transcriptase activities of hexane extracts from some asian medicinal plants. **J. Med. Plant Res.** 5(19): 4899-4906.
- Silprasit, K., R. Thammaporn, S. Tecchasakul, S. Hannongbua and K. Choowongkomon. 2011. Simple and rapid determination of the enzyme kinetics of HIV-1 reverse transcriptase and anti-HIV-1 agents by a fluorescence based method. **J. Virol. Methods.** 171(2): 381-387.
- Sittisombut C., Michel S., Tillequin F., Pohmakotr M., and Reutrakul V. Survey of potential products as anti-cancer agents from plants in families of Rutaceae and Dipterocarpaceae inThailand. Annual TRF Meeting: Young scientists meet Senior Scientists, Regent Hotel Cha-Am. Phetchaburi, Thailand. 13-15 Oct., **2005**.
- Sittisombut C., Michel S., Tillequin F., Pohmakotr M., and Reutrakul V. Investigation of anti-cancer activity of plants in families of Rutaceae and Dipterocarpaceae inThailand. Annual TRF Meeting: Young scientists meet Senior Scientists, Regent Hotel Cha-Am. Phetchaburi, Thailand. October 12-14, **2006**
- Sluis-Cremer, N. and G. Tachedjian. 2008. Mechanisms of inhibition of HIV replication by non-nucleoside reverse transcriptase inhibitors. **Virus Res.** 134(1-2): 147-156.
- Sri, A., N. Aznam, R. Arianingrum, Y. Takaya and N. Masatake. 2008. Resveratrol Derivatives from Stem Bark of *Hopea* and Their Biological Activity Test. **J. Phys. Sci.** 19(2): 7-21.

- Sun, B., J. Hoshino, K. Jermihov, L. Marler, J.M. Pezzuto, A.D. Mesecar and M. Cushman. 2010. Design, synthesis, and biological evaluation of resveratrol analogues as aromatase and quinone reductase 2 inhibitors for chemoprevention of cancer. **Bioorg. Med. Chem.** 18(14): 5352-5366.
- Suphavanich, K., P. Maitarad, S. Hannongbua, P. Sudta, S. Suksamrarn, Y. Tantirungrotechai and J. Limtrakul. 2009. CoMFA and CoMSIA studies on a new series of xanthone derivatives against the oral human epidermoid carcinoma (KB) cancer cell line. **Monatsh. Chem.** 140(3): 273-280.
- SYBYL/QSAR, Molecular Modelling Software, Tripos Inc., 1699 S, Hanley Road, St. Louis, MO 63944, USA.
- Thengyai, S., P. Maitarat, S. Hannongbua, K. Suwanborirux and A. Plubrukarn. 2010. Probing the structural requirements for antitubercular activity of scalarane derivatives using 2D-QSAR and CoMFA approaches. **Monatsh. Chem.** 141(6): 621-629.
- Vingtdeux, V., U. Dreses-Werringloer, H. Zhao, P. Davies and P. Marambaud. 2008. Therapeutic potential of resveratrol in Alzheimer's disease. **BMC Neurosci.** 9(Suppl 2): S6.
- Wibowo, A., N. Ahmat, A.S. Hamzah, A.S. Sufian, N.H. Ismail, R. Ahmad, F.M. Jaafar and H. Takayama. 2011. Malaysianol A, a new trimer resveratrol oligomer from the stem bark of *Dryobalanops aromatica*. **Fitoterapia** 82(4): 676-681.
- Wibowo, A., N. Ahmat, A.S. Hamzah, N.H. Ismail, R. Ahmad and F.M. Jaafar. 2012. Resveratrol oligomers from the stem bark of *Dryobalanops aromatica*. **Biochem. System. Ecol.** 40(0): 62-64.



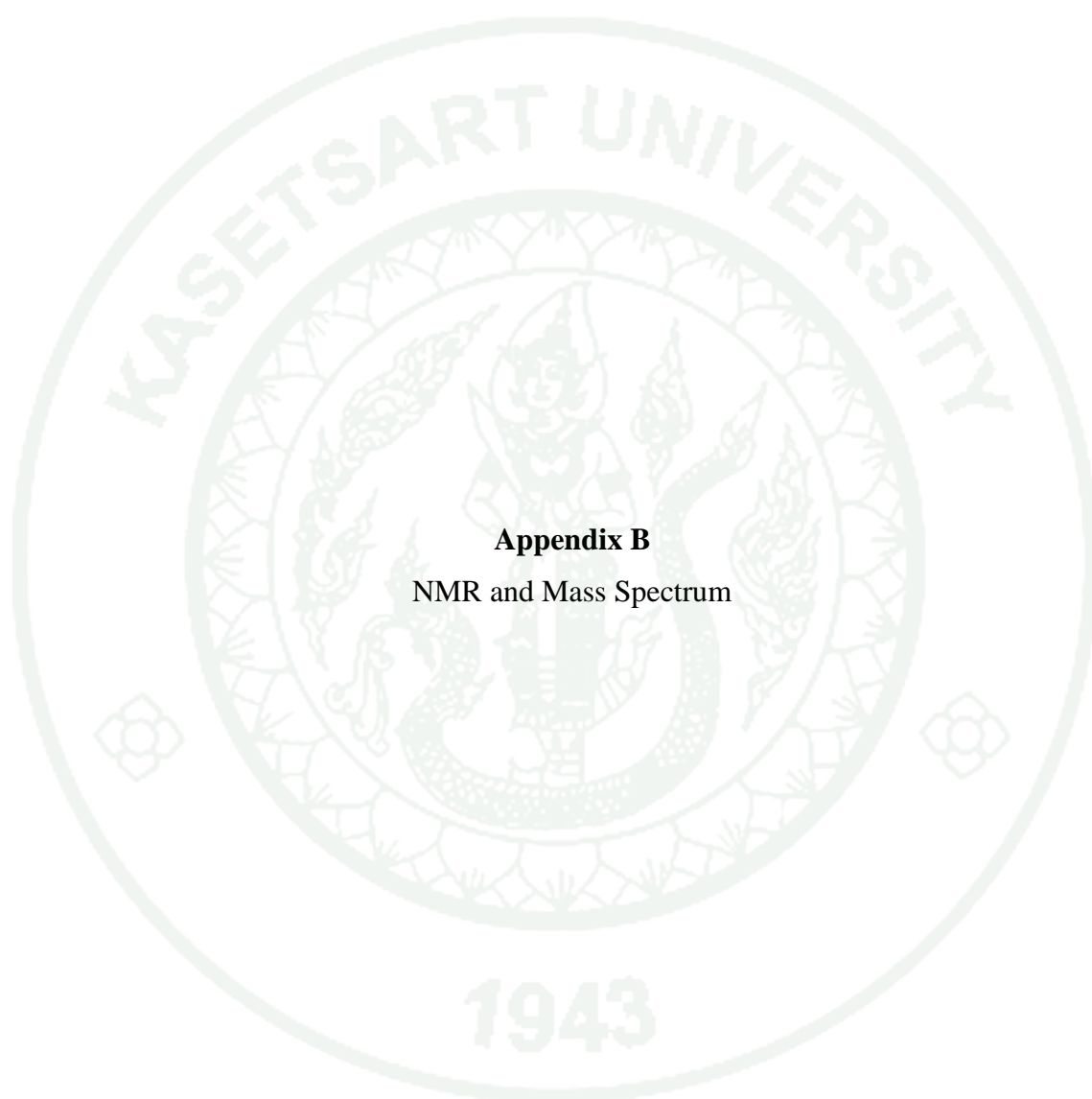
**APPENDICES**



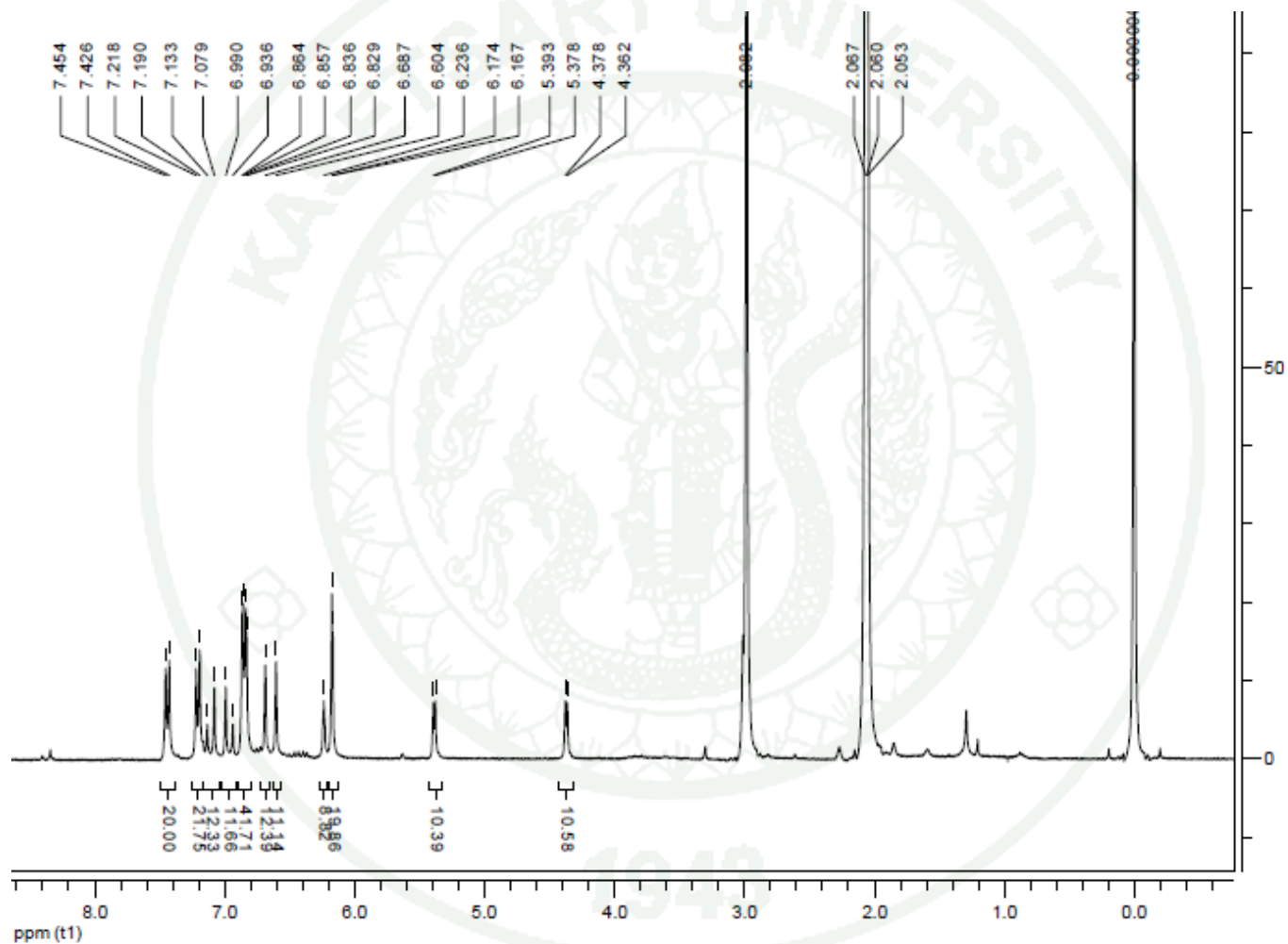
**Appendix A**  
IC<sub>50</sub> for HIV-1 RT assay

### **IC<sub>50</sub> for HIV-1 Reverse transcriptase activity assay**

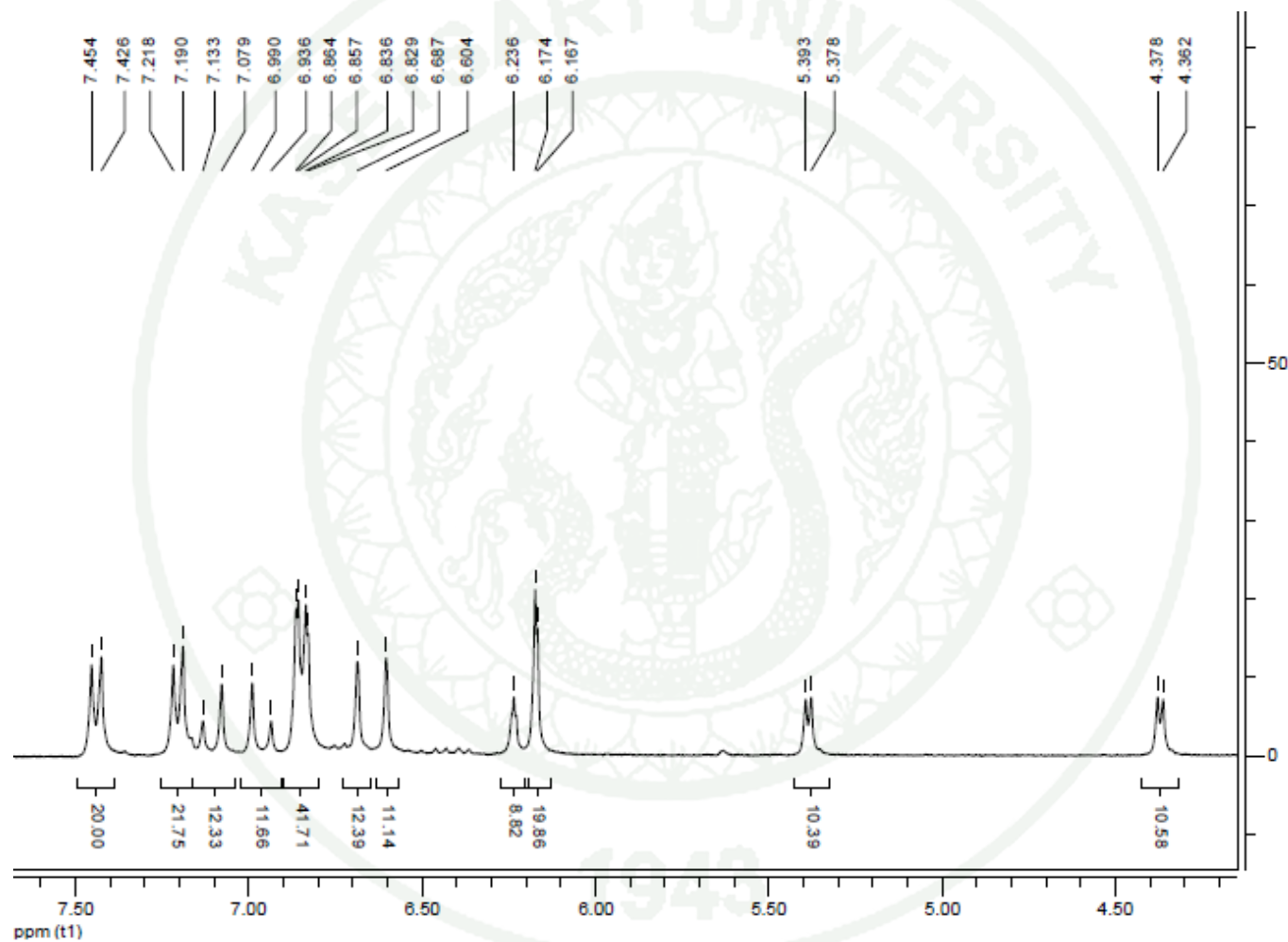
The determination of IC<sub>50</sub> values for compounds against HIV-1 RT was based on fluorescence measurement. All reagents were obtained from Molecular Probes' EnzChek<sup>®</sup> Reverse Transcriptase Assay Kit. The mixture of 5 µl of 1 mg/mL poly(A) ribonucleotide template and 5 µl of 50 µg/mL oligo d(T)16 primer was incubated for 1 hour at room temperature and diluted to 200 fold with polymerization buffer (60 mM Tris.HCl, 60 mM KCl, 8 mM MgCl<sub>2</sub>, 13 mM DTT, 100 µM dTTP, pH 8.1). PicoGreen reagent was diluted by adding into TE buffer (10 mM Tris-HCl, 1 mM EDTA, pH 7.5) with ratio 1:2000. Two-fold serial dilutions of inhibitors were prepared and 2 µl of each inhibitor concentration was added to 96 well plates. The 4 µl of template/primer polymerization buffer and 2 µl of 30 ng/µl HIV-1 RT were added and mixed to 96 well plates containing each inhibitor concentration. The mixtures were incubated at 37 °C for 10 minutes. The reactions were stopped by 200 mM EDTA and kept at 4°C until the reactions will be measured. The PicoGreen reagent were added to the reactions and incubated for 2-5 minutes by protecting from the light. The fluorescence measurement was performed by fluorescence microplate reader with excitation wavelengths at 485 nm and emission wavelengths at 535 nm.



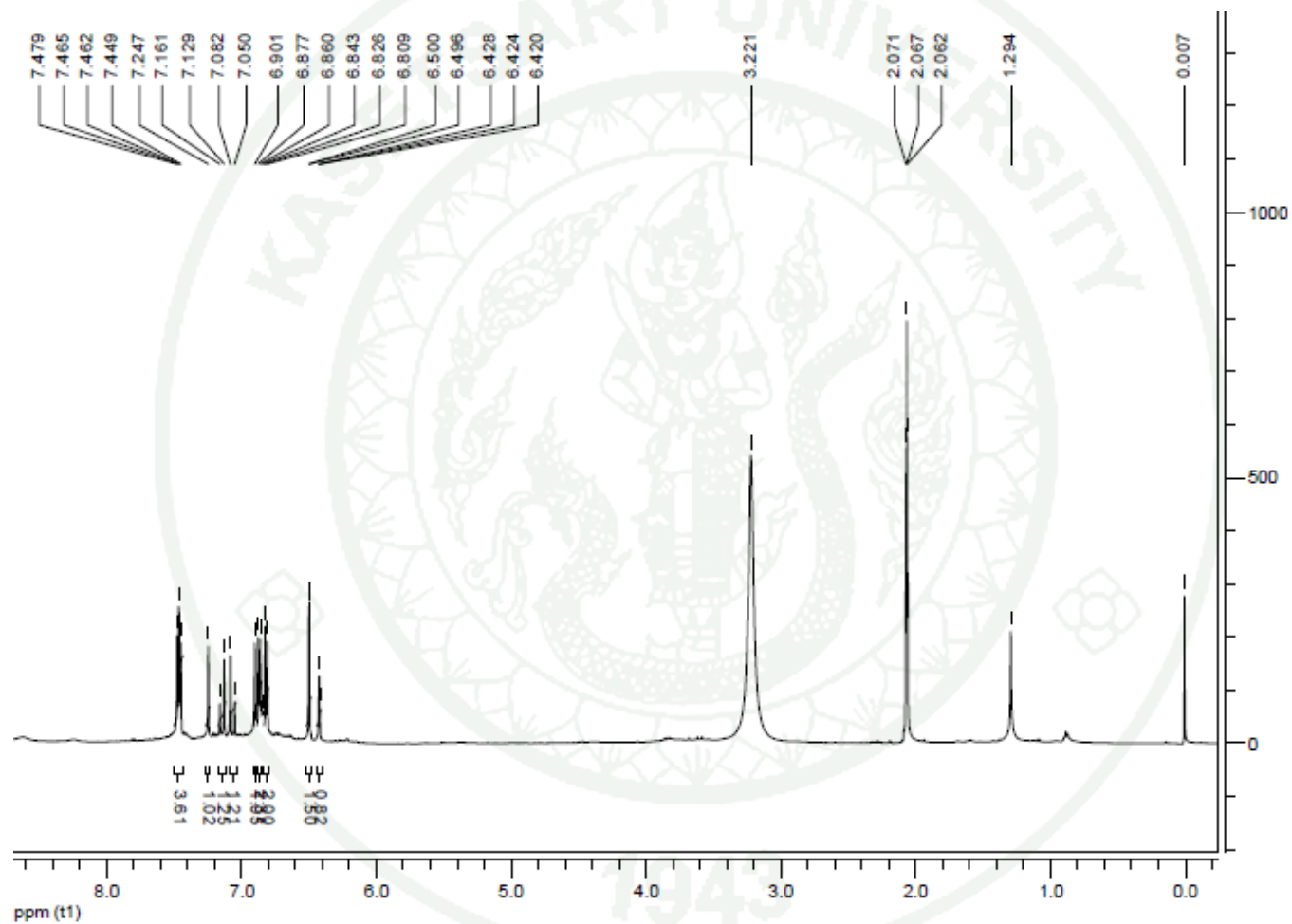
**Appendix B**  
NMR and Mass Spectrum



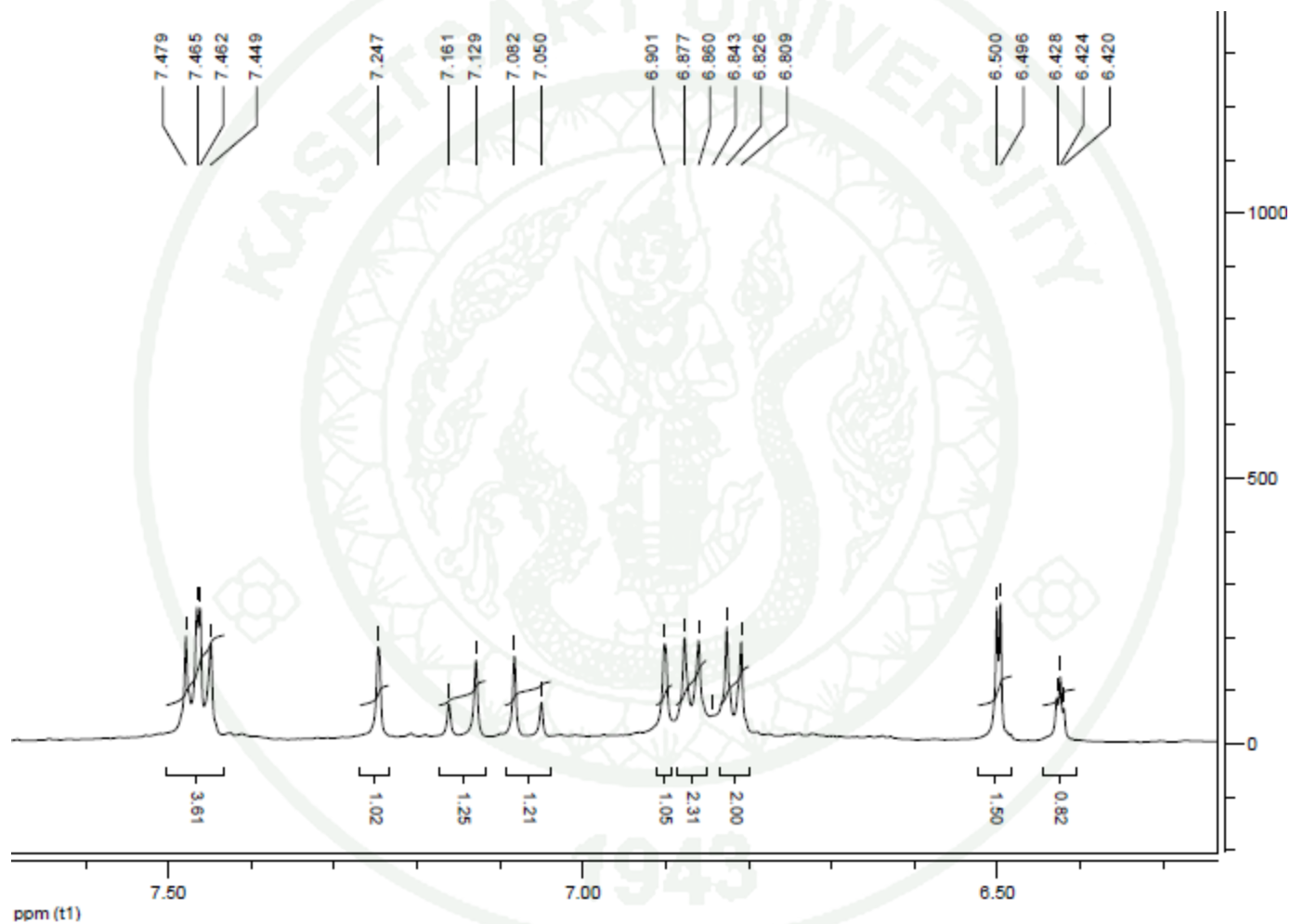
**Appendix Figure B1**  $^1\text{H}$  NMR spectrum (Acetone- $d_6$ ) of Gnetin C.



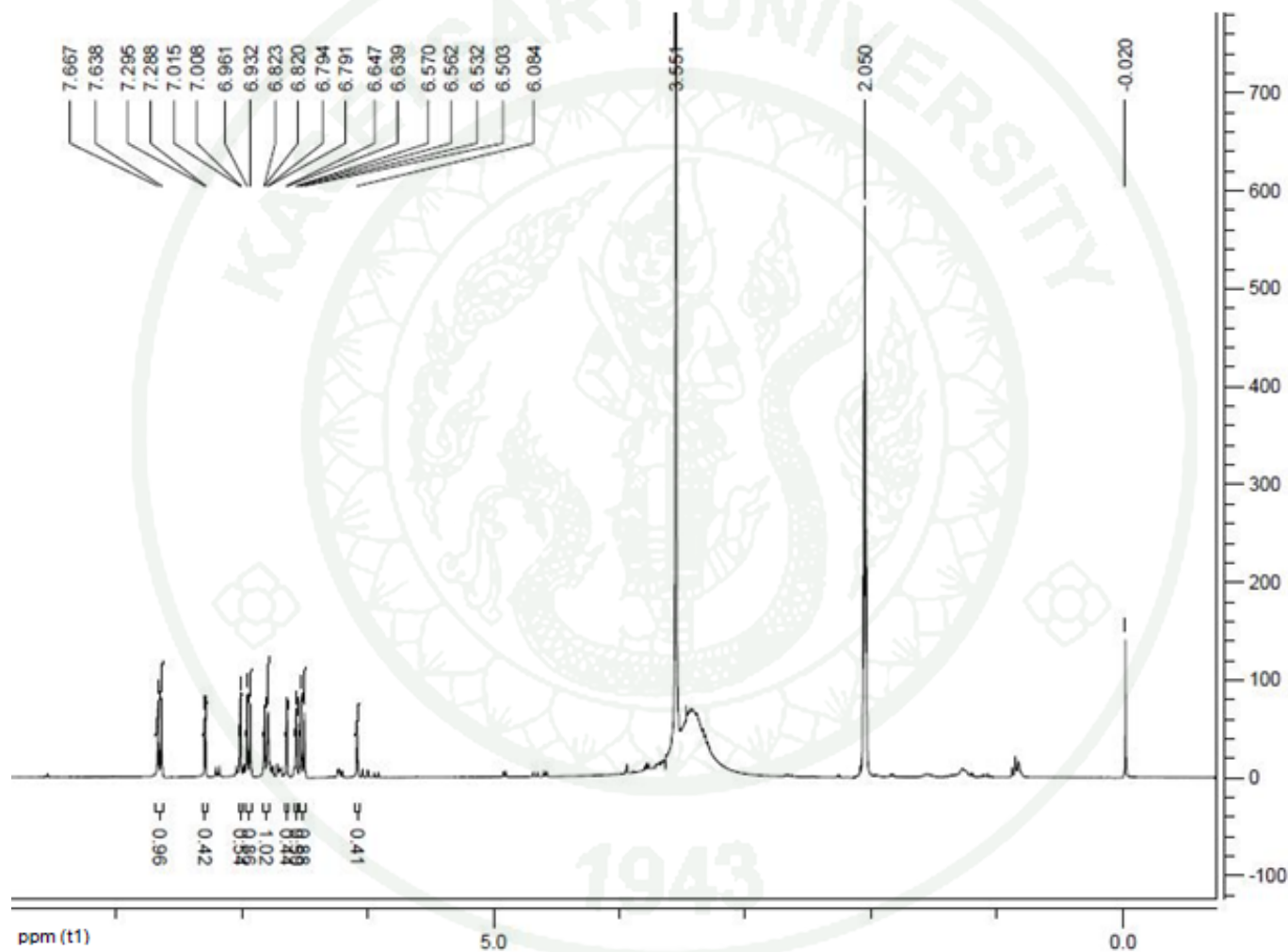
**Appendix Figure B2**  $^1\text{H}$  NMR spectrum (Acetone- $d_6$ ) of Gnetin C (Continued).



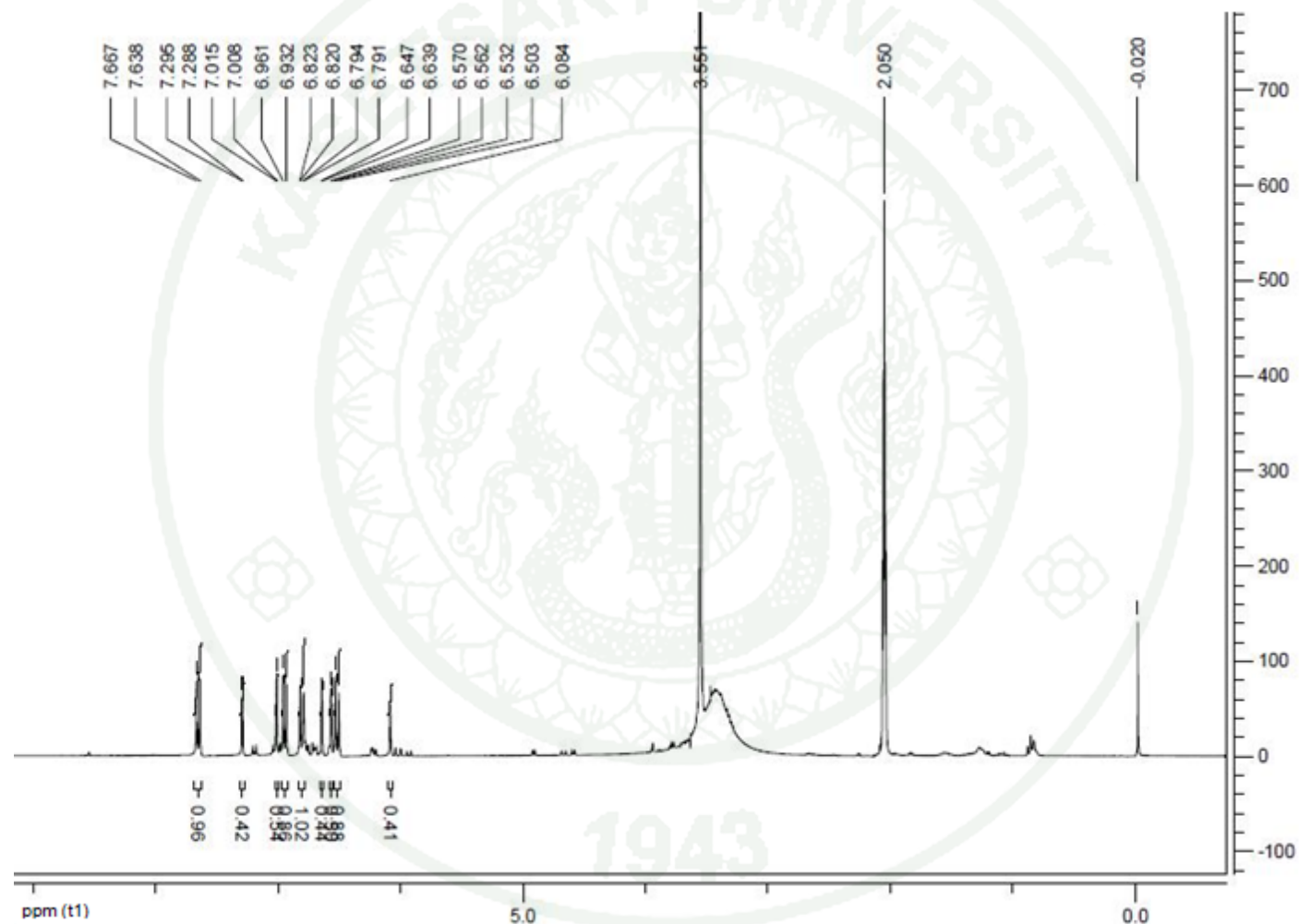
Appendix Figure B3 <sup>1</sup>H NMR spectrum (Acetone-*d*<sub>6</sub>) of Anigopreissin A.



**Appendix Figure B4**  $^1\text{H}$  NMR spectrum (Acetone- $d_6$ ) of Anigopreissin A (Continued).



Appendix Figure B5  $^1\text{H}$  NMR spectrum (Acetone- $d_6$ ) of Hopeafuran.

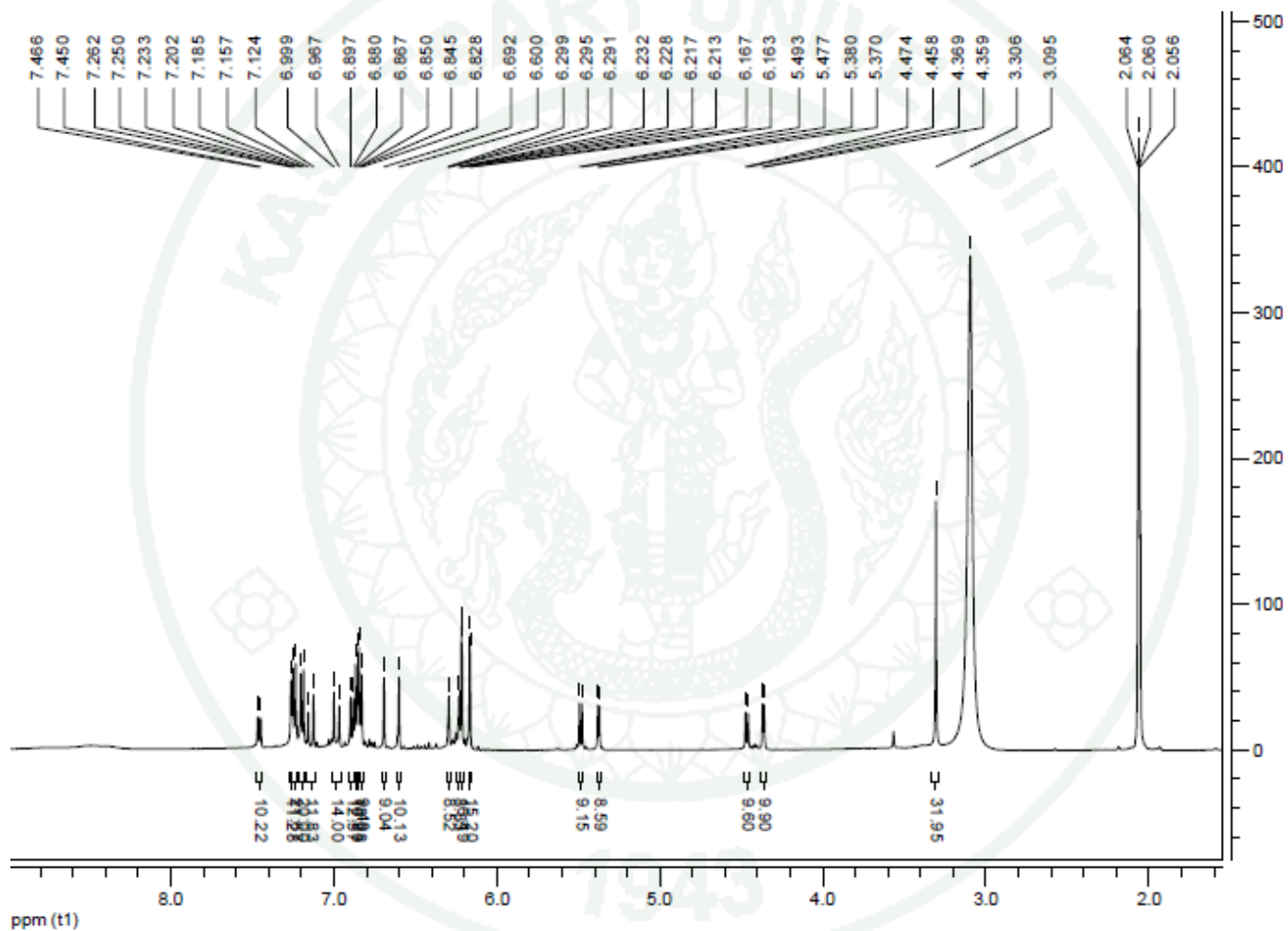


Appendix Figure B6  $^1\text{H}$  NMR spectrum (Acetone- $d_6$ ) of Hopeafuran (Continued).

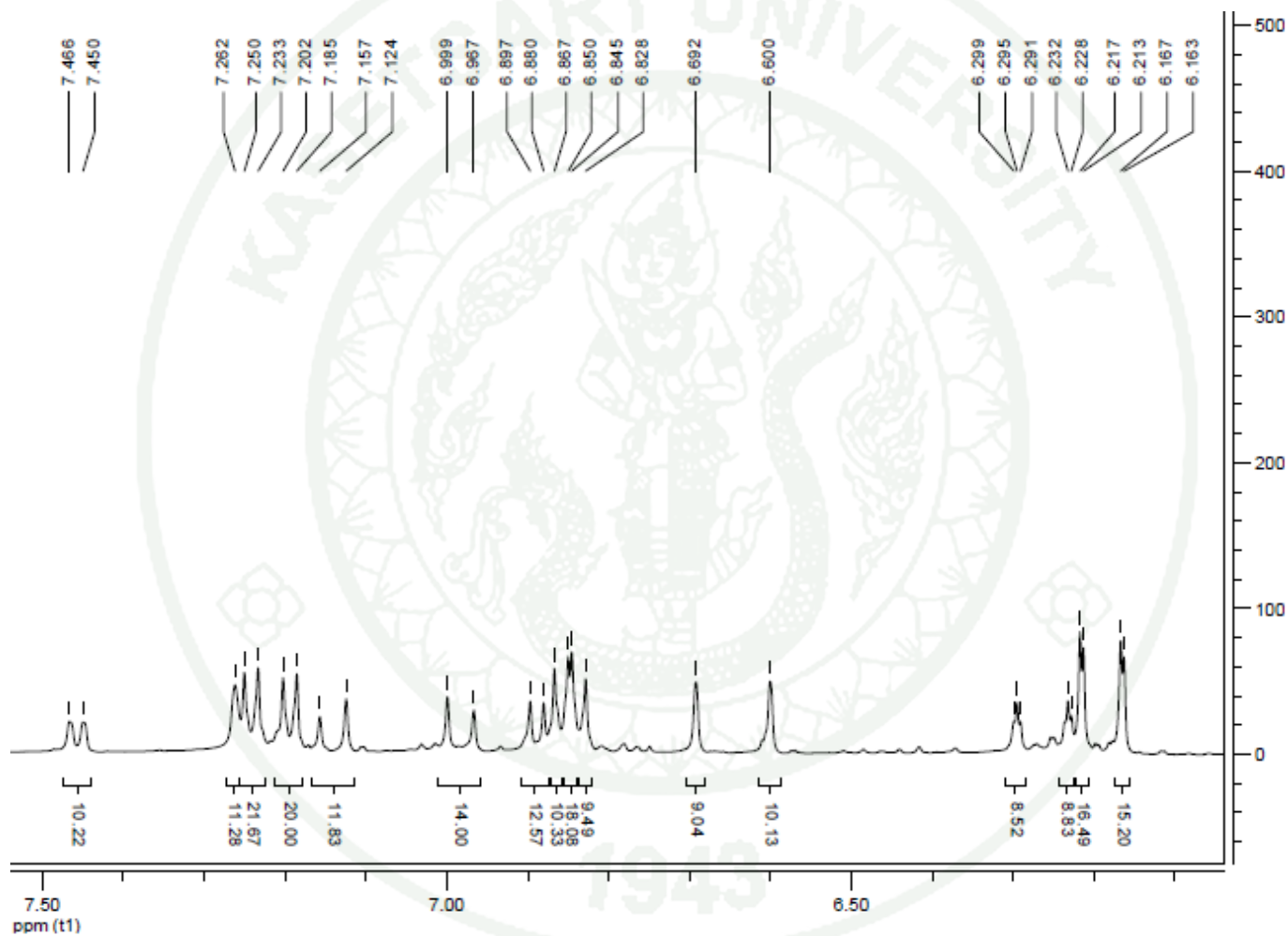
**Appendix Table B1** NMR Spectroscopic data of New resveratrol trimer<sup>a</sup>.

Position	$\delta_C$	$\delta_H$ (J in Hz)	$^1H$ - $^{13}C$ HMBC
1a	132.6		
2a,6a	128.6	7.25(d,8.5)	4a, 7a
3a,5a	116.2	6.86(d,8.5)	4a, 1a
4a	158.4		
7a	94.1	5.47(d,8.0)	8a, 5b, 1a, 9a, 1b
8a	57.9	4.48(d,8.0)	7a, 10a, 14a,3b, 4b, 2b, 1a,9a, 1b
9a	145.3		
10a,14a	107.5	6.21(d,2.0)	8a, 12a, 11a/13a
11a,13a	159.8		
12a	102.4	6.30(br.s)	11a/13a, 10a, 14a
1b	160.7		
2b	132.3		
3b	124.0	7.28(br.s)	1b, 7b, 5b
4b	131.8		
5b	128.7	7.46(d,8.5)	3b, 7b, 1b
6b	110.2	6.89(d,8.5)	1b, 4b, 2b
7b	129.3	7.15(d,16.0)	3b, 9b, 4b, 5b
8b	127.2	7.00(d,16.0)	14b, 10b, 12b, 9b, 4b, 7b
9b	141.2		
10b	108.2	6.59(br.s)	11b, 8b, 14b, 12b, 8c
11b	155.3		
12b	115.2		
13b	163.2		
14b	99.3	6.71(br.s)	10b, 12b, 8b, 11b, 13b
1c	134.1		
2c,6c	127.9	7.20(d,8.5)	7c, 12b, 8b, 11b, 13b
3c,5c	116.2	6.84(d,8.5)	4c, 2c/6c, 1c
4c	158.2		
7c	93.7	5.38(d,5.0)	8c, 12b, 2c, 6c, 1c
8c	56.0	4.39(d,5.0)	7c, 10c, 14c, 12b, 1c, 9c, 11b, 13b
9c	146.3		
10c,14c	106.7	6.16(d,2.0)	8c, 12c, 11c/13c
11c,13c	159.6		
12c	102.0	6.26(br.s)	10c/14c, 11c/13c

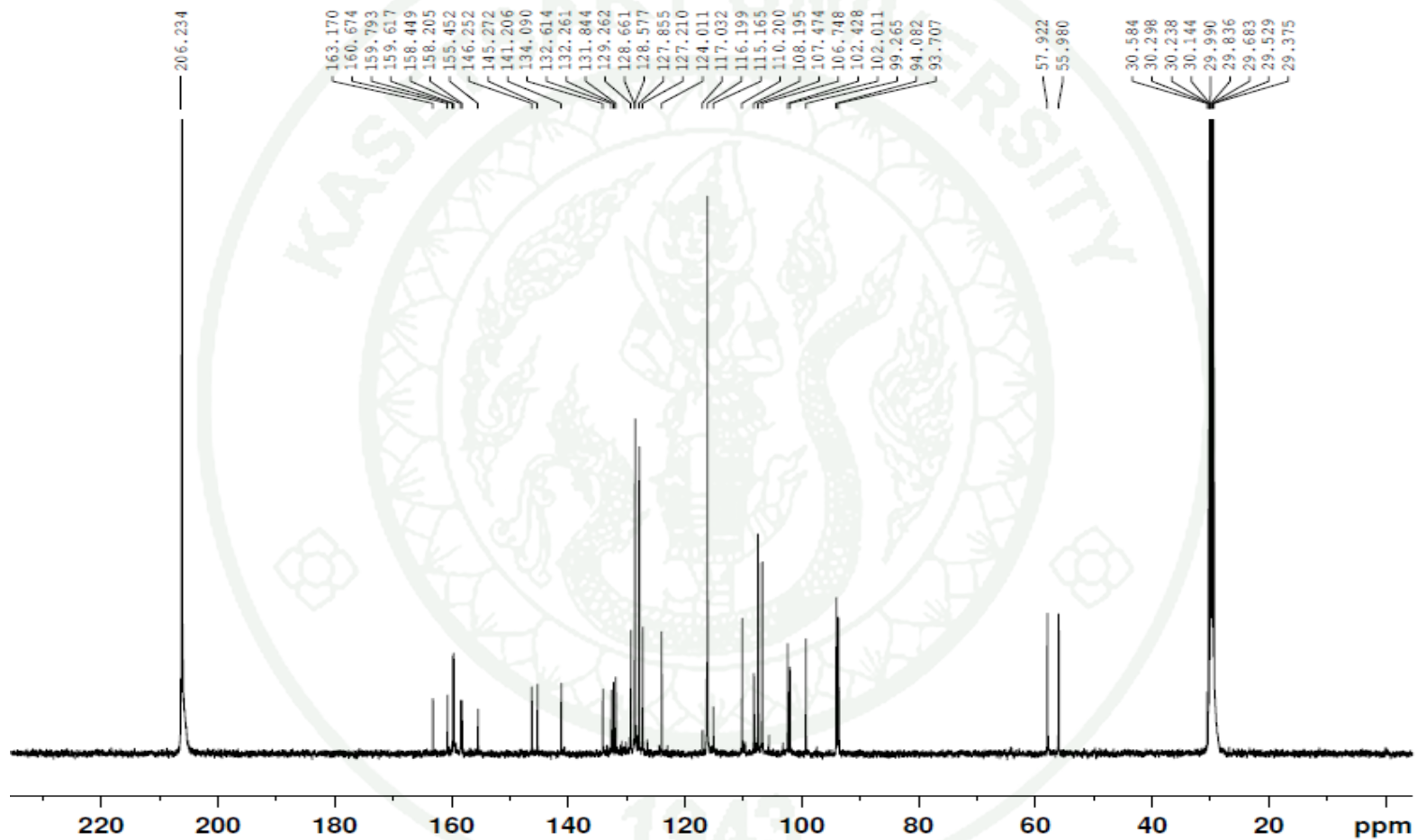
<sup>a</sup> Measure in acetone-*d*<sub>6</sub> at 500 MHz ( $^1H$  NMR) and 125 MHz ( $^{13}C$  NMR)



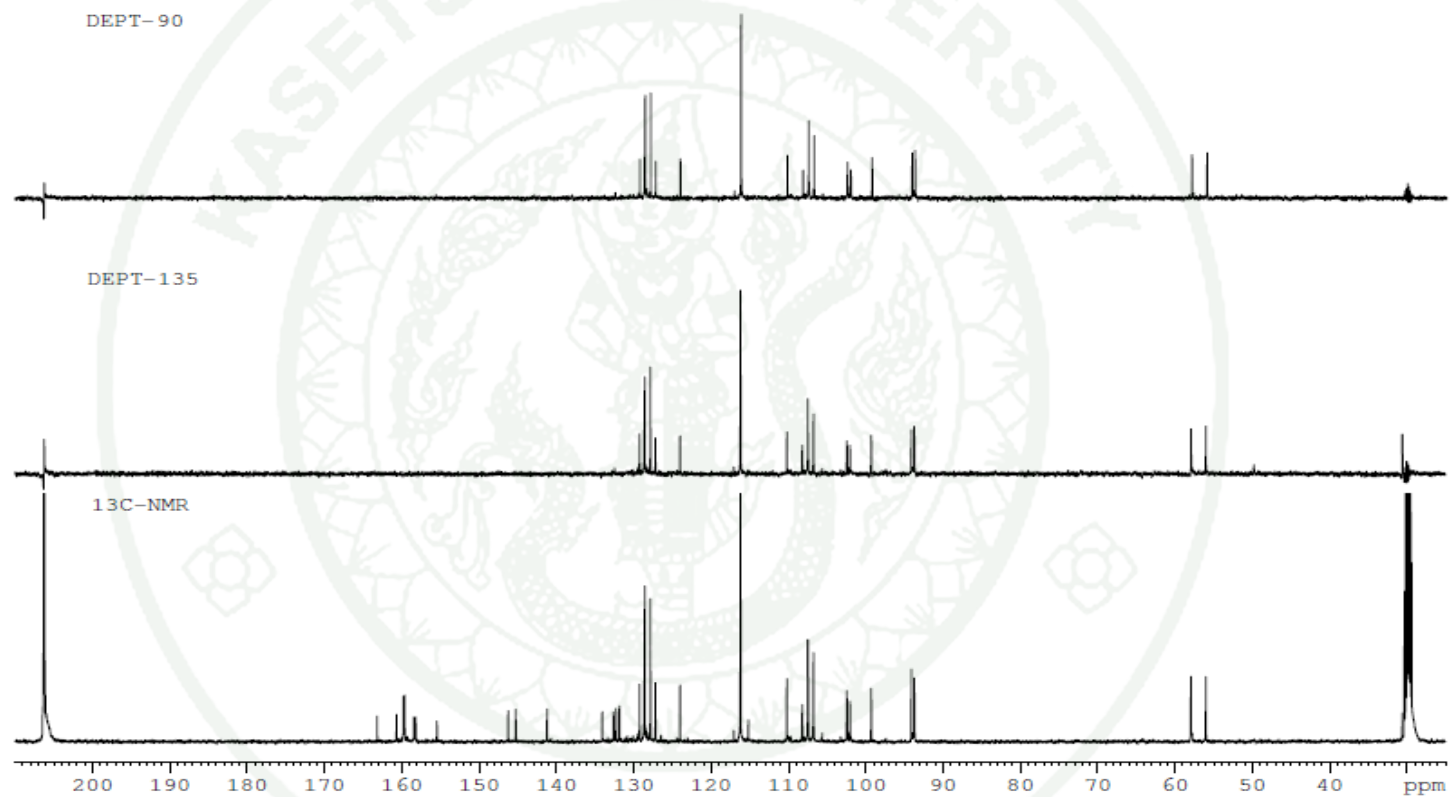
**Appendix Figure B7**  $^1\text{H}$  NMR spectrum (Acetone- $d_6$ ) of New resveratrol trimer.



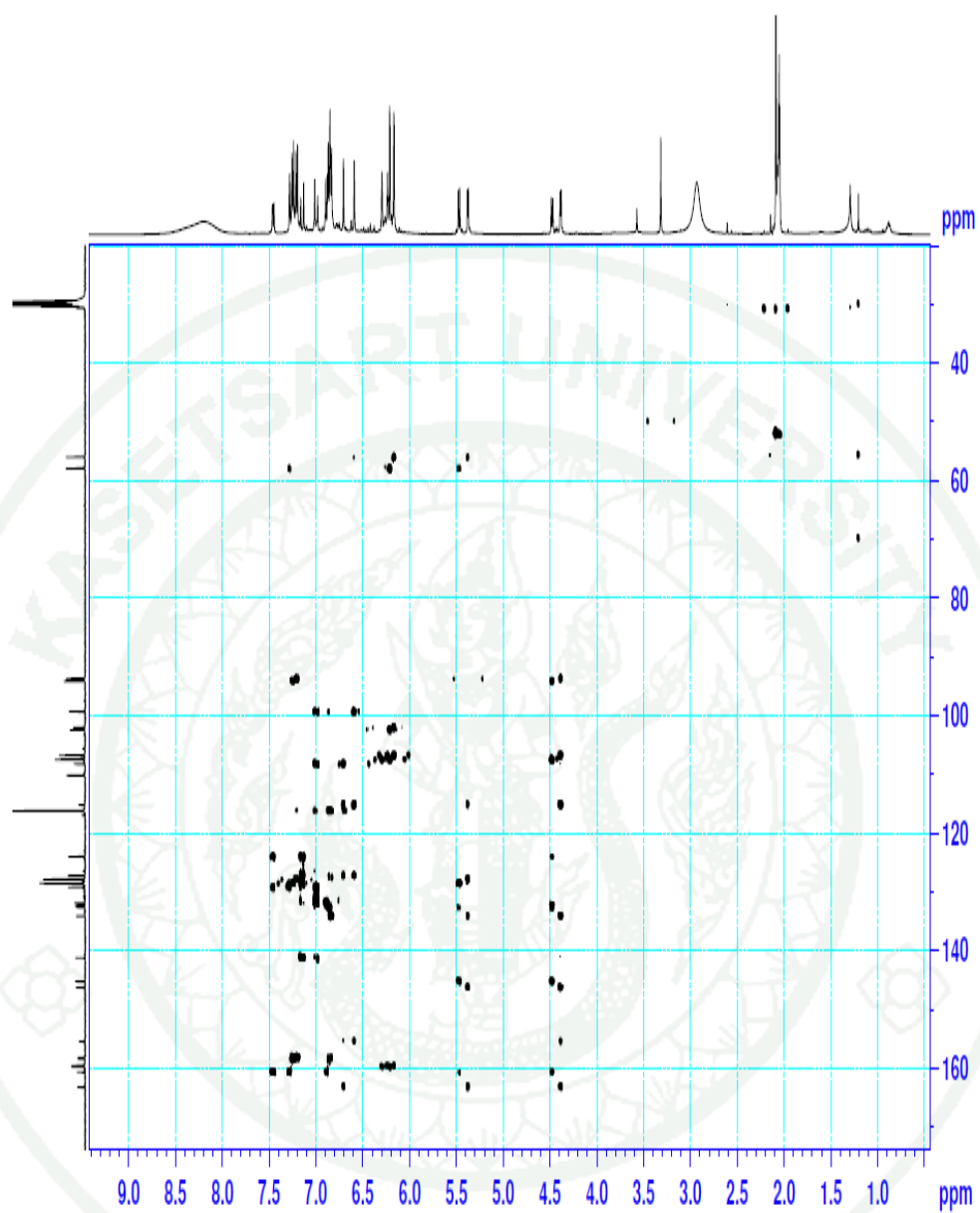
**Appendix Figure B8**  $^1\text{H}$  NMR spectrum ( $\text{Acetone-}d_6$ ) of New resveratrol trimer (Continued).



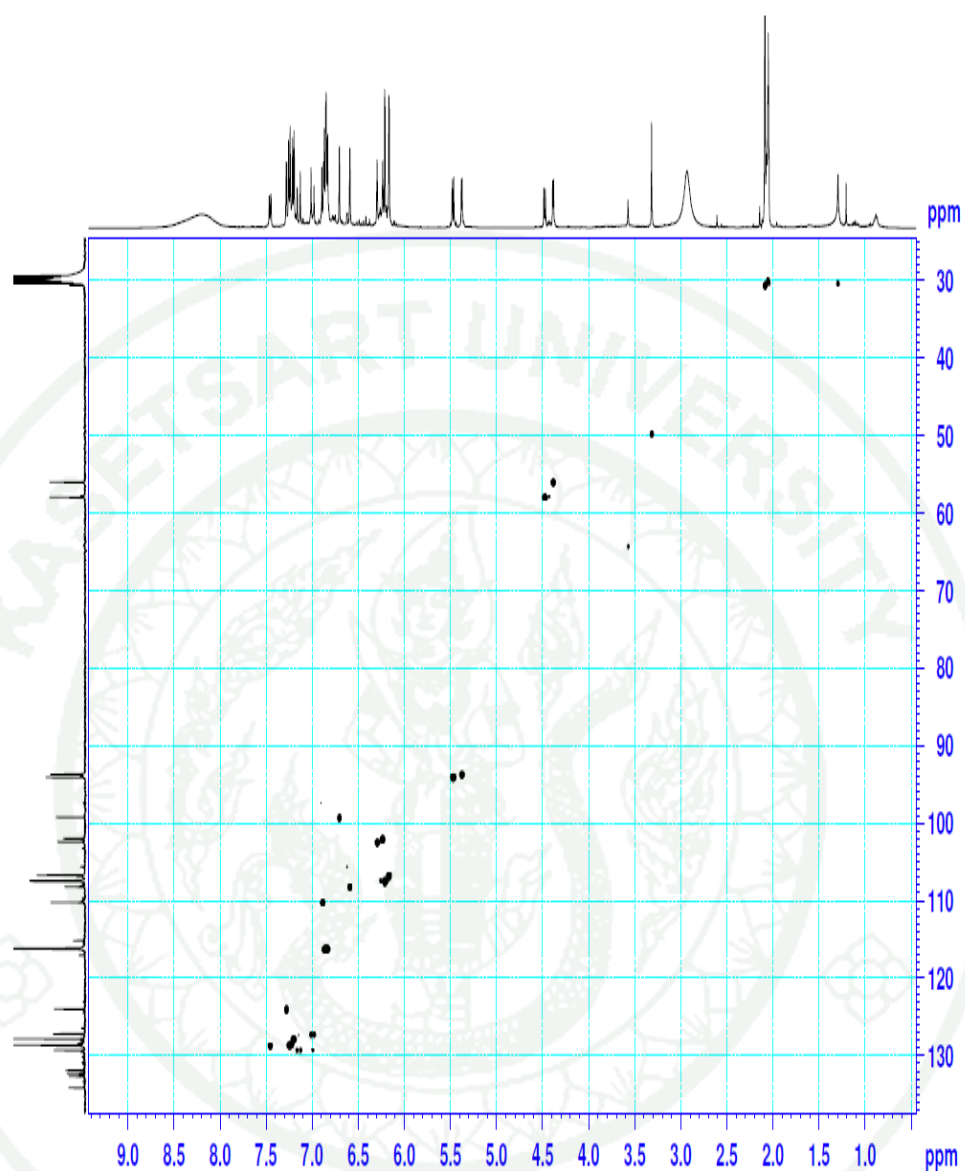
**Appendix Figure B9**  $^{13}\text{C}$ -NMR spectrum (Acetone- $d_6$ ) of New resveratrol trimer (Continued).



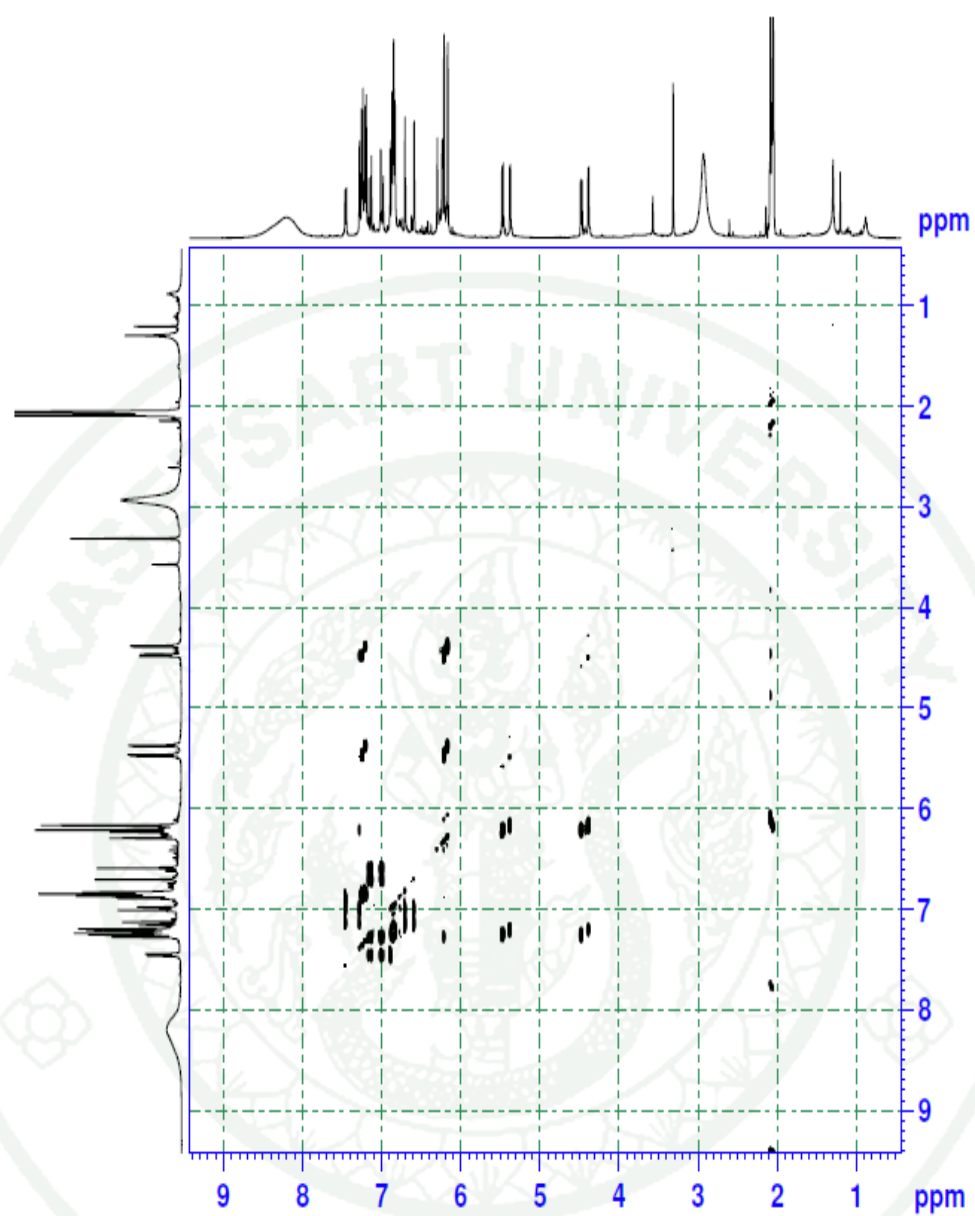
**Appendix Figure B10** DEPT 90 and 135 spectrum (Acetone-*d*<sub>6</sub>) of New resveratrol trimer.



**Appendix Figure B11** HMBC spectrum (Acetone-*d*<sub>6</sub>) of New resveratrol trimer.



**Appendix Figure B12** HSQC spectrum (Acetone-*d*<sub>6</sub>) of New resveratrol trimer.



**Appendix Figure B13** ROESY spectrum (Acetone-*d*<sub>6</sub>) of New resveratrol trimer.

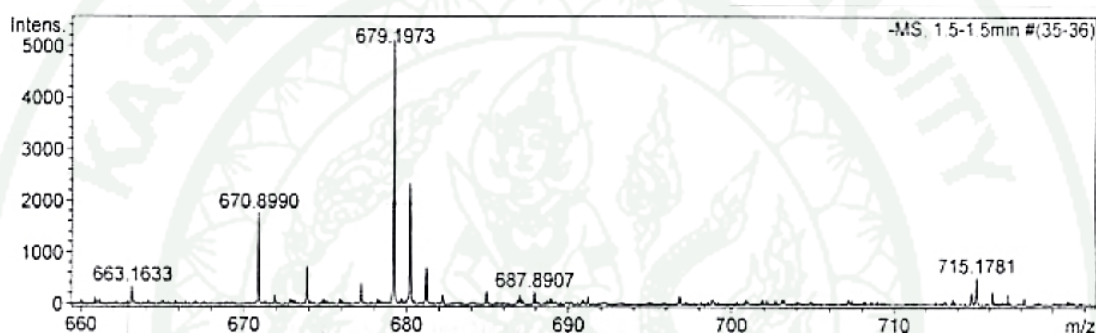
## Mass Spectrum List Report

### Analysis Info

Analysis Name TOFKU012044 Prapasiri BB20-45 E- Acquisition 1/20/2012 3:01:53  
 .d PM  
 Method Apci\_neg\_low-nitirat1.m Operator Administrator  
 Sample Name ESINEG Operator :Nitirat Instrument micrOTOF

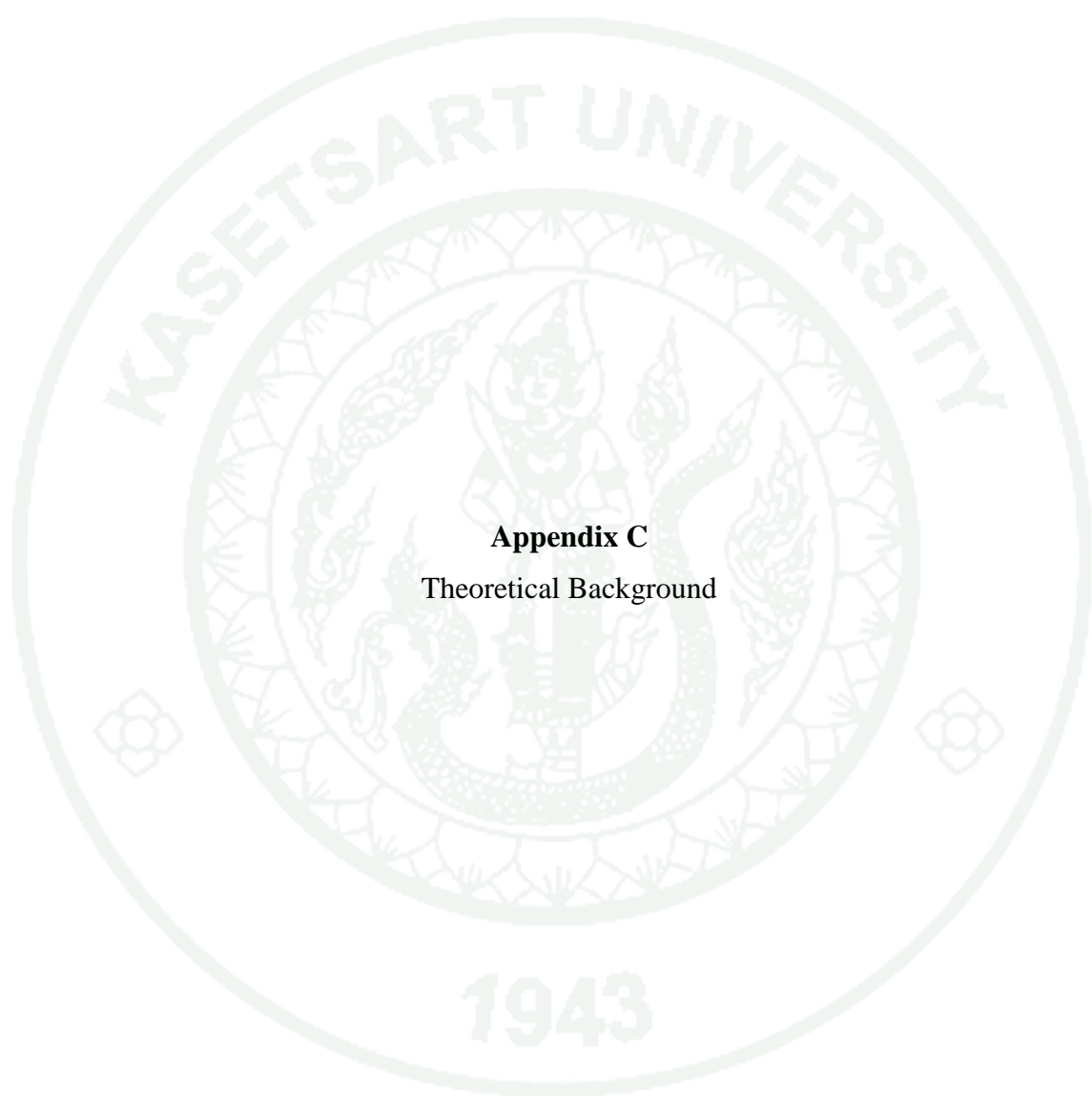
### Acquisition Parameter

Source Type	APCI	Ion Polarity	Negative	Set Corrector Fill	56 V
Scan Range	n/a	Capillary Exit	-90.0 V	Set Pulsar Pull	409 V
Scan Begin	120 m/z	Hexapole RF	120.0 V	Set Pulsar Push	409 V
Scan End	1000 m/z	Skimmer 1	-30.0 V	Set Reflector	1300 V
		Hexapole 1	-24.0 V	Set Flight Tube	9000 V
				Set Detector TOF	2285 V



#	m/z	Res.	S/N	I	FWHM
1	154.9741	6260	2460.7	41113	0.0248
2	180.9720	6590	1027.8	26150	0.0275
3	197.9616	7082	200.3	6246	0.0280
4	204.9690	6849	587.3	19682	0.0299
5	210.8821	7261	447.7	15894	0.0290
6	212.8789	7213	311.7	11278	0.0295
7	221.7981	7465	268.7	10232	0.0297
8	223.7957	7514	439.8	16904	0.0298
9	225.7937	7475	237.2	9212	0.0302
10	230.8194	7408	102.1	4067	0.0312
11	232.7631	7705	135.6	5447	0.0302
12	234.7600	7587	102.8	4171	0.0309
13	248.9581	7669	3779.7	162837	0.0325
14	249.9608	7797	167.0	7241	0.0321
15	288.8993	8356	242.1	11107	0.0346
16	290.9010	8018	111.9	5097	0.0363
17	299.8159	8254	312.2	13670	0.0363
18	301.8141	8025	371.1	16103	0.0376
19	303.8110	8501	164.9	7103	0.0357
20	316.9473	8861	334.8	13568	0.0358
21	377.8344	8868	120.6	4516	0.0426
22	379.8320	9202	117.3	4399	0.0413
23	384.9362	9058	1150.4	43114	0.0425
24	452.9230	9238	694.6	19309	0.0490
25	520.9102	9524	1007.5	22528	0.0547
26	588.8977	10027	423.2	8528	0.0587
27	656.8856	10218	363.7	7068	0.0643
28	679.1973	10053	243.8	5115	0.0676
29	724.8730	10381	156.1	3488	0.0698
30	725.2023	11099	158.9	3547	0.0653

Appendix Figure B14 Mass Spectrum of New resveratrol trimer.



**Appendix C**  
Theoretical Background

## Molecular Docking

Molecular docking is a key tool in structural molecular biology and computer-assisted drug design. The goal of ligand–protein docking is to predict the predominant binding mode(s) of a ligand with a protein of known three-dimensional structure. Successful docking methods search high-dimensional spaces effectively and use a scoring function that correctly ranks candidate dockings. Docking can be used to perform virtual screening on large libraries of compounds, rank the results, and propose structural hypotheses of how the ligands inhibit the target, which is invaluable in lead optimization. The setting up of the input structures for the docking is just as important as the docking itself, and analyzing the results of stochastic search methods can sometimes be unclear. The key steps common to all docking protocols was shown in Appendix Figure 1. The 3D structures for the target macromolecule and the small molecule must first be chosen, and then each structure must be prepared in accordance with the requirements of the docking method being used. Following the docking, the results must be analyzed, selecting the binding modes with the best scores.

### Docking Program

Program GOLD (Genetic Optimization for Ligand Docking) are used to perform ligand-protein docking. GOLD is an automated ligand docking program that uses genetic algorithm to explore the full range of conformational flexible ligand with partial flexible protein, and find an optimized one with fundamental requirement. The binding result is showed as fitness function. Goldscore function is a molecular mechanics which is made up of four components:

$$GOLD\ Fitness = S_{hb\_ext} + 1.3750S_{vdw\_ext} + S_{hb\_int} + S_{vdw\_int} \quad (6)$$

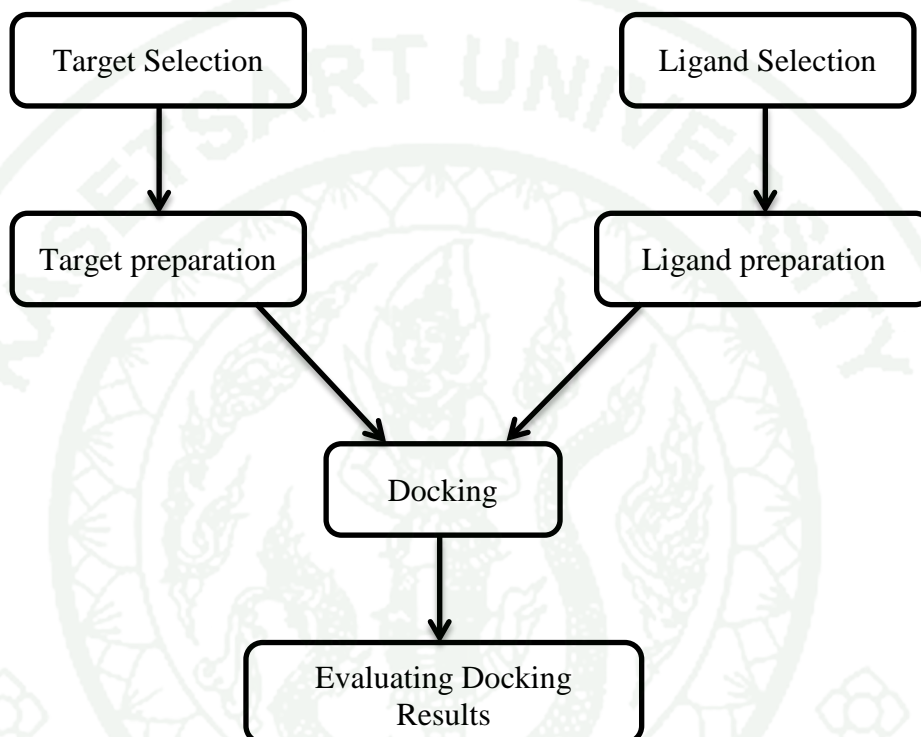
where  $S_{hb\_ext}$  is the protein-ligand hydrogen bond energy or score (external H-bond).

$S_{vdw\_ext}$  is the protein-ligand van der Waals (vdw) energy or score (external vdw). (This term is multiplied by a factor of 1.375 when total fitness score is

computed. This is an empirical correction to encourage protein-ligand hydrophobic contact).

$S_{hb\_int}$  is the ligand internal vdw energy or score (internal vdw).

$S_{vdw\_int}$  is the ligand torsional strain energy (internal torsion).



**Appendix Figure C1** Key flowchart for all docking protocols.

## Quantitative Structure-Activity Relationships Analysis

Finding an accurate method for estimating the affinity of protein ligands activity is one of the most challenging tasks in computer-aided molecular design. QSAR (Quantitative structure-activity relationship) is a mathematical relationship between a biological activity of a molecule and its geometric and chemical characteristics, has been proven to be the principle method used for activity prediction in drug design.

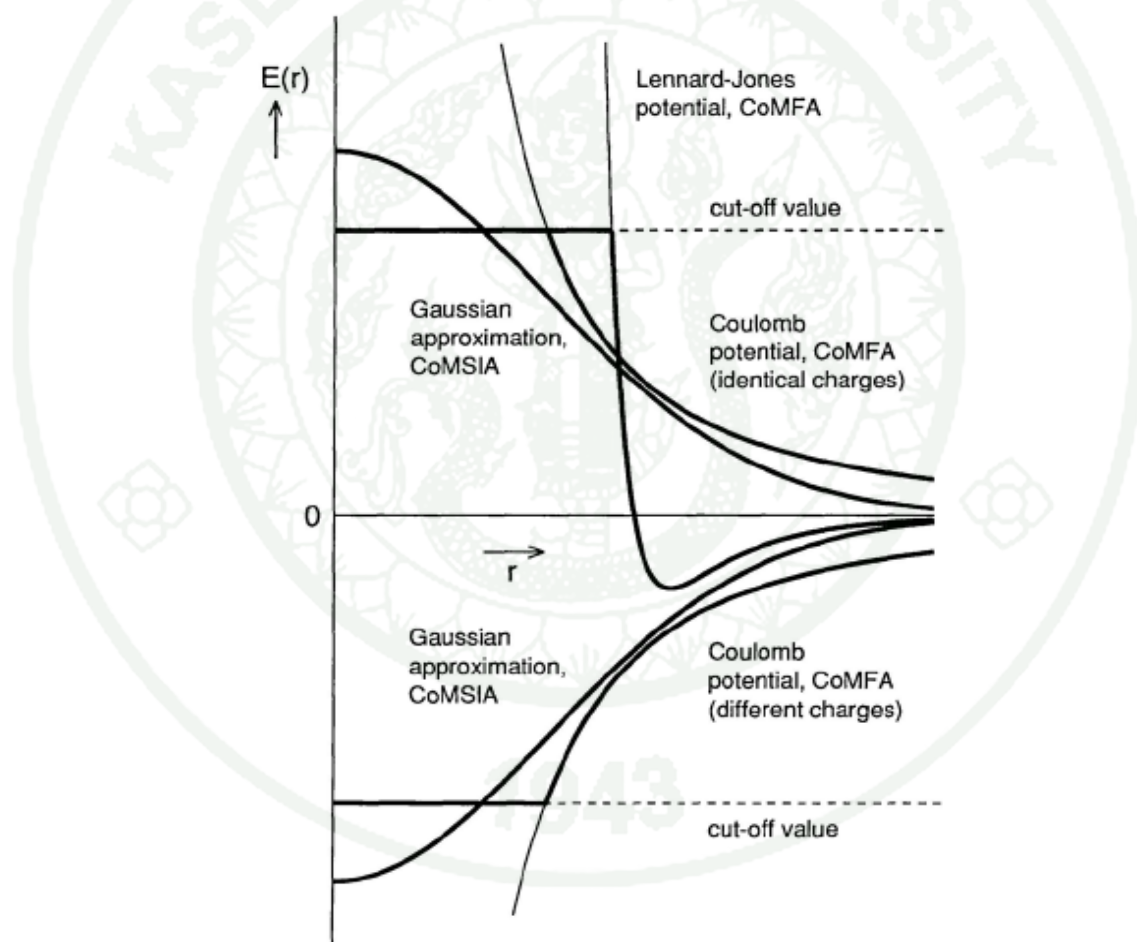
Activity should be a function of the geometric and chemical characteristics of the compounds. QSAR attempts to find consistent relationship so that can be used to evaluate the activity of new compounds.

3D-QSAR techniques are routinely used in analog-based drug design. The ability to produce quantitative correlation between three-dimension properties of molecules and biological activity of these compounds is of inestimable value in deciding upon the choice of further synthetic chemistry.

Comparative Molecular Similarity Indices Analysis (CoMSIA) was developed by Klebe *et al.*, 1994. CoMSIA is known as one of the newer 3D-QSAR descriptors. This technique is most commonly used in drug discovery to find the common features that are important in binding to the relevant biological receptor. The CoMSIA technique is of particular interest, as it involves a hydrophobic, hydrogen bond donor and hydrogen bond acceptor fields. CoMSIA is an extension of the Comparative Molecular Filed Analysis (CoMFA) methodology that search for relationships between the biological activity of a set of compounds (with specified alignment) and their three-dimension electronic and steric properties (so called molecular filed). Both of them method are based on the same assumption. CoMSIA approach differ in that Gaussian functions rather than Lennard-Jones and Coulombic functions are used in CoMFA. Gaussian functions describe the physicochemical similarity between a probe placed at each grid point and each compound. The values computed at the grid points are subjected to PLS analysis to derive a 3D-QSAR. The field contribution maps

show regions that are important for activity within the molecules, rather than around them as in CoMFA.

In CoMSIA, five different similarity fields are calculated: steric, electrostatic, hydrophobic, hydrogen bond donor and hydrogen bond acceptor. These fields were selected to cover the major contributions to ligand binding. Similarity indices are calculated at regularly spaced grid points for the pre-aligned molecules. A comparison of the relative shapes of CoMSIA and CoMFA field is shown in Appendix Figure C2.



**Appendix Figure C2** Gaussian-type functional form of CoMSIA field defines a significantly smoother distance dependence compared to the Lennard-Jones and Coulomb potential of CoMFA field (Klebe 1994).

For the distance dependence between the probe atom and the molecule atoms a Gaussian function is used. Because of the different shape of the Gaussian function, the similarity indices can be calculated at all grid points, both inside and outside the molecular surface.

The equation used to calculate the similarity indices is as follows:

$$A_{F,k}^q(j) = \sum_{i=1}^n W_{probe,k} W_{ik} e^{-\alpha r_{iq}^2} \quad (7)$$

where

$A$  is the similarity index at grid point  $q$ , summed over all atoms  $i$  of the molecule  $j$  under investigation.

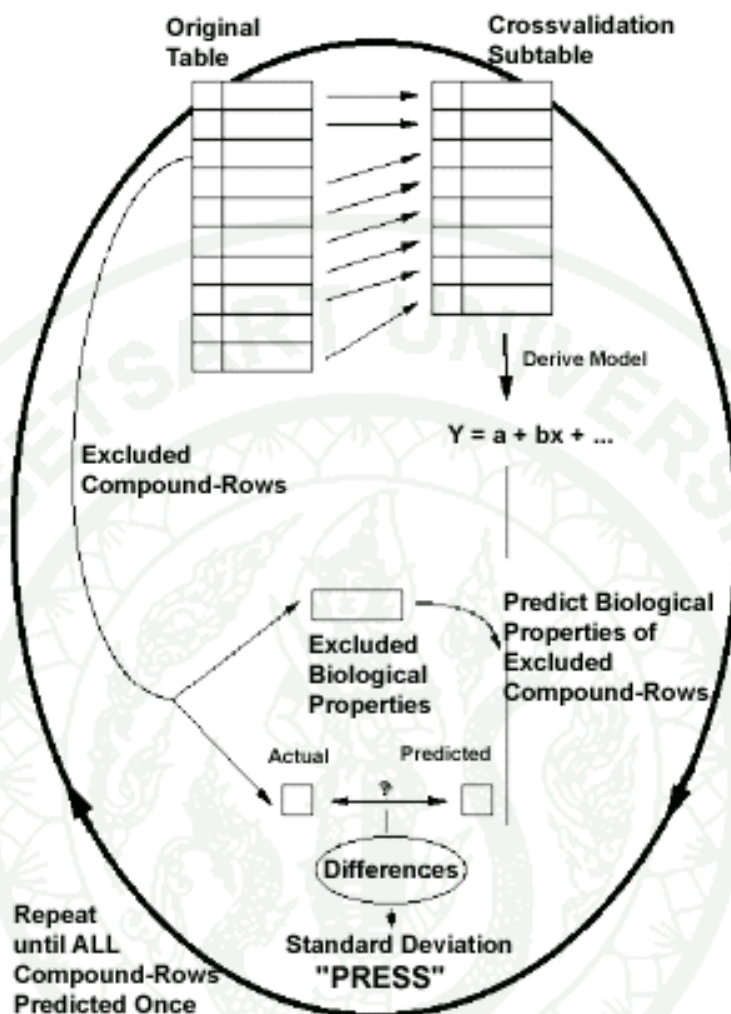
$W_{probe, k}$  is the probe atom with radius 1 Å, charge +1, hydrophobicity +1, hydrogen bond donating +1, hydrogen bond accepting +1.

$W_{ik}$  is the actual value of the physicochemical property  $k$  of atom  $i$ .

$r^{iq}$  is the mutual distance between the probe atom at grid point  $q$  and atom  $i$  of the test molecule.

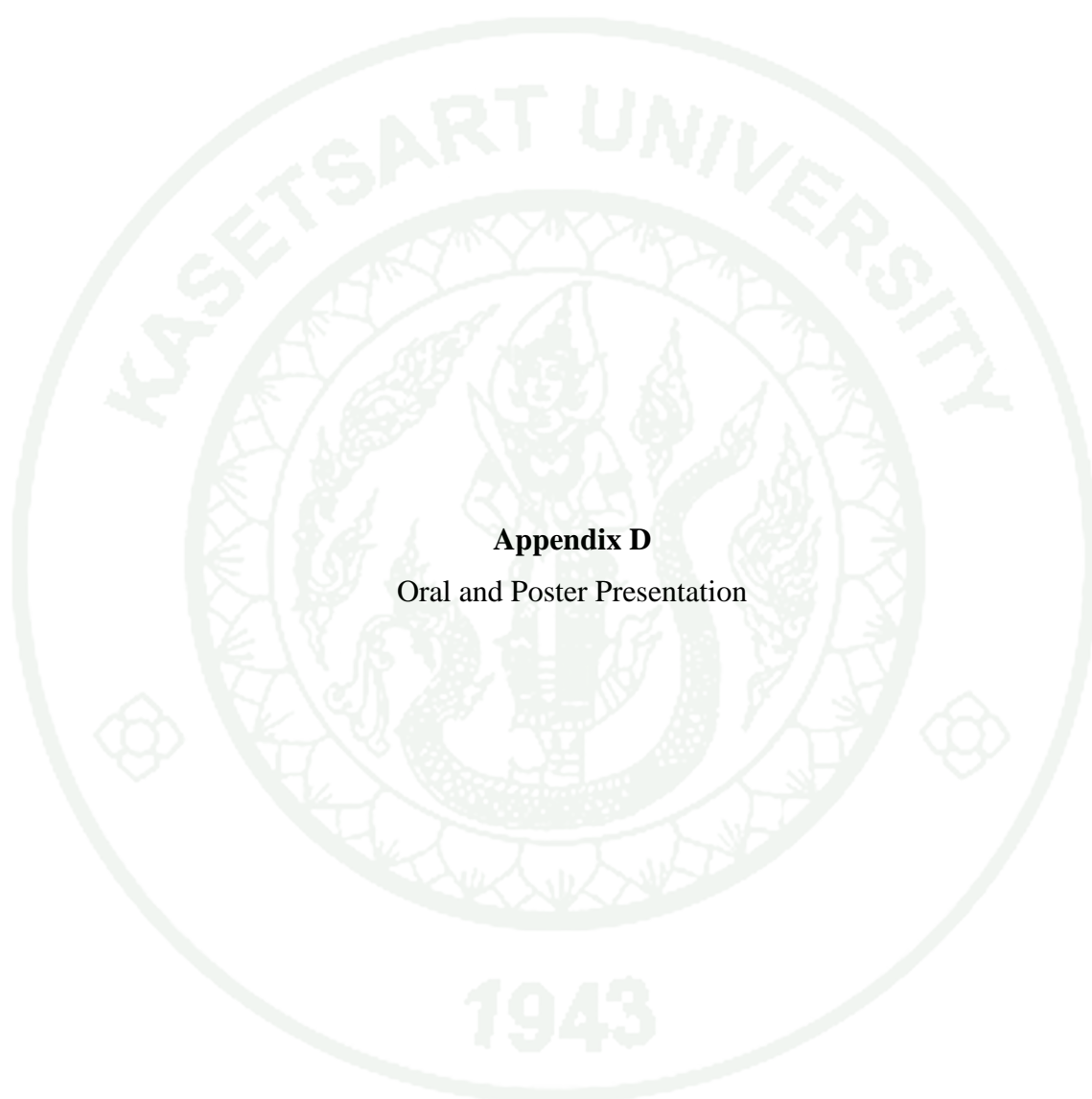
$\alpha$  is the attenuation factor, with a default value of 0.3, and an optimal value normally between 0.2 and 0.4. Larger values result in a steeper Gaussian function, and a strong attenuation of the distance-dependent effects of molecular similarity.

Partial least squares (PLS) methodology was used for all 3D-QSAR analyses. The CoMFA and CoSIA descriptors were used as independent variables and  $\log(1/K_i)$  values were used as dependent variables in partial least squares regression analyses to derive 3D-QSAR models using the standard implementation in the SYBYL 8.0 package. PLS analysis was carried out using the leave-one-out option to obtain the optimal number of components to be used subsequently in the final analysis as shown in the procedure in Appendix Figure C3.



Appendix Figure C3 Cross-validated procedure (Kubinyi 1993)

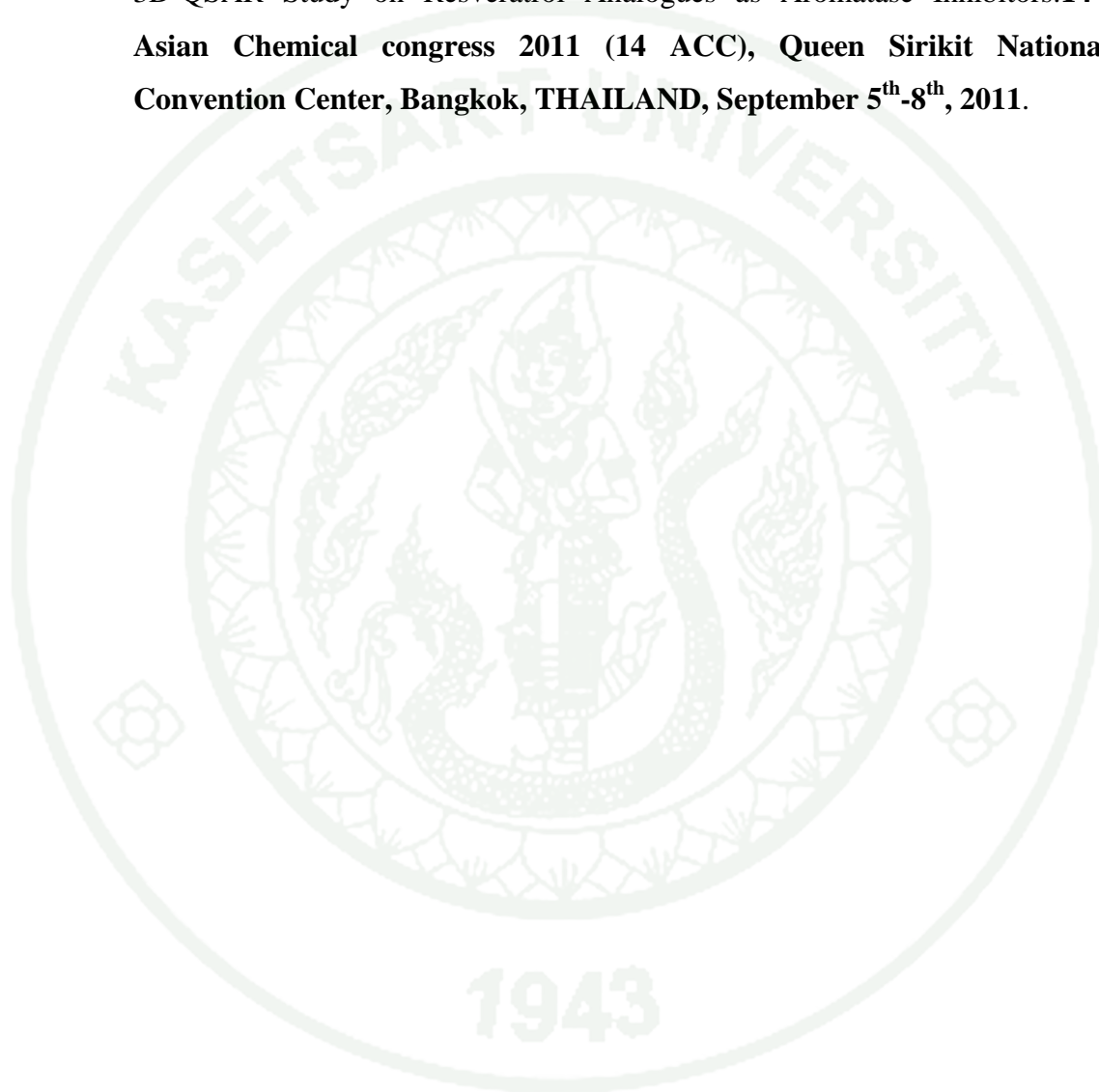
1943



**Appendix D**  
Oral and Poster Presentation

**Proceeding**

**Chompoonuch Tancharoen, Phornphimon Maitarad, Nuttapong Ithiapa, Songwut Suramitr, Patchreenart Saparpakorn and Supa Hannongbua**  
3D-QSAR Study on Resveratrol Analogues as Aromatase Inhibitors.14<sup>th</sup>  
Asian Chemical congress 2011 (14 ACC), Queen Sirikit National  
Convention Center, Bangkok, THAILAND, September 5<sup>th</sup>-8<sup>th</sup>, 2011.



### 3D-QSAR Study on Resveratrol Analogues as Aromatase Inhibitors

Chompoonuch Tanchaoren<sup>1,2</sup>, Phornphimon Maitarad<sup>1,2\*</sup>, Nuttapong Ithiapa<sup>1,2</sup>, Songwut Suramitr<sup>1,2</sup>, Patchareenart Saparpakorn<sup>1,2</sup> and Supa Hannongbua<sup>1,2\*</sup>

<sup>1</sup>Department of Chemistry, Faculty of Science, Kasetsart University, Bangkok 10900, Thailand

<sup>2</sup>Center of Nanotechnology KU, Kasetsart University, Bangkok 10900, Thailand.

\*E-mail: pmaitarad@gmail.com, Tel: +66-2562-5555 ext. 2163 Fax: +66-2562-5555 ext. 2176

\*E-mail: fscisph@ku.ac.th, Tel: +66-2562-5555 ext. 2111 Fax: +66-2562-5555 ext. 2176

#### Abstract

Aromatase is a potential enzyme in the prevention or treatment of estrogen-dependent breast cancers. In this study, the three dimensional quantitative structure-activity relationships (3D-QSAR) using Comparative Molecular Similarity Indices Analysis (CoMSIA) technique was performed on a series of resveratrol analogues (18 compounds) to find the linear relationship between structural properties and their aromatase inhibitory activities. The obtained CoMSIA model exhibited good statistical results of  $r^2_{cv}$  (0.683),  $r^2_{nv}$  (0.974),  $S_{press}$  (0.355),  $s$  (0.101) and  $F$  (56.556) values. The model revealed that H-bond acceptor and electrostatic fields contributed significantly with 36.9% and 49.1%, respectively whereas H-bond donor and steric fields showed the minor contributions with 6.8% and 7.2% respectively. Our CoMSIA contour map and equation are useful to understand and guide the new designed inhibitors and also can predict the biological activity before doing an experiment.

**Keywords:** CoMSIA, 3D-QSAR, Breast cancer, Aromatase, Resveratrol analogues

#### References

- [1]. Partha Pratim Roy & Kunal Roy. (2010). *Journa of Molecular Modeling*.16(10): 1597-1616.
- [2]. Bin Sun, Juma Hoshino, Katie Jermihov, Laura Marler, John M. Pezzuto, Andrew D. Mesecar & Mark Cushman. (2010). *Bioorg. Med. Chem.* 18(14): 5352-5366.
- [3]. Joseph A. Baur & David A. Sinclair. (2006). *Nat Rev Drug Discov*5(6): 493-506.
- [4]. Debashis Ghosh, Jennifer Griswold, Mary Erman & Walter Pangborn. (2009). *Nature*457(7226): 219-223.
- [5]. SYBYL 8.0, Tripos Associates Inc., 1699 South Hanley Road, Suite 303, St Louis, Missouri 63144, USA.
- [6]. Ketthip Suphavanich, Phornphimon Maitarad, Supa Hannongbua, Pichit Sudta, Sunit Suksamrarn, Yuthana Tantirungrotechai & Jumras Limtrakul. (2009). *Monatsh Chem.* 140(3): 273-280.
- [7]. Phornphimon Maitarad, Patchareenart Saparpakorn, Supa Hannongbua, Sumalee Kamchonwongpaisan, Bongkoch Tarnchompoo & Yongyuth Yuthavong. (2009). *J EnzInh Med Chem.* 24 (2): 471-479.
- [8]. Pornpan Pungpo, Patchareenart Saparpakorn, Peter Wolschann & Supa Hannongbua. (2006). *SAR QSAR Environ Res.* 17 (4): 353-370.
- [9]. Supa Hannongbua, Pornpan Pungpo, Jumras Limtrakula & Peter Wolschann. (1999). *J. Comput. Aided Mol. Des.* 13 (6), 563-577.
- [10]. Phornphimon Maitarad, Sumalee Kamchonwongpaisan, Jarunee Vanichtanankul, Tirayut Vilaivan, Yongyuth Yuthavong & Supa Hannongbua. (2009). *Journal of Computer-Aided Molecular Design.* 23: 241-252.
- [11]. Suriyan Thengyai, Phornphimol Maitarat, Supa Hannongbua, Khanit Suwanborirux & Anuchit Plubrukarn. (2010). *Monatsh Chem.* 141(6): 621-629.

14<sup>th</sup> Asian Chemical Congress 2011 (14 ACC), Queen Sirikit National Convention Center, Bangkok, THAILAND, September 5<sup>th</sup>-8<sup>th</sup>, 2011

Sokendai Asian Winter School "Basics and Frontiers in Molecular Science",  
Okazaki Conference Center, National Institutes for Natural Sciences, Okazaki,  
JAPAN, January 10<sup>th</sup>-13<sup>th</sup>, 2012.



## A CoMSIA Study on Resveratrol Derivatives Active against Aromatase Enzyme of Breast Cancer

Chompoonuch Tancharben<sup>1,2</sup>, Phornphimon Maitarad<sup>1,2,3</sup>, Nuttapong Ithiapa<sup>1,2</sup>, Songwut Suramitri<sup>1,2</sup>, Patchareenart Saparakorn<sup>1,2</sup>, and Supa Hannongbua<sup>1,2\*</sup>

<sup>1</sup>Department of Chemistry, Faculty of Science, Kasetsart University, Bangkok 10900, Thailand  
<sup>2</sup>Center of Nanotechnology KU, Kasetsart University, Bangkok 10900, Thailand.  
<sup>3</sup>Nano Science and Technology Research Center Shanghai University, Shanghai 200444, China

### Abstract

Resveratrol derivatives and their aromatase inhibitory activities were used to apply on the Comparative Similarity Indices Analysis (CoMSIA) technique, aiming to understand the structural requirements of aromatase inhibitors. The obtained CoMSIA model exhibited the good statistical results of  $R^2_{\text{steric}}$ ,  $R^2_{\text{electrostatic}}$ ,  $S_{\text{HBD}}$ ,  $s$  and  $F$  values with 0.683, 0.974, 0.355, 0.101 and 56.556, respectively. This model consisted of minor structural contributions (steric = 6.8% and hydrogen-bond donor = 7.2%) whereas the electrostatic and hydrogen-bond acceptor were mainly the structural properties that effecting to the antiaromatase activity.

### Introduction

Breast cancer is the most commonly diagnosed type of cancer in women and is the second leading cause of death from cancer in women. Estrogens are known to play pivotal role in the cancer cell proliferation. High levels of estrogens promote the progression of breast cancer. Aromatase enzyme catalyzes the rate limiting step in estrogen biosynthesis. This enzyme is an important enzyme responsible for converting androgens to estrogens as a target of other biological interest for the development of new agents for the treatment of breast cancer. Thus, inhibition of the enzyme aromatase is an attractive target for Endocrine treatment of breast cancer depending on hormones. Resveratrol (3,5,4'-trihydroxystilbene) has been reported to exert a variety of biological effects including antioxidant, anti-inflammatory, anti-proliferative and cancer chemopreventive activity. In this work, we aim to construct the three-dimensional quantitative structure activity relationship (3D-QSAR) on resveratrol derivatives active against of the aromatase enzyme using the Comparative Molecular Similarity Indices Analysis (CoMSIA) technique. The results would be useful to understand the basic structural requirement of resveratrol inhibitors that will increase the anti-aromatase activity.

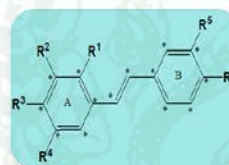


Figure 1 Resveratrol template with 6 substitution positions for resveratrol derivatives (Bin Sun and colleagues *Bioorg. Med. Chem.* 18 (2010) 5352–5366)

### Methodology

18 resveratrol derivatives were reported the structures and their aromatase inhibitory activities by Sun, et al. as shown in Table 1. The processes of structural modifications, optimizations and Gasteiger-Hückel charge calculations were performed on the Sybyl 8.0 program package. All structures generated were aligned in a 3D lattice by fitting them with 14 aligned positions as marked by asterisks (Fig 1) by using fit-atom and superimpose. The CoMSIA process was performed on Sybyl 8.0.

Table 1. Data set for CoMSIA analysis and experimental and calculated  $pIC_{50}$  value in aromatase enzyme.

Comp	R <sup>1</sup>	R <sup>2</sup>	R <sup>3</sup>	R <sup>4</sup>	R <sup>5</sup>	R <sup>6</sup>	Expt. $pIC_{50}$	Calc. $pIC_{50}$ <sup>a</sup>
1	H	OCH <sub>3</sub>	H	OCH <sub>3</sub>	H	NH <sub>2</sub>	6.2291	6.1031
2	OCH <sub>3</sub>	H	OCH <sub>3</sub>	H	H	NH <sub>2</sub>	6.1192	6.1112
3	OCH <sub>3</sub>	H	OCH <sub>3</sub>	H	NH <sub>2</sub>	H	4.9531	4.8951
4	OCH <sub>3</sub>	H	H	OCH <sub>3</sub>	H	NH <sub>2</sub>	5.7399	5.8479
5	OCH <sub>3</sub>	OCH <sub>3</sub>	H	H	H	NH <sub>2</sub>	6.0088	5.9168
6	H	OCH <sub>3</sub>	OCH <sub>3</sub>	H	H	NH <sub>2</sub>	4.8383	-
7	H	OCH <sub>3</sub>	OCH <sub>3</sub>	OCH <sub>3</sub>	NH <sub>2</sub>	H	4.7846	4.8566
8	H	OCH <sub>3</sub>	OCH <sub>3</sub>	OCH <sub>3</sub>	H	NH <sub>2</sub>	6.0458	6.0578
9	OCH <sub>3</sub>	OCH <sub>3</sub>	OCH <sub>3</sub>	H	H	NH <sub>2</sub>	5.4473	5.4153
10	OCH <sub>3</sub>	OCH <sub>3</sub>	H	OCH <sub>3</sub>	H	NH <sub>2</sub>	5.6421	5.6351
11	H	-OCH <sub>2</sub> O-	H	H	NH <sub>2</sub>	H	4.6604	4.6484
12	H	-OCH <sub>2</sub> O-	H	H	H	NH <sub>2</sub>	5.0711	-
13	H	H	NO <sub>2</sub>	H	NO <sub>2</sub>	H	5.0794	5.0754
14	H	OCH <sub>3</sub>	H	H	H	NH <sub>2</sub>	5.5114	5.7124
15	H	NH <sub>2</sub>	H	H	H	NH <sub>2</sub>	5.1267	5.1427
16	H	NH <sub>2</sub>	H	NH <sub>2</sub>	H	NH <sub>2</sub>	5.0701	4.9951
17	H	OAc	H	OAc	H	NH <sub>2</sub>	5.5316	5.5266
18	H	OH	H	OH	H	NH <sub>2</sub>	5.3010	5.256

<sup>a</sup> CoMSIA model with  $R^2_{\text{steric}} = 0.683$ ,  $R^2_{\text{electrostatic}} = 0.974$ ,  $S_{\text{HBD}} = 0.355$ ,  $s = 0.101$  and  $F$  value = 56.556.

### Acknowledgement

- ◇ Thailand Research Fund (TRF)
- ◇ KU Research and Development Institute (KURDI)
- ◇ National Electronics and Computer Technology (NECTEC)
- ◇ Laboratory for Computational and Applied Chemistry (LCAC)
- ◇ National Nanotechnology Center at Kasetsart University
- ◇ The Graduate School, Kasetsart University

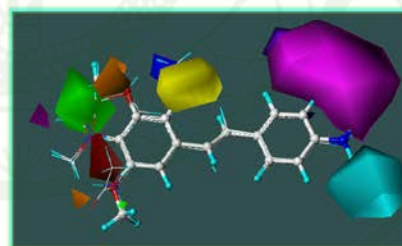


Figure 2 CoMSIA contour maps for steric, electrostatic, hydrogen-bond donor and acceptor properties. Sterically favored regions are in green and disfavored regions in yellow. Positive charge-favored areas in blue and negative-charged-favored areas in red. H-bond donor favored regions are in cyan and disfavored regions in purple. H-bond acceptor favored areas in magenta and disfavored areas in orange.

### Results & Discussion

Considering of CoMSIA contour maps (Fig 2), we can conclude that

- (i) R<sup>1</sup> is favorable the positive charge or electron donating group
- (ii) R<sup>2</sup> is favorable the steric group.
- (iii) R<sup>3</sup> and R<sup>4</sup> are favorable the negative charge or electron withdrawing group
- (iv) R<sup>5</sup> is favored the H-bond acceptor interaction implying that the H-donor group is suitable for this region
- (v) R<sup>6</sup> has both H-bond donor and H-bond acceptor regions merging together which means that the substituent that can act both H-donor and H-acceptor is fit for this position, such as NH<sub>2</sub> group.

The CoMSIA results provide a useful information for designing and predicting the affinities of resveratrol derivatives with enhanced activities prior to synthesis.

## CURRICULUM VITAE

**NAME** : Miss Chompoonuch Tancharoen

**BIRTH DATE** : December 23, 1986

**BIRTH PLACE** : Ratchaburi, THAILAND

<b>EDUCATION</b>	<b><u>:YEAR</u></b>	<b><u>INSTITUTION</u></b>	<b><u>GREE/DIPLOMA</u></b>
	2008	Kasetsart University	B.Sc.(Chemistry)

**POSITION/TITLE** : Postgraduates student

**SCHOLARSHIPS** : 1) The NSTDA Chair Professor, Kasetsart University Research and Development Institute (KURDI).  
2) Thailand Research Fund (RTA 5380010).

### PRESENTATION AND PUBLICATION

Chomoonuch Tancharoen, Phornphimon Maitarad, Nuttapong Ithiapa, Songwut Suramitr, Patchreenart Saparpakorn and Supa Hannongbua. **3D-QSAR Study on Resveratrol Analogues as Aromatase Inhibitors**. 14<sup>th</sup> Asian Chemical congress 2011 (14 ACC), Queen Sirikit National Convention Center, Bangkok, THAILAND, September 5<sup>th</sup>-8<sup>th</sup>, 2011.

Kanokorn Sudto, Chompoonuch Tancharoen, Srunya Vajrodaya, Supanna Techasakul, Yan Hua Qin, Hui Ming Ge, Ren xiang Tan and Supa Hannongbua. **Resvertrol Oligomers from Stem Bark of Thai Dipterocarpaceous Plants (Shorea Roxburghii G. Don)**. 14<sup>th</sup> Asian Chemical congress 2011 (14 ACC), Queen Sirikit National Convention Center, Bangkok, THAILAND, September 5<sup>th</sup>-8<sup>th</sup>, 2011.

Chompoonuch Tancharoen, Phornphimon Maitarad, Nuttapong Ithiapa, Songwut Suramitr, Patchreenart Sarpapakorn and Supa Hannongbua. **A CoMSIA Study on Resveratrol Derivatives Active against Aromatase Enzyme of Breast Cancer** Sokendai Asian Winter School "Basics and Frontiers in Molecular Science", Okazaki Conference Center, National Institutes for Natural Sciences, Okazaki, JAPAN, January 10<sup>th</sup>-13<sup>th</sup>, 2012.

Chompoonuch Tancharoen, Kanokorn Sudto, Yan Tong, Hui Ming Ge, Kanokwan Changwichit, Kornkanok Ingkaninan, Supanna Techasakul, Srunya Vajrodaya, Ren xiang Tan and Supa Hannongbua. **New Resveratrol Trimers from the Bark of *Shora Siamensis* Miq.** 2012, to be submitted.